Proportional Miniaturization of Microscale Features into the Nanoscale Using Pre-stressed Polymer Films and Formation of Plasmonic Nanostructures

Proportional Miniaturization of Microscale Features into the Nanoscale Using Pre-stressed Polymer Films and Formation of Plasmonic Nanostructures

By

Shady Abosree, B.Sc., M.Sc.

A Thesis

Submitted to the School of Graduate Studies in Partial Fulfillment of the Requirements

for the Degree Doctor of Philosophy

McMaster University

DOCTOR OF PHILOSOPHY (2021) McMaster University

(Mechanical Engineering) Hamilton, Ontario, Canada

TITLE:	Proportional Miniaturization of Microscale Features into the Nanoscale Using Pre-stressed Polymer Films and Formation of Plasmonic Nanostructures
AUTHOR:	Shady Abosree B.Sc. in Mechanical Engineering (Military Technical College) M.Sc. in Mechanical Engineering (Military Technical College)
SUPERVISOR:	Professor P. Ravi Selvaganapathy
NUMBER OF PAGES:	136

Abstract

Fabrication of nano structures and patterns is the basis of diverse technologies and applications in our life ranging from microelectronics and semiconductors to nanofludics, biosensors and lab-on-chip devices. However, creation of nano patterns by means of conventional nanofabrication techniques such as electron beam lithography is expensive and time consuming. Pre-stressed polymer films have been used as a miniaturization technique to fabricate features with smaller size than the initial patterned features. Microscale patterns can be miniaturized by shrinking induced due to thermal stress release of the pre-stressed films. However, there are several challenges such as lack to achieve sub-micron resolution, lack of proportional miniaturization and limited shrinkage ratio that prevent the use of current technology for effective and scalable approach to fabricate nanoscale patterns. This thesis presents development of new miniaturization approaches using shrinkable films that can proportionally miniaturize microscale patterns into nanoscale down to sub 100 nm. Low-cost, rapid and scalable method to fabricate high resolution nano patterns was demonstrated by developing a constrained shrinking process. This process was able to overcome the loss of resolution after thermal shrinking of imprinted polymer films. Moreover, the process design allowed to perform iterative miniaturization which significantly reduced the size of the initial patterns by more than 99% reduction in area. These new capabilities were applied to fabricate tunable plasmonic structures in order to demonstrate the potential of the developed miniaturization approaches that can be used in various applications including microelectronics, sensors and functional surfaces.

Acknowledgment

I am very grateful to my supervisor, Prof. P. Ravi Selvaganapathy, for his continuous support, encouragement, and advice. I would like to thank him for being always available to provide answers, research guidance, and discussions throughout this critical time. Thanks for being so understanding as I worked through critical time requirements. I have learnt extensively from him valuable lessons, both professional and personal. Your excessive support, teaching, and encouragement are appreciated more than you know.

I would like to express my sincere gratitude to Prof. Matiar Howlader for his precious support and sharing his knowledge and laboratory facilities. Without this guidance it would not be possible to conduct this research. I also would like to thank Centre for Emerging Device Technologies (CEDT) and its people Doris Stevanovic and Shahram Tavakoli for all the provided facilities and assistance.

Next, I would like to thank all colleagues and members of CAMEF group, special thanks to Islam, Nidhi, Aliakbar, Mohammadhossein, Mohamed Fathalla, Rong, Sreekant, Vinay, Shadi and all others for all your help, guidance, friendship and unforgettable memories.

Lastly, I would like to express my indebtedness to my parents for their prayers, unconditional love, support, and blessed wishes throughout my life. Thanks to all my family, my brother and sister for their love and support. Words cannot express my gratitude to my wife Nourhan Hussein and my son Zeineldein for all the patience, love, and endless support.

Table of Contents

List of Figures

1 Chapter 1

Introduction and Background

1.1 Introduction

Miniaturization of micro and nano structures is crucially required in many applications such as microelectronics, semiconductors and nanoelectromechanical systems (NEMS) as well as nanofluidics and biosensors. The current advancement in integrated circuit (IC) manufacturing rely on continued miniaturization of the patterned areas on the substrate surface in order to increase the density of transistors while decreasing the overall size and dimensions of the chip [1, 2]. Photolithography, the most known micro fabrication technology, has rapidly evolved to improve the resolution and achieve smaller size patterns [3]. However, it has limitations due to the optical diffraction of the light and it requires using masks that are highly expensive at sub-micron resolution [4]. Alternatively, high resolution nanofabrication technologies, including focused ion beam and electron beam lithography, are used to fabricate nano patterns at high precision which are generally used as master mold for subsequent scalable fabrication [5-8]. However, these technologies are expensive and time consuming particularly for large-area patterning [9, 10], so they are not suitable for low-cost, scalable applications. Thus, development of alternative micro fabrication and miniaturization methods that can miniaturize the size of microscale features to nanoscale can be potentially valuable for rapid, low-cost and scalable nanofabrication.

Size reduction approaches using pre-stressed polymer films have been developed in order to miniaturize the size of the original patterns fabricated by conventional methods [11-13]. Pre-stressed polymer films are basically shape memory polymers (SMP) which are composed of randomly oriented polymer chains that can be plastically deformed to retain an embedded pre-stress [14, 15]. They are responsive to external stimuli that can be triggered by, for example, heating above the glass transition temperature T_g as in the heat shrinkable polymer films [16, 17]. When an external stimulus is applied, shape recovery of the SMP takes place by relaxation of the internal stresses whereupon the polymer reorganizes to its minimum energy state and the overall polymer film tends to recover to its original shape. By imposing a topographical pattern on the pre-stressed polymer film and letting it shrink, the pattern size can be miniaturized as well and new smaller size patterns could potentially be fabricated. This offers a simple and low-cost way to generate micro and nano features at smaller sizes than the original patterns. This can overcome the limitations of mask fabrication that is needed, for example, for photolithography.

Heat shrinkable polymer films have been patterned by different methods to transfer the patterns from the master template to the shrinkable film. In particular, pattern transfer methods have been used to pattern either the shrinkable film itself [18-21] or other materials deposited on top of the film [22, 23]. The main aspect to be considered when patterning the heat shrinkable films directly or using other materials is the ability of the pattern to shrink without distortion. This is profoundly challenging at sub-micron/nano scale resolution. When other materials are patterned on the heat shrinkable films typically they do not have the same pre-stress as the underlying heat shrinkable films. Therefore, when the composite layer is shrunk by heating, the shrinkage of the underlying heat shrink

films impose a compressive stress on the patterned layer on the top. Typically, the pattern will deform and in some cases generates wrinkles. This phenomenon has been exploited in a number of other applications such as for creating high surface area electrodes [24-27] but is not useful in proportional miniaturization of defined patterns as needed in microelectronics. Alternatively, when the heat shrink polymers themselves are patterned through hot embossing or etching, they do allow proportional miniaturization in the millimeter and hundreds of micrometer scale [13]. Nevertheless, significant challenges have been found that prevent the use of these methods in the sub micrometer and nanometer scales which is crucial in microelectronics. The main objective of this thesis is to overcome these challenges and to develop a new method that can achieve proportional miniaturization below the 100 nm scale which is suitable for microelectronics.

This chapter summarizes the main contributions as well as research efforts of using pre-stressed polymer films as a size reduction technique to miniaturize the pattern size and generate new features induced by thermal shrinking process. Various patterning methods that have been used to pattern heat shrinkable films directly are discussed in detail along with their limitations and resolution limits. In addition, the method of introducing wrinkles by depositing other materials on pre-stressed polymer films is also discussed. The fundamental phenomenon of shape memory effect of pre-stressed polymers is described along with the different modeling approaches. Next, the motivation of the thesis is presented which aims to research challenges in the fabrication of high resolution nanoscale patterns by miniaturization of patterned pre-stressed films. Finally, the thesis objectives and the main contributions as well as the thesis outline are presented.

1.2 Literature review

The field of micro and nanofabrication has experienced rapid growth in the past decade due to the rapid advancement in the applications that rely on micro/nano structures. Photolithography has been the work horse for microfabrication for decades [28, 29]. In conventional photolithography process, an image on a mask that contains dark and transparent areas is transferred to a photosensitive polymer by illuminating UV light through the mask. Various photolithography methods were developed based on the location of the mask relative to the substrate surface including contact, proximity, and projection photolithography. In contact and proximity methods, the mask is placed in direct contact or close proximity to the photoresist while the projection method utilizes an optical projection system to transfer the image on the mask. Contact photolithography is straightforward and less expensive, thus it is widely used in research laboratories. However, the image on the mask is transferred in scale 1:1 and the resolution is generally limited by the wavelength of light and the optical diffraction limits. For instance, lithography using i-line mercury lamps (wavelength of 365 nm) generally can produce patterns of 500 nm or larger. Projection photolithography was developed to avoid the contact between the mask and the photoresist in contact lithography and to extend the lifetime of the mask. The separation of the mask and the substrate leads to loss of resolution which can be corrected using an optical lens system which increases the complexity and cost of the system. Nevertheless, this method also is limited in the resolution achieved by the wavelength of light used and the optical diffraction limits.

The main approach that has been taken to improve the resolution of projection photolithography has been to develop new light sources and optical projection systems that

have a lower wavelength and to increase the numerical aperture (NA) of the optical lens system. Deep UV systems were developed using shorter wavelengths of excimer lasers for KrF (248 nm) and ArF (193 nm) lasers to increase the resolution [30]. One of the significant techniques that improved NA is immersion lithography which increases NA by using high refractive index medium (mainly water) instead of air along with 193 nm laser [31]. Further improvements resulted in developing extreme UV systems to reduce the wavelength at 13.5 nm which represents more than 10 times reduction from 193 nm [32]. However, this method requires the entire system to be in an evacuated chamber as well as using fully reflective optical path to reduce absorption of 13.5 nm extreme UV. Due to these requirements, the cost and complexity of such systems are very high.

An alternative approach that has been adopted is to use existing nanofabrication methods that are low throughput such as electron beam lithography or focused ion beam lithography to fabricate a master that can be replicated quickly and at lower cost using mechanical methods such as hot embossing. These nanofabrication approaches consist of two processes: writing and replication. Writing is the process in which the master is fabricated using high resolution but slow direct write techniques such as focused ion beam and electron beam lithography. Replication is the transfer of nano structures on the master into another substrate by nanoimprint lithography (NIL), hot embossing or soft lithography techniques. Focused ion beam lithography is a mask-less process; it utilizes accelerated ion beam which is focused to a spot size less than 10 nm [33]. Due to the heavy ions and their high momentum, the ions can travel in straight path through matter resulting in direct etch high resolution patterns through different materials including metals. Similarly, electron beam lithography uses high energy electron beams to expose electron-sensitive resists. It

can achieve high resolution nano patterns of about 10 nm without diffraction limits [34]. However, the low throughput limits its application in mask production and in research (an approximation to write 1 in^2 area with pattern density 25% is about 45 hour) [30]. Therefore, it is often used to create an expensive master and combined with a replication method like NIL which has a high throughput at relatively low cost. In NIL, a master mold with surface patterns is physically embossed into polymer or resist film with the aid of heating as in thermal-NIL or UV light as in UV-NIL to leave its imprint [35]. In contrast with photolithography where the image of a photomask is transferred by optical illumination, the pattern of a mold is replicated by physical pressure in NIL. Therefore, the main advantage of NIL is that it does not require optical system and can overcome the resolution limitation of photolithography such as diffraction. NIL is a 1:1 replication process in both lateral and vertical directions. Thus, the lateral resolution and depth of the imprinted patterns are determined by the master mold. This makes fabrication of masters more difficult specially over large area and at sub 100 nm resolution. In summary, the replication process is usually a simple, rapid and inexpensive step. However, most writing methods are expensive and time consuming to be used for mass production. Thus, developing a combination between writing of a high-resolution master and replication of this master with fast and low-cost step leads to the most practical route for nanofabrication.

Since it is expensive and difficult to fabricate a master with nanoscale resolution over large area using direct write methods, alternative unconventional approaches have been taken to proportionally miniaturize larger patterns made more easily in the millimeter or hundreds of micrometer scales and used in applications such as sensors [36-38], diffraction gratings [39, 40], microfluidic devices [41-43] and stretchable electrodes [44].

These size reduction techniques are based on physical or mechanical deformation of elastic materials such as polydimethylsiloxane (PDMS) [45, 46] or shrinkage of pre-stressed materials such as heat shrinkable polymers [26, 47]. These techniques are not only cost-effective but also can produce complex structures over large areas which are applicable for certain types of micro structures that can be fabricated without using high-resolution lithography methods. However, they have so far been restricted to millimeter or micrometer dimensions.

Pre-stressed polymer films have been the widely used materials for these size reduction techniques due to their availability, flexibility, and the ease of processing, control and integration with other micro lithography methods, which make them effective for simple, rapid, and low-cost micro fabrication. In order to pattern the heat shrinkable films, various methods have been used. They can be divided into two general categories, patterning by means of pattern-transfer methods (lithography) and surface-induced patterns due to shrinking behavior (wrinkles). These two approaches are discussed in detail below.

1.2.1 Pattern-transfer methods

Pattern-transfer methods are used to fabricate micro/nano structures on the heat shrinkable films by replicating patterns of a master template. The size of the fabricated structures is then reduced after shrinkage which improves the resolution compared to the original pattern. Thus, a combination between the heat shrinkable polymers and lithography techniques can produce less expensive fabrication approaches with higher resolution. Patterning heat shrinkable films directly has been done by reactive ion etching (RIE) [18], hot embossing [20], and contact etching lithography [21]. While other materials have been

patterned on heat shrinkable films by printing [11, 48], soft lithography [22], and photolithography [23].

1.2.1.1 Patterning heat shrinkable films directly

The pre-stressed polymer films have been patterned by removing material in specified areas using RIE. Physical masks with relief structures were used to define the pattern area to be etched on Polystyrene (PS) heat shrinkable films [18, 19]. Then, the surface of the films were etched by exposing to O_2 plasma. The patterned PS films were heated at 110 ^oC to allow shrinking in the plane of the film while increasing the height of the micro structures. High aspect ratio polymeric structures were fabricated with an aspect ratio of ≈10 and up to 120 μm in height, showing 100-fold increase in the aspect ratio. Figure 1-1 shows SEM images of a mask used in RIE and the patterned polystyrene film before and after thermal shrinking. The patterns created by the shrunk PS films were also used by replica molding to create the inverse of the micro structures on other materials such as silver epoxy, polyurethane (PU) and carbon. The patterns were miniaturized proportionally by shrink ratio of 75% in a single miniaturization step. Although microstructures have been generated, the resolution was limited to few microns. Moreover, it needs fabrication of physical masks which is difficult and expensive at sub-micron scale.

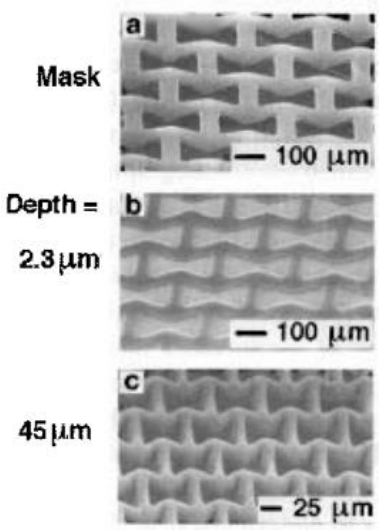

Figure 1-1 SEM images of (a) mask used in RIE (b) patterned heat shrinkable PS film before shrinking (c) after shrinking.[19]

Alternatively, hot embossing with a rigid master has been used to directly imprint patterns on the heat shrinkable films at controlled pressure and temperature. Unlike removing the material in RIE, hot embossing results in the polymer reflow to replicate the pattern in the master mold. Therefore, after shrinking when the pattern's lateral size decreases, the depth of the embossed pattern also decreases rather than increasing as with the case of RIE. This happens because of the relaxation of the pre-stressed polymer when heated which known as the shape memory effect. In order to overcome this issue, an approach was developed to change the shrinkage behavior by physically removing some of the material from the embossed pattern [20]. In particular, after hot embossing a pre-pattern on a PS heat shrinkable film, the projected structure was partially removed by a polishing process. After this process, the embossed pattern increased in height 6 times after shrinking. This modification enabled higher aspect ratio micro features to be formed. Figure 1-2 shows a microneedle array mold used for hot embossing, and the resulted shrunk pattern. However, it was used to fabricate only relatively large micro structures of tens of

micrometers with a minimum feature size obtained in the order of 25 µm. Moreover, the surface roughness of the polished surface increased significantly after shrinking. The shrunk features were miniaturized proportionally by shrink ratio of 60% in a single miniaturization step. These factors prevent this polishing approach from being applied to shrink patterns to sub micrometer or nanometer scale.

Another approach to protect the embossed patterns from diminishing in height and aspect ratio during the shrinking step was presented in [12]. A surface protection layer of poly(vinyl alcohol) was applied on the patterned heat shrinkable film. After shrinking, this layer was removed by dissolving in water. The minimum features obtained were 60 nm, while the depth reduced to 33% of the original pattern. For another pattern which has larger size and depth, the depth after shrinking decreased more to 25% of the original pattern. The features were miniaturized proportionally by 40-60% in a single miniaturization step. Although nanoscale patterns were imprinted and miniaturized, the depth of the pattern still decreased significantly. Therefore, this method cannot be used for successive miniaturization and require a master that is also made using conventional nanofabrication processes.

Leveraging the usage of hot embossing in micro/nano fabrication, nanoscale features were fabricated by embossing heat shrinkable films [47]. Polyolefin (PO) shrinkable films were embossed by sharp edge Ni mold at high pressure to cut imprinted patterns through the films. After heat treatment of the PO films, the shrunk films were used as shadow masks for metal deposition. Metal lines as small as 21 nm were fabricated by sputtering. Figure 1-3 shows a scheme of the shrink lithography process and SEM images for the mold and the fabricated nano features. In this work, the authors were able to fabricate different line

widths using a single mold by controlling the embossing pressure and the shrinkage temperature. High shrink ratio of more than 90% was achieved in a single miniaturization step by increasing the shrinking temperature. Moreover, they applied this technique to fabricate a biosensor based on a suspended graphene nanoribbon. This low-cost nanofabrication approach shows the potential to be applied for nano devices and integrated circuits. However, this technique is a specialized one and can only be used for limited feature shapes. In particular, the use of anisotropic etch of silicon to form the wedge shape structure, put a limit on the spacing between the features as well as the ability to form angled features.

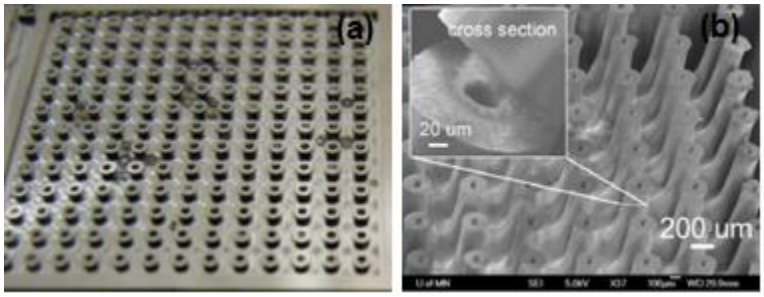

Figure 1-2 (a) microneedle array mold used for hot embossing, (b) SEM view for the shrunk pattern.[20]

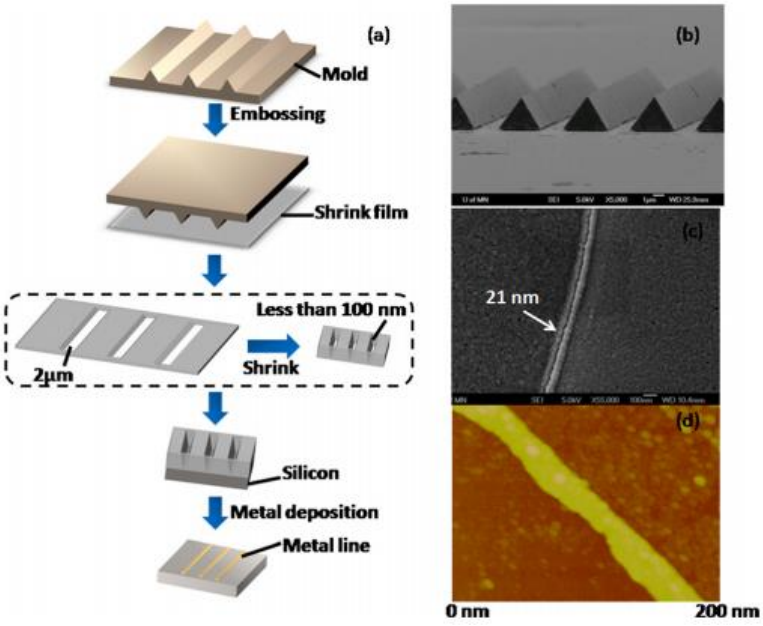

Figure 1-3 (a) A scheme of the embossing process of the shrinkable film to be used as a mask for metal deposition. SEM images of (b) the mold, and (c) the fabricated metal line. (d) AFM image of the line.[47]

In another approach, contact etching lithography has been used to transfer patterns to shrinkable films by means of elastomeric molds [21]. Polydimethylsiloxane (PDMS) templates were swollen with a solvent and pressed against the shrinkable films to partially dissolve and reshape the surface of the polymer films. Nanoscale pillars were patterned on the surface of the shrinkable film. After thermal shrinkage, the patterns were miniaturized. The highest resolution pattern shown was a PDMS template in the form of a hole array of 0.25 µm diameter with same spacing (pitch=0.5µm). After imprint, the pitch of the transferred pillars was 0.6 µm. After thermal shrinking, the pitch reduced to 0.44 µm. Figure 1-4 shows different sizes of PDMS molds that were used to pattern the shrinkable films, and the transferred patterns before and after shrinkage. The reduction in size after shrinking was only around 25% of the original patterns. However, a second miniaturization

step was performed to achieve more size reduction, the pattern was significantly deformed and considerably diminished (the height of the pattern decreased from 1µm to 70 nm).

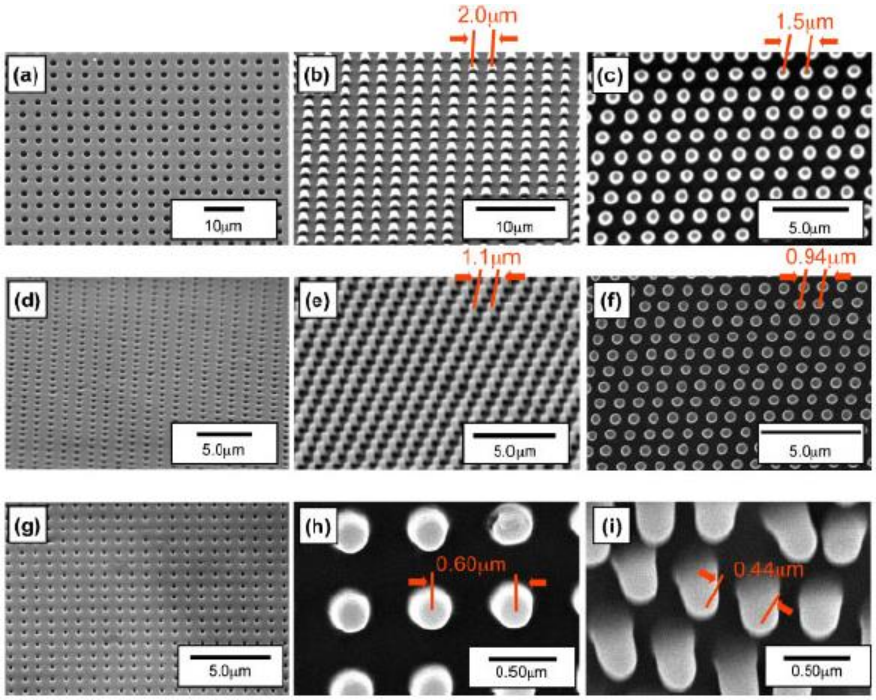

Figure 1-4 SEM images of (a),(d),(g) the PDMS molds, (b),(e),(h) patterned shrinkable polymer films before shrinking, and (c),(f),(i) after shrinking.[21]

1.2.1.2 Patterning other materials on the heat shrinkable films

Instead of patterning the heat shrinkable film itself by removing or reflowing the polymer material, other materials can be patterned on top of the shrinkable film. One of these methods, which is extremely rapid and low-cost, is printing. Printing on the heat shrinkable film is a simple process that can produce micro structures by printing using a laser-jet printer or an ink-jet printer and heating the film to allow shrinking [11, 48-51]. The ability to create rapid and low-cost microfluidic devices by printing on heat shrinkable films was first demonstrated in [48]. Instead of using expensive silicon or glass masters that usually fabricated by photolithography, printed PS shrinkable films were used. First, the pattern of a microfluidic device was printed on the PS film by laser-jet printer. Then,

the film was heated in an oven to shrink in-plane while the thickness increased. After shrinking, the printed line was reduced in width from 800 to 300 µm (shrink ratio 63%) and the height increased to 80 µm. This resulted in increasing the height of the printed pattern which was used as a master mold. PDMS was cast onto this master to create the negative microfluidic channels. Finally, the PDMS mold was bonded to a glass substrate to complete the microfluidic device. Figure 1-5 shows the process flow and a fabricated gradient generator as a microfluidic device. The minimum width of the fabricated channels was 65 µm.

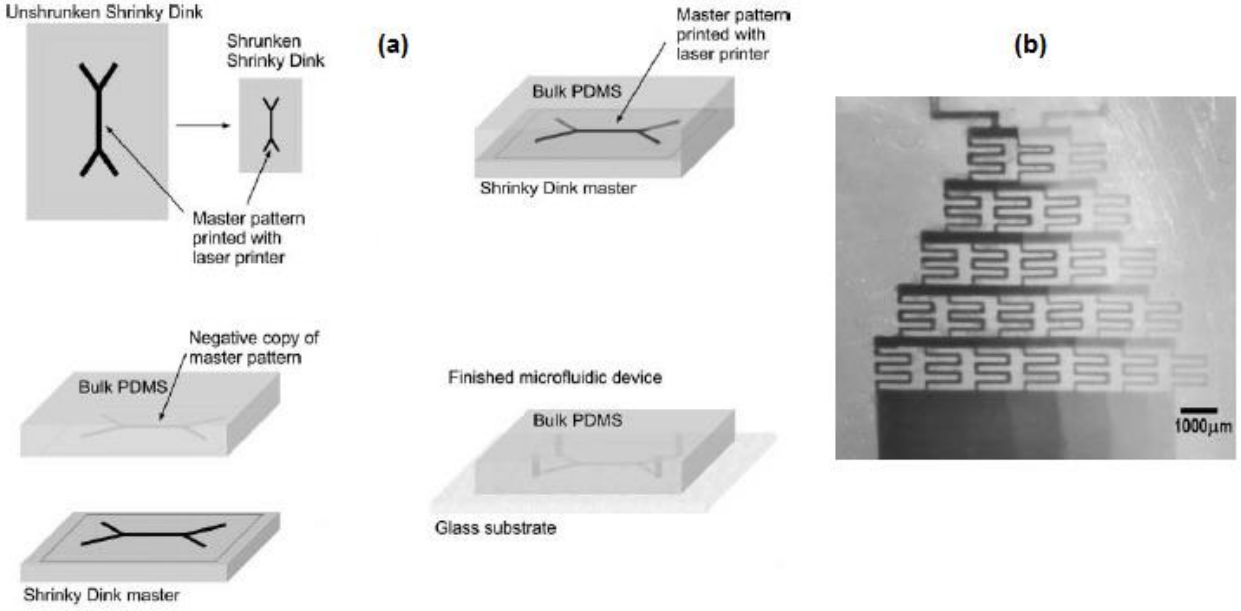

Figure 1-5 (a) Process flow of creating a microfluidic device by printing on the heat shrinkable film (b) PDMS gradient generator.[48]

Printing on the heat shrinkable film approach is suitable for relatively large micro channels (20-100 µm in width), because the printed features size is limited by the resolution of the laser printer. Moreover, the depth of the micro channels can't be easily controlled and depends on the height of the printed layer and the particle size of the printer toner. In order to increase the height of the printed patterns, templates with multilayer prints were

fabricated using both ink-jet and laser-jet printers [11]. However, the additional layers did not lead to a uniform and proportional increase in the height of the structures formed after shrink over the entire reprinted area and the surface roughness significantly increased with the number of printed layers rendering the technique unsuitable for sub micron miniaturization.

Alternatively, soft lithography has been used to pattern photoresists on the heat shrinkable films to fabricate nanoparticle arrays [22]. In this method, a PDMS mold which was cast from a master template was used to transfer the patterns to shrinkable films. The PDMS mold was first wet with photoresist, then placed into contact with a heat shrinkable film until the pattern was solidified. Photoresist features were created on top of the film. By shrinking the film, the spacing between the features was decreased to create arrays with higher densities than the original master. Moreover, lower density pattern was produced by stretching the film instead of shrinking. Thus, by using a single master, arrays of nano patterns were reproduced with different densities (increase or decrease the spacing between patterns) by stretching or shrinking the thermoplastic PS film while keeping same feature size, as shown in Figure 1-6. The initial pitch of 400 nm was reduced to 200 nm after shrinking (shrink ratio 50%). Although, nanoscale patterns can be created using this approach, it had several limitations. The use of the nanoparticles as templates means that patterns such as periodic arrays of pillars are easier to assemble and fabricate. However, line patterns and other arbitrary patterns that are important in electronic designs cannot be fabricated. In addition, this method is used to reduce the spacing between the pattern while the pattern itself retains its size. Therefore, proportional miniaturization is not possible.

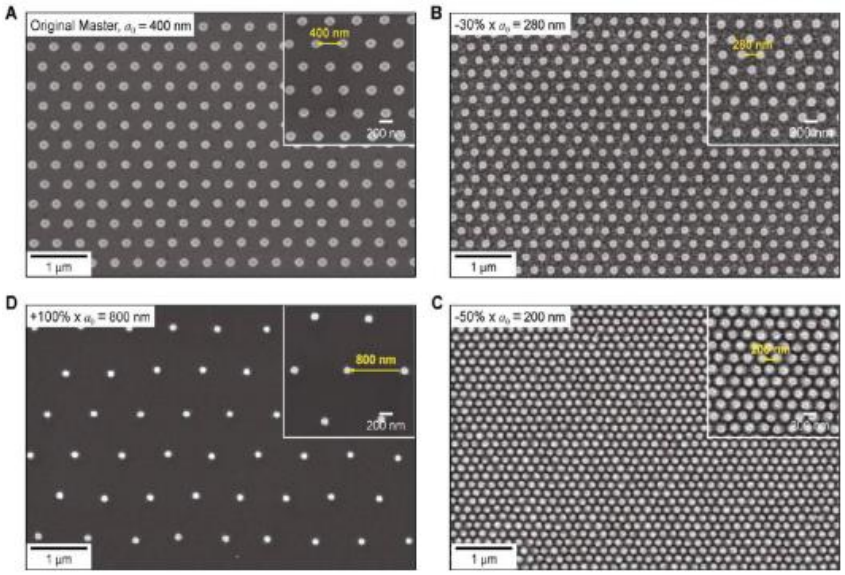

Figure 1-6 SEM images of different nano pattern densities. (A) Original master, (B) -30% smaller pitch, (C) -50% smaller pitch, (D) +100% larger pitch.[22]

In a different approach, photolithography was also used to pattern photoresist features on a polyolefin shrink-wrap film [23]. The mask that was used in photolithography was also fabricated by printing on a PS shrinkable film and shrinking it. Then, the mask was used to pattern photoresist coated on a polyolefin shrinkable film. After shrinking, smooth convex photoresist bumps were created with size of around 65-70 µm. Thus, two sequential miniaturization steps were achieved with an almost 99% reduction in area (shrink ratio 90% reduction in size). The shrunk pattern was used to fabricate microlens arrays by molding a PDMS on the shrunk pattern to create a negative mold. This PDMS mold was then pressed onto cyclic olefin copolymer (COC) which is an optically attractive plastic to create microlens arrays. Although promising, this approach has not been demonstrated with sub micrometer features probably due to patterning resolutions. In addition, similar issues as with the previous method where a resist was use is expected such as the lack of the ability to proportionally shrink both the pattern as well as the spacing.

The challenges in extending the reported approaches for pattern miniaturization using heat shrinkable polymers can be mainly categorized into 1) lack of the ability to achieve sub micrometer resolution, 2) lack of the ability to proportionally miniaturize both patterns and spacing, 3) lack of a versatile low cost method to scale the process to multi-steps so that higher degree of miniaturization can be achieved. Most of these methods were designed for microfabrication where the resolution was limited to few micrometers. Although nano features were fabricated using, in particular, soft lithography, the patterns did not shrink proportionally and the patterns were limited to certain shapes such as dot array. Hot embossing, for example, is a well known replication process that can easily replicate nano patterns on polymer films over large area. However, thermal shrinking of imprinted films failed to preserve topographical features where the pattern height significantly decreased due to shape memory effect. The maximum reduction in size that can be achieved was also a limitation, for example, in contact etching lithography where the shrink ratio was very low. In order to increase the overall reduction in size, the miniaturization cycle can be repeated sequentially by using the shrunk pattern of the first cycle as master for the next cycle. However, the process designs reported so far were not able to generate suitable features that could be used as masters for the second miniaturization cycle. In addition, a master template is required for any replication process to replicate the patterns onto another substrate. Thus, to create different pattern sizes, new masters have to be fabricated for each pattern. Moreover, fabricating master molds is difficult and expensive at sub-micron and nanoscale. In summary, the approach of miniaturization using heat shrinkable polymers still requires more development to overcome these limitations in order to be suitable at the nanoscale.

1.2.2 Surface-induced patterns due to shrinking (wrinkles)

Micro/nano structures can also be formed on the surface of the pre-stressed polymers after shrinking due to generation of wrinkles. When the heat shrinkable films are heated, the pre-stressed polymer softens and shrinks to the original shape. If there is another material layer on top of the heat shrinkable film, it doesn't shrink with the film. Instead, it is compressed and buckles creating wrinkled structures [52]. This occurs due to the mismatch of the mechanical properties between the different layered materials [53]. Many strategies have been developed to produce and control periodic surface topographies. Usually elastomers, such as PDMS, are used as a soft substrate while a thin rigid layer is attached to it to form the wrinkles [54]. Alternatively, pre-stressed polymer films with attached stiff layers have also been used to generate wrinkles and buckled structures. The stiff layer can be formed, for example, by metal deposition [55], oxidation [56], and chemical treatment by RIE [57].

An interesting aspect of this method is the generated surface topography has a characteristic wavelength which depends on the geometry and the skin layer material. Thus, the wavelength and the amplitude of the periodic wrinkles can be programmed and controlled by adjusting the thickness of the skin layer and the elastic properties of the two layers [58, 59]. The ability to control the characteristic wavelength was discussed in [57], by changing the skin layer thickness. The skin layer was formed on PS shrinkable films by RIE with CHF_3 gas. Simply, the thickness of the deposited layer was controlled by the RIE exposure time. As shown in Figure 1-7, wrinkles with different wavelengths were obtained by increasing the exposure time. This work showed a direct relation between the generated wrinkles wavelength and the thickness of the deposited skin layer. Tunable wavelengths

from 30 to 500 nm were obtained. This approach has the potential to fabricate large area tunable nano wrinkles for optical and electronic applications.

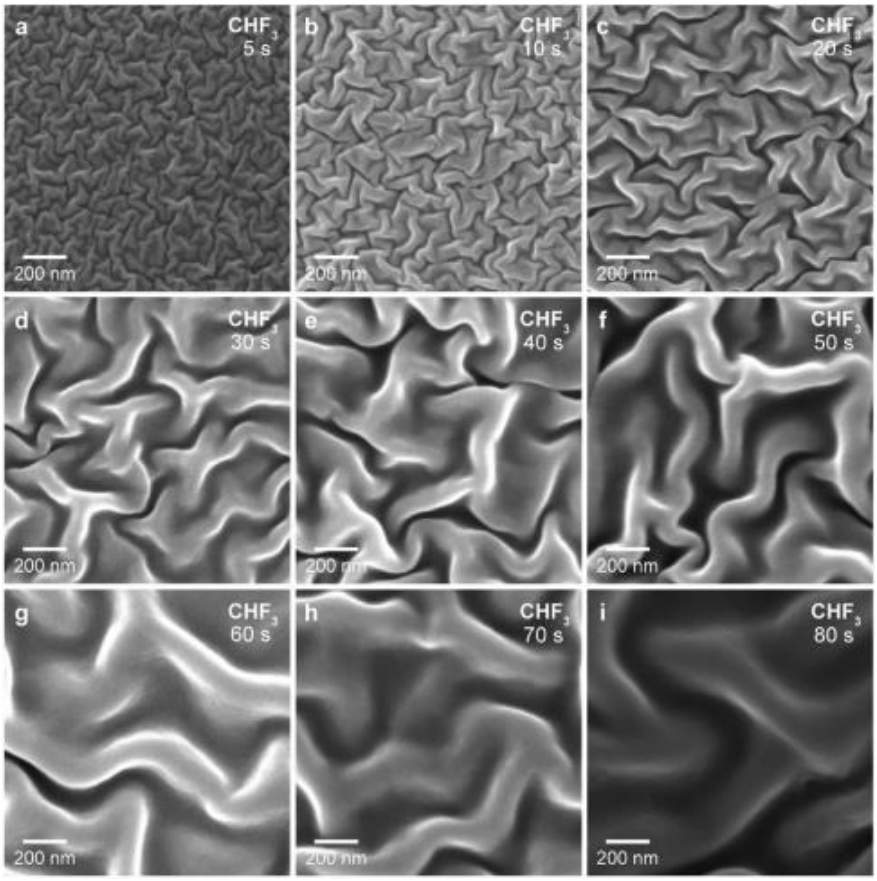

Figure 1-7 Characteristic wavelengths (λ) of PS films tuned by changing the RIE exposure time. SEM images of 2D nano wrinkles formed by RIE with CHF3 and times of (a) 5 s (λ = 34 nm), (b) 10 s (λ = 44 nm), (c) 20 s (λ = 107 nm), (d) 30 s (λ = 162 nm), (e) 40 s (λ = 198 nm), (f) 50 s (λ = 228 nm), (g) 60 s (λ = 303 nm), (h) 70 s (λ = 360 nm), and (i) 80 s (λ = 431 nm).[57]

Uniaxial and biaxial wrinkles were formed on the pre-stressed PS films by changing the boundary constraints during shrinking to allow shrinking in one direction only or in two directions [60]. A thin gold layer was deposited on the PS films to create wrinkles after shrinking. The wrinkles size was controlled by varying the thickness of the deposited gold layer. Figure 1-8 shows the uniaxial and biaxial wrinkles created from buckling of the gold layer. By this simple approach, wrinkles with sizes of 200 nm and 300 nm were created for

the uniaxial and biaxial wrinkles, respectively. Overall, the wrinkles geometry and the corresponding wavelength can be controlled by varying the thickness of the skin layer, the mechanical properties of the base and skin layers, and the applied strain due to shrinking of the pre-stressed shrinkable films.

Although these composite layers produced self generated nanoscale features, they lack control over precise dimensions of features and independent control of spacing and aspect ratio. In addition, over the large area, the patterns may not be exactly identical to each other making them not suitable for microelectronic applications.

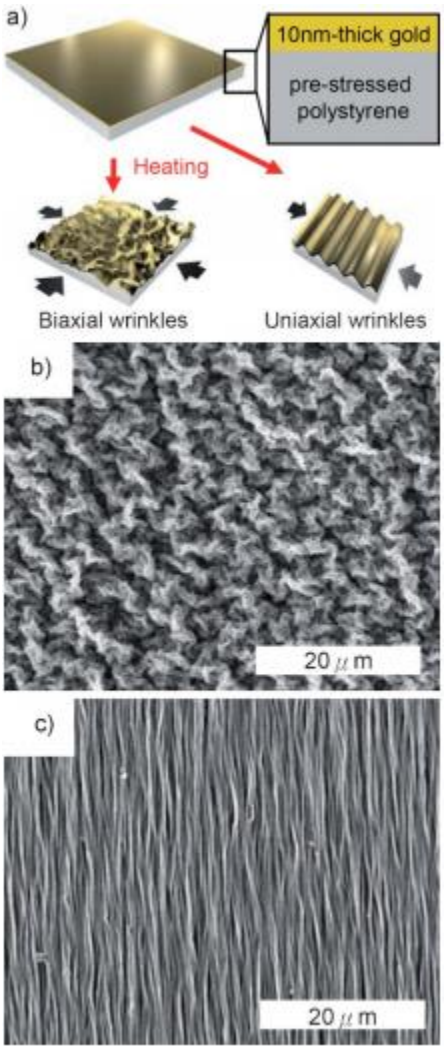

Figure 1-8 Nanowrinkles fabrication. (a) Scheme of fabrication of biaxial and uniaxial wrinkles. SEM images of (b) biaxial wrinkles, and (c) uniaxial wrinkles of a 10 nm gold layer on PS films.[60]

1.2.3 Fundamentals of shape memory polymers (SMPs)

A shape memory polymer (SMP) is a polymer which can be stretched and reshaped into a temporary shape by application of external stress. It has the ability to recover to its original (unstretched) shape when triggered by external stimuli such as heat, light, or chemical [61, 62]. When an external stimulus is applied, shape recovery occurs by releasing the internal stresses. The contraction of SMP during recovery can be programmed as it reverses the mechanical deformation that happened to form the temporary shape [63]. Thermally-

induced SMPs, which are responsive to temperature change, are the most widely used responsive polymers due to the ease of applying and control the temperature change. Recently, thermally-induced shrinking of SMPs was introduced in microfabrication as a facile and rapid strategy to form micro/nano features [13]. It was first reported by Whitesides group to miniaturize pre-defined micro patterns using SMP films [18, 19].

1.2.3.1 Mechanism of thermally-induced shape memory polymers

In order to allow shape memory effect, the polymer should have a suitable molecular architecture which generally consists of molecular switches and netpoints. Additionally, the polymer should have sufficient elasticity to enable deformation. The chain segments must be flexible enough to obtain the required deformability which increases as the length of chains increases. The netpoints are connected by chain segments and they determine the permanent shape of the polymer. The polymer can be recovered to the permanent shape by recoiling of the chain segments which represent the molecular switches [64]. The molecular mechanism of thermally-induced SMP for programming the temporary shape and recovery of the permanent shape is illustrated in Figure 1-9.

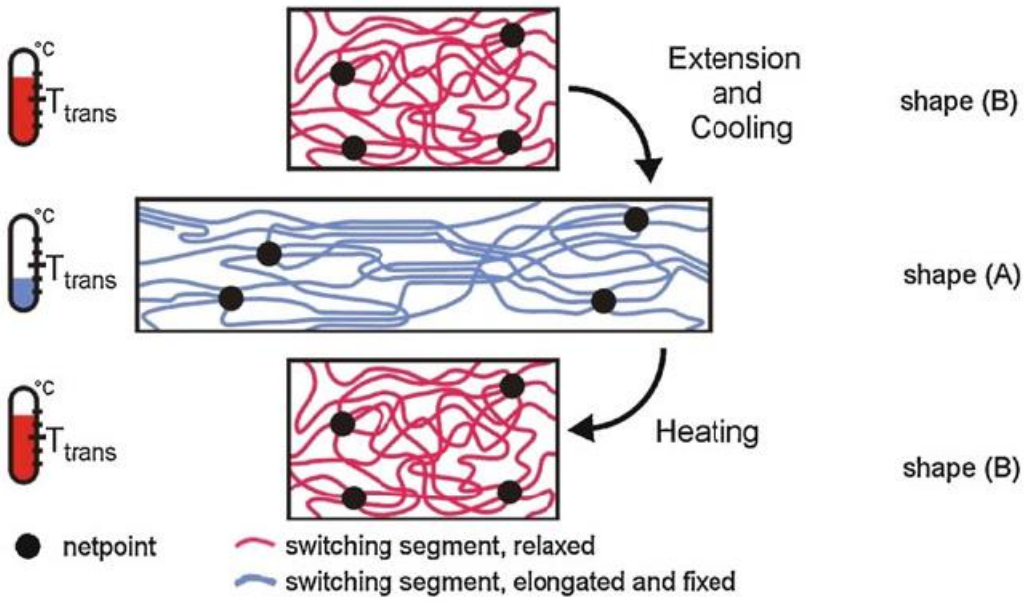

Figure 1-9 Molecular mechanism of thermally-induced SMP. A polymer network with transition temperature $T_{trans} = T_g$.[64]

The transition temperature of the polymer from the glassy state to the rubbery (elastic) state is defined by the glass transition temperature T_g. Below T_g, the polymer is in the glassy state where the movements of the polymer chains are limited. Increasing the temperature above T_g enables the transition to the rubbery state where the chains mobility increases as well as the rotation around chain bonds [14, 65]. This allows polymer chains to form compact random coils where such conformation is entropically favored over the stretched conformation. When an external tensile stress is applied during heating, the polymer chains tend to disentangle and stretch into a temporary shape. This temporary shape can be fixed by cooling down to a temperature under T_g. When the temperature is subsequently raised above T_g, the chains relax again and the mechanical stress in the material is released. This results in forming the entropically favored random coils and recovery of the original shape.

1.2.3.2 Macroscopic thermomechanical mechanism

The shrinkage mechanism of thermally-induced SMPs can be quantified by cyclic testing of thermomechanical behavior. A tensile tester that is equipped with temperature-controlled chamber can be used for the measurements. The important parameters to be determined to characterize shape memory effect are the strain recovery rate (R_r) and the strain fixity rate (R_f) [66]. The strain recovery rate defines the ability of the material to recover to its permanent shape, while the strain fixity rate defines the ability to fix the mechanical deformation of the temporary shape [67]. A schematic illustration of the thermomechanical test results is shown in Figure 1-10. First, the sample is heated to a temperature above the switching temperature and deformed to the maximum strain (ε_m) (step 1). Then, the sample is cooled below the switching temperature while keeping the strain constant at ε_m to obtain the temporary shape (step 2). The sample is unloaded and a stress-free state is achieved, at which the sample is slightly retracted to a strain ε_u (step 3). Finally, the sample is heated again above the switching temperature to allow shape recovery to the permanent shape while leaving a residual strain of ε_p (step 4). The thermomechanical cycle can be started again. For Nth cycle, the strain recovery rate (R_r) and the strain fixity rate (R_f) can be determined as follows:[65]

$$R_r(N) = \frac{\varepsilon_m - \varepsilon_P(N)}{\varepsilon_m - \varepsilon_P(N-1)} \tag{1.1}$$

$$R_f(N) = \frac{\varepsilon_u(N)}{\varepsilon_m} \tag{1.2}$$

It is clear that for an ideal case R_r and R_f should be 100%. However, the achieved temporary shape at stress-free state (ε_u) can be different from the shape at the maximum deformation (ε_m). In addition, after the first cycle the shape does not completely recover to

the original shape (where $\varepsilon_{=0}$) due to the remaining residual strain (ε_p) which determines the permanent shape. Although the first few cycles can be different from each other, the results tend to be more similar at higher number of cycles which allows high reproducibility of the process. This can be explained as during the initial cycles, the polymer chains are rearranged on the molecular scale in a more favorable way with respect to the deformation direction.

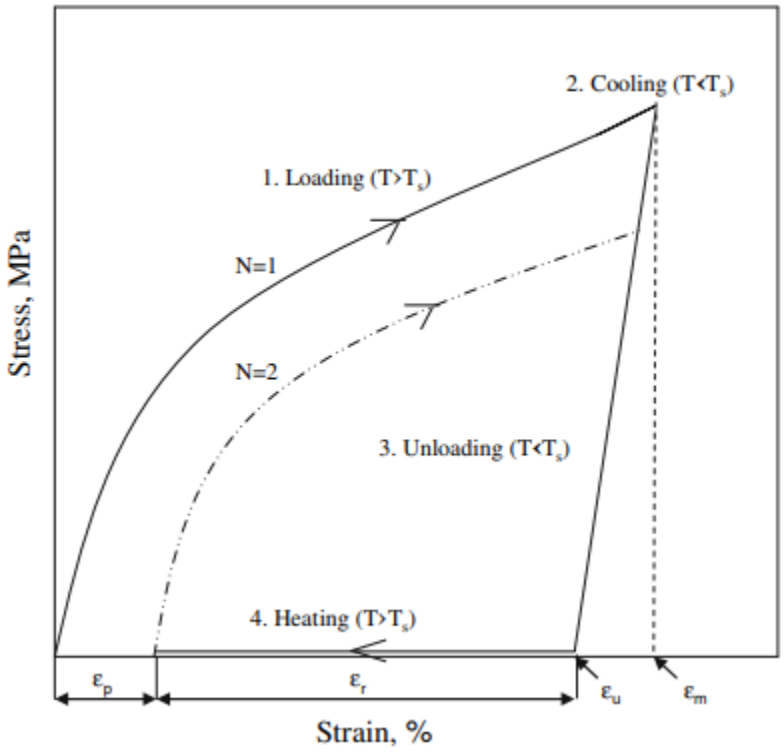

Figure 1-10 Schematic illustration of the cyclic thermomechanical testing.[66]

Another important parameter which cannot be determined by the previous two dimensional measurements is the switching (transition) temperature. Thus, three dimensional measurements including the temperature change are required. This test is performed in a stress-controlled programming cycle where the sample is cooled down under constant stress σ_m. A typical three dimensional test for thermally-induced SMP is shown in Figure 1-11. After stretching to ε_m, the sample is held at this strain for a short

time to allow relaxation of the polymer chains. Then, the sample is cooled at temperature below the switching temperature while the stress is kept constant. The strain is then decreased until achieving the stress-free state. Finally, the sample is heated to allow shape recovery while maintaining constant tensile stress at 0 MPa. During the contraction of the sample, the mechanical movement is recorded as a function of the temperature and hence the transition temperature can be determined. For polystyrene shrinkable films, the glass transition temperature T_g is around 100 ^oC. These films shrink uniformly by 60% in both lateral directions while the thickness increases by 625%.

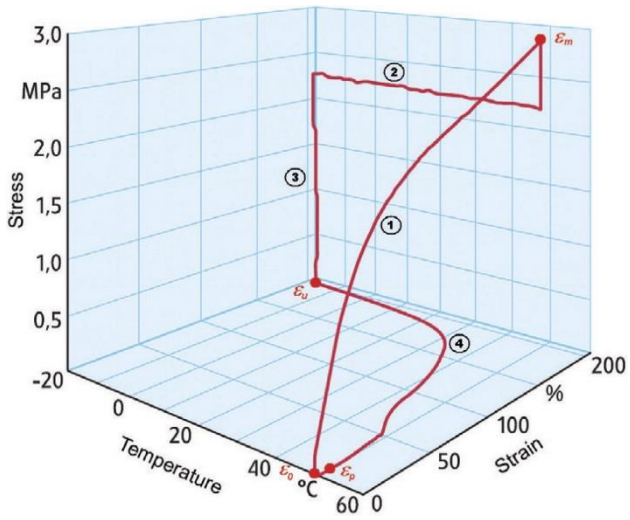

Figure 1-11 Typical stress-strain-temperature diagram for thermally-induced SMP.[64]

1.2.3.3 Modeling of shape memory effect in thermally-induced SMPs

Several models have been developed to predict the shape memory and recovery behavior of the SMPs. They were mainly focusing on the uniaxial deformation but use either mechanical [68-71] or thermodynamic [72, 73] approaches. One of the more common approach is based on modeling the SMP as elastic and viscous units where their properties depend on the temperature change. Based on this approach, a mechanical model was

developed to investigate the stress-strain-time behavior of both stretching the polymer (crosslinked polyethylene) at high temperature and strain recovery [68]. This three-element model consists of a Kelvin unit (spring E and dashpot η_1, in parallel) and a single dashpot η_2 in series ($\eta_2 >> \eta_1$). The mechanical model is shown in Figure 1-12, illustrating the steps of deformation to build up the recovery force and its release to obtain shape recovery. The total deformation was initially transferred to the Kelvin unit. During stress relaxation at cooling step, part of the deformation was gradually transferred from the Kelvin unit to the single dashpot while maintaining the total strain constant. When the model is heated again above transition temperature, shape recovery takes place but not a full recovery. The viscous (irrecoverable) strain can be determined by following the derived equation:

$$\eta_1 \frac{\mathrm{d}\gamma}{\mathrm{d}t} + E\gamma = \sigma_0 \frac{1 + \frac{\eta_1}{\eta_2}}{1 + \frac{\eta_1}{\eta_2} + \frac{t}{\tau}} \tag{1.3}$$

where γ is the strain of the Kelvin unit, t is the holding time, σ_0 is the initial stress before stress relaxation, and τ is the relaxation time of the model ($\tau = \eta_2 / E$).

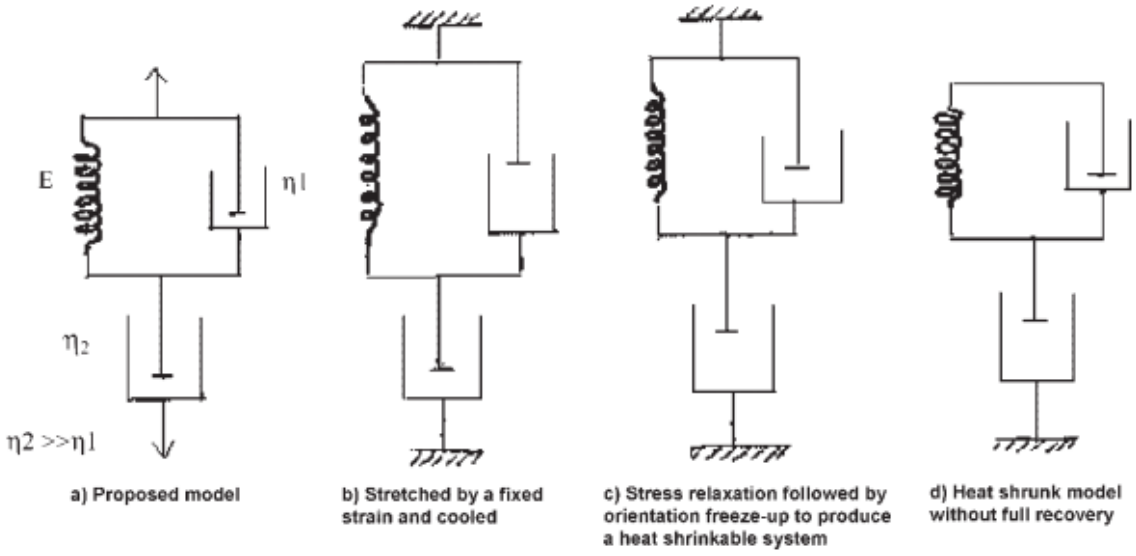

Figure 1-12 Mechanical model for thermally-induced shape memory effect.[68]

This model allowed the prediction of the irrecoverable strain which was mainly related to the stress relaxation which occurs at the holding-cooling time step. It was found that the stress relaxation occurs only during the holding-cooling step before crystallization to fix the temporary shape. If this time is too long, the recovering force is completely released, which results in no shrinkage.

Based on the same mechanical model, the full shape recovery process was investigated by including a temperature dependency to the Kelvin unit (viscosity of η_1) [74] which was useful in exhibiting a temperature dependent recovery that is seen in experiments. Another approach represented the viscoelastic response as the response of a generalized Voigt model [75]. The model was adapted with retardation times and relaxed compliance. The normalized retardation spectrum and limiting compliances were obtained from experimental creep tests and used to predict shape recovery behavior. This model allowed prediction of the temperature of maximum recovery rate and the recovery temperature interval. Hence, it can control the onset and intensity of the recovery transition.

Another modelling approach is based on thermodynamic considerations associated with temperature dependent stress-strain behavior of SMPs. The temperature-dependent behavior of SMPs can be represented by thermodynamic concepts of entropy and internal energy [72]. The shape memory effect is mainly related to the change of entropy during the elastic deformation in the rubbery state that can be stored by transition into glassy state. In the rubbery state (well above the transition temperature), the deformation energy is converted to a change in entropy and the interaction of the polymer chain molecules becomes relatively negligible [76]. In the glassy state (well below transition temperature), the entropic change is fixed due to the limited mobility of individual chains. Any small

strain in the glassy state, where the polymer is assumed to behave as elastic solid, causes a change in internal energy. Thus, the resulting stress due to deformation in the rubbery state is stored and can be only released when heated above the transition temperature to drive the entropic changes.

Based on this general approach, several models were developed by introducing the SMP as a mixture of two phases: a frozen phase controlled by the internal energy and an active soft phase associated with entropy changes [72, 77-79]. The transition of a state is represented by a change of relative volume fractions of the frozen and soft phases while the fraction of one phase is usually used as a state variable. The material parameters are determined by fitting the experimental results and used as inputs to the model. The constitutive equations of the model are then solved to determine the shape memory behavior. Using a two-phase mixture model, shape memory response at small strains for an epoxy resin was investigated in both uniaxial tension and compression [72]. Following the generalized Hooke's law, the constitutive equation of the model was derived as:

$$\sigma = \frac{\varepsilon - \varepsilon_s - \int_{T_h}^{T} \alpha \, \mathrm{d}T}{\frac{\phi_f}{E_i} + \frac{1-\phi_f}{E_e}} = E(\varepsilon - \varepsilon_s - \int_{T_h}^{T} \alpha \, \mathrm{d}T) \tag{1.4}$$

where ϕ_f is the frozen phase fraction $\phi_f = 1 - \frac{1}{1+C_f(T_h - T)^n}$

E is Young's modulus, α is coefficient of thermal expansion, and ε_s is the stored elastic strain in the frozen phase. The two parameters c_f and n in the frozen fraction ϕ_f are determined from experimental tests. This model was able to predict the stress-strain response for small uniaxial strains. In addition, it was used to explore the recovery response under different flexible external constraints.

1.3 Motivation

Despite the many research efforts investigating the use of pre-stressed polymer films in micro/nano fabrication, there are several challenges that prevent the use of current technology for effective and scalable approach to fabricate nanoscale custom designed patterns. As discussed earlier, the resolution was limited to few micrometers. Although some methods were able to generate nanoscale features, the patterns did not shrink proportionally and/or the reduction in size was limited. Developing a new fabrication method that can proportionally miniaturize patterns from tens of micrometers which are easy to fabricate at scale to sub 100 nm dimensions would solve a major challenge in producing nanoscale patterns for microelectronics as well as other applications including sensors and functional surfaces and lab on chip devices. In particular, pre-stressed polymer films tend to lose patterns and features embedded on them in the sub micrometer scale. Overcoming this challenge and scaling the process so that a variety of shapes, features and sizes can be proportionally miniaturized is the main motivation of this thesis. Secondary motivations include characterizing the process and understanding the mechanisms as well as demonstration of control over the process to produce different shapes and sizes by control of process parameters. Finally, this thesis aims to demonstrate the application of this technique in a practical application such as generation of a photonic grating structure. The development of such a method is expected to have a significant impact in microelectronic fabrication, sensors as well as lab on chip devices.

1.4 Research Objectives

The main objective of the thesis is to develop a low-cost, rapid, and scalable micro/nano fabrication technique by using heat shrink materials that can achieve a resolution

comparable to conventional nanolithography methods without the need to use a master fabricated by high resolution nanolithography methods. This approach can be applied to fabricate tunable diffraction gratings and plasmonic structures. This objective was accomplished by achieving the following aims:

1. Developed a new multi-step miniaturization approach that allows iterative shrinking of patterns proportionally to sub-micron resolution using pre-stressed polymer films. It is a low-cost, rapid and scalable fabrication method that can achieve high reduction in size.
2. Discovered and developed a new miniaturization approach by constrained shrinking to enhance and control the shrinking behavior of hot embossed patterns. This approach allows fabrication of nanoscale patterns below 50 nm. Fabrication of tunable plasmonic structures.
3. Extended the new miniaturization approach by constrained shrinking to develop a multi-step miniaturization approach that can achieve nanoscale resolution starting with a master fabricated by a low resolution microfabrication method.

1.5 Thesis outline

Overall, the main results of the thesis have been included in three journal articles. The thesis consists of five chapters. The first chapter introduces the literature review, thesis motivation, objectives and the main contributions. The other chapters are summarized as following:

Chapter 2 introduces a new multi-step miniaturization approach using pre-stressed polymer films that offers a sequential size reduction to fabricate sub-micron patterns. A pattern transfer method was developed by integration of soft imprint lithography and RIE

that allows to use the shrunk patterns from one step as new master for the subsequent miniaturization step without the need of fabricating hard or metal templates. The developed method eliminates defects from one cycle propagating into the next one and hence enables scalable miniaturization. Thus, from a single master, new patterns were created with different smaller feature sizes. Sequential size reduction of different patterns was demonstrated showing a 20x reduction in size of the original patterns, and achieving features as small as 750 nm. The vertical aspect ratio was investigated in order to identify the ratio that is mechanically strong to allow successive miniaturization. In addition, to show that the fabricated patterns are not limited to polymeric materials and can be converted into a functional substrate, the patterns were transferred to a silicon substrate.

Chapter 3 presents the discovery and development of a new miniaturization approach by applying mechanical constraints during shrinking of imprinted pre-stressed films. This miniaturization approach is able to reduce the feature size of the initial imprinted pattern while maintaining the height of pattern. It allows controlling the polymer reflow of not only the in-plane direction but also the out-off plane direction. Thus, the height of the shrunk patterns was preserved instead of vanishing and well-defined patterns were generated. The constrained shrinking overcomes the limitations of using hot embossing with the shrinkable films. Direct shrinking of embossed patterns results in loss of the topographical features due to stress relaxation and flow of material causing a shape memory effect. However, the developed approach was able to generate shrunken nanoscale patterns of sub-50 nm without losing the topographical features. The hot embossing process parameters were optimized by investigating the effect of these parameters on the quality of the imprinted patterns and the effect on the ability of the embossed film to shrink. The

programmability of this approach was demonstrated by fabricating different scale patterns with different feature sizes from the same initial master pattern. Finally, these new capabilities were applied to fabricate tunable and gradient plasmonic structures and hence different optical properties.

Chapter 4 details the development of multi-step miniaturization approach based on the constrained shrinking process to significantly reduce the patterns size from micro to nanoscale without using a master fabricated by nanolithography methods. Thus, it overcomes the limitations of fabricating nanoscale master molds which often involves using expensive and time consuming processes. This approach allows using the miniaturized pattern to fabricate a new master which was then used as a master for the next miniaturization cycle. This powerful approach reduced the patterns size by 10x over three cycles, and generated high resolution patterns as small as 100 nm. In addition, the aspect ratio of the features can be maintained even after shrinking multiple times which improves the pattern fidelity. The developed approach can be used to fabricate masters for nanoimprint lithography.

Chapter 5 summarizes all achievements in this thesis and the research contributions. Finally, recommendations for the future work are discussed.

References

[1] S. Sreenivasan, "Nanoimprint lithography steppers for volume fabrication of leading-edge semiconductor integrated circuits," *Microsystems & nanoengineering,* vol. 3, pp. 1-19, 2017.

[2] E. M. Sebastian, S. K. Jain, R. Purohit, S. Dhakad, and R. Rana, "Nanolithography and its current advancements," *Materials Today: Proceedings,* vol. 26, pp. 2351-2356, 2020.

[3] D. P. Sanders, "Advances in patterning materials for 193 nm immersion lithography," *Chemical reviews,* vol. 110, pp. 321-360, 2010.

[4] N. Liaros and J. T. Fourkas, "Ten years of two-color photolithography," *Optical Materials Express,* vol. 9, pp. 3006-3020, 2019.

[5] L. Bruchhaus, P. Mazarov, L. Bischoff, J. Gierak, A. Wieck, and H. Hövel, "Comparison of technologies for nano device prototyping with a special focus on ion beams: A review," *Applied Physics Reviews,* vol. 4, p. 011302, 2017.

[6] A. Cattoni, D. Mailly, O. Dalstein, M. Faustini, G. Seniutinas, B. Rösner, and C. David, "Sub-10 nm electron and helium ion beam lithography using a recently developed alumina resist," *Microelectronic Engineering,* vol. 193, pp. 18-22, 2018.

[7] P. van Assenbergh, E. Meinders, J. Geraedts, and D. Dodou, "Nanostructure and microstructure fabrication: from desired properties to suitable processes," *Small,* vol. 14, p. 1703401, 2018.

[8] M. Roeder, T. Guenther, and A. Zimmermann, "Review on fabrication technologies for optical mold inserts," *Micromachines,* vol. 10, p. 233, 2019.

[9] H. Lan and H. Liu, "UV-nanoimprint lithography: structure, materials and fabrication of flexible molds," *Journal of nanoscience and nanotechnology,* vol. 13, pp. 3145-3172, 2013.

[10] H. Matsumoto, H. Inoue, H. Yamashita, H. Morita, S. Hirose, M. Ogasawara, H. Yamada, and K. Hattori, "Multi-beam mask writer MBM-1000 and its application field," in *Photomask Japan 2016: XXIII Symposium on Photomask and Next-Generation Lithography Mask Technology,* 2016, p. 998405.

[11] P. J. Goodrich, F. Sharifi, and N. Hashemi, "Rapid prototyping of microchannels with surface patterns for fabrication of polymer fibers," *RSC Advances,* vol. 5, pp. 71203-71209, 2015.

[12] A. Yokoo, K. Wada, and L. C. Kimerling, "Pattern size reduction of nanoprint-fabricated structures on heat-shrinkable film," *Japanese Journal of Applied Physics,* vol. 46, p. 6395, 2007.

[13] S. Lin, E. K. Lee, N. Nguyen, and M. Khine, "Thermally-induced miniaturization for micro-and nanofabrication: progress and updates," *Lab on a Chip,* vol. 14, pp. 3475-3488, 2014.

[14] A. Lendlein, *Shape-memory polymers* vol. 226: Springer, 2010.

[15] J. Hu, Y. Zhu, H. Huang, and J. Lu, "Recent advances in shape–memory polymers: Structure, mechanism, functionality, modeling and applications," *Progress in Polymer Science,* vol. 37, pp. 1720-1763, 2012.

[16] P. T. Mather, X. Luo, and I. A. Rousseau, "Shape memory polymer research," *Annual Review of Materials Research,* vol. 39, pp. 445-471, 2009.

[17] W. Small IV, P. Singhal, T. S. Wilson, and D. J. Maitland, "Biomedical applications of thermally activated shape memory polymers," *Journal of materials chemistry,* vol. 20, pp. 3356-3366, 2010.

[18] X.-M. Zhao, Y. Xia, O. J. Schueller, D. Qin, and G. M. Whitesides, "Fabrication of microstructures using shrinkable polystyrene films," *Sensors and Actuators A: Physical,* vol. 65, pp. 209-217, 1998.

[19] X. M. Zhao, Y. Xia, D. Qin, and G. M. Whitesides, "Fabrication of polymeric microstructures with high aspect ratios using shrinkable polystyrene films," *Advanced materials,* vol. 9, pp. 251-254, 1997.

[20] X. Zhu and T. Cui, "Polymer shrinkage of hot embossed microstructures for higher aspect ratio and smaller size," *Sensors and Actuators A: Physical,* vol. 195, pp. 21-26, 2013.

[21] H. Yabu and M. Shimomura, "Miniaturization of surface patterns by combination of contact etching lithography and multi-step shrinking of stretched polymer films," *Polymer journal,* vol. 40, p. 534, 2008.

[22] M. H. Lee, M. D. Huntington, W. Zhou, J.-C. Yang, and T. W. Odom, "Programmable soft lithography: solvent-assisted nanoscale embossing," *Nano letters,* vol. 11, pp. 311-315, 2010.

[23] D. Dyer, S. Shreim, S. Jayadev, V. Lew, E. Botvinick, and M. Khine, "Sequential shrink photolithography for plastic microlens arrays," *Applied Physics Letters,* vol. 99, p. 034102, 2011.

[24] U. Manna, M. C. Carter, and D. M. Lynn, "“Shrink-to-Fit” Superhydrophobicity: Thermally-Induced Microscale Wrinkling of Thin Hydrophobic Multilayers Fabricated on Flexible Shrink-Wrap Substrates," *Advanced materials,* vol. 25, pp. 3085-3089, 2013.

[25] S. J. Park, J. Kim, M. Chu, and M. Khine, "Flexible piezoresistive pressure sensor using wrinkled carbon nanotube thin films for human physiological signals," *Advanced Materials Technologies,* vol. 3, p. 1700158, 2018.

[26] J. D. Pegan, A. Y. Ho, M. Bachman, and M. Khine, "Flexible shrink-induced high surface area electrodes for electrochemiluminescent sensing," *Lab on a Chip,* vol. 13, pp. 4205-4209, 2013.

[27] L. R. Freschauf, J. McLane, H. Sharma, and M. Khine, "Shrink-induced superhydrophobic and antibacterial surfaces in consumer plastics," *PLoS One,* vol. 7, 2012.

[28] C. Wagner and N. Harned, "Lithography gets extreme," *Nature Photonics,* vol. 4, pp. 24-26, 2010.

[29] A. Lio, "EUV resists: What's next?," in *Extreme Ultraviolet (EUV) Lithography VII*, 2016, p. 97760V.

[30] A. Sarangan, *Nanofabrication: Principles to Laboratory Practice*: CRC Press, 2016.

[31] W. Hinsberg, G. M. Wallraff, C. E. Larson, B. W. Davis, V. Deline, S. Raoux, D. Miller, F. A. Houle, J. Hoffnagle, and M. I. Sanchez, "Liquid immersion lithography: evaluation of resist issues," in *Advances in Resist Technology and Processing XXI*, 2004, pp. 21-33.

[32] N. Fu, Y. Liu, X. Ma, and Z. Chen, "EUV lithography: state-of-the-art review," *J. Microelectron. Manuf,* vol. 2, pp. 1-6, 2019.

[33] A. Pimpin and W. Srituravanich, "Review on micro-and nanolithography techniques and their applications," *Engineering Journal,* vol. 16, pp. 37-56, 2012.

[34] M. Altissimo, "E-beam lithography for micro-/nanofabrication," *Biomicrofluidics,* vol. 4, p. 026503, 2010.

[35] D. Wagner and A. Jayatissa, "Nanoimprint lithography: Review of aspects and applications," in *Nanofabrication: Technologies, Devices, and Applications II*, 2005, p. 60020R.

[36] S. J. Park, J. Kim, M. Chu, and M. Khine, "Highly flexible wrinkled carbon nanotube thin film strain sensor to monitor human movement," *Advanced Materials Technologies,* vol. 1, p. 1600053, 2016.

[37] K. Takashima, H. Kamizono, M. Takenaka, and T. Mukai, "Force sensor utilizing stiffness change of shape-memory polymer based on temperature," *ROBOMECH Journal,* vol. 4, pp. 1-8, 2017.

[38] F. Greco, L. Ventrelli, P. Dario, B. Mazzolai, and V. Mattoli, "Micro-wrinkled palladium surface for hydrogen sensing and switched detection of lower flammability limit," *International journal of hydrogen energy,* vol. 37, pp. 17529-17539, 2012.

[39] S. Schauer, R. Schmager, R. Hünig, K. Ding, U. W. Paetzold, U. Lemmer, M. Worgull, H. Hölscher, and G. Gomard, "Disordered diffraction gratings tailored by shape-memory based wrinkling and their application to photovoltaics," *Optical Materials Express,* vol. 8, pp. 184-198, 2018.

[40] Z. Li, R. Sun, M. A. Rahman, J. Feng, A. Olah, and E. Baer, "Scaling effects on the optical properties of patterned nano-layered shape memory films," *Polymer,* vol. 167, pp. 182-192, 2019.

[41] M. Long, M. A. Sprague, A. A. Grimes, B. D. Rich, and M. Khine, "A simple three-dimensional vortex micromixer," *Applied Physics Letters,* vol. 94, p. 133501, 2009.

[42] S. Sonney, N. Shek, and J. M. Moran-Mirabal, "Rapid bench-top fabrication of poly (dimethylsiloxane)/polystyrene microfluidic devices incorporating high-surface-area sensing electrodes," *Biomicrofluidics,* vol. 9, p. 026501, 2015.

[43] D. Nawarathna, N. Norouzi, J. McLane, H. Sharma, N. Sharac, T. Grant, A. Chen, S. Strayer, R. Ragan, and M. Khine, "Shrink-induced sorting using integrated nanoscale magnetic traps," *Applied Physics Letters,* vol. 102, p. 063504, 2013.

[44] J. Yoon, Y. An, S. B. Hong, J. H. Myung, J. Y. Sun, and W. R. Yu, "Fabrication of a Highly Stretchable, Wrinkle-Free Electrode with Switchable Transparency Using a Free-Standing Silver Nanofiber Network and Shape Memory Polymer Substrate," *Macromolecular Rapid Communications,* p. 2000129, 2020.

[45] N. Unno, S.-i. Satake, and J. Taniguchi, "Super-resolution technique for nanoimprint mold using elastic UV-curable resin," *Microelectronic Engineering,* vol. 110, pp. 167-172, 2013.

[46] Y. Xia and G. M. Whitesides, "Extending microcontact printing as a microlithographic technique," *Langmuir,* vol. 13, pp. 2059-2067, 1997.

[47] B. Zhang, M. Zhang, and T. Cui, "Low-cost shrink lithography with sub-22 nm resolution," *Applied Physics Letters,* vol. 100, p. 133113, 2012.

[48] A. Grimes, D. N. Breslauer, M. Long, J. Pegan, L. P. Lee, and M. Khine, "Shrinky-Dink microfluidics: rapid generation of deep and rounded patterns," *Lab on a Chip,* vol. 8, pp. 170-172, 2008.

[49] D. Nguyen, J. McLane, V. Lew, J. Pegan, and M. Khine, "Shrink-film microfluidic education modules: Complete devices within minutes," *Biomicrofluidics,* vol. 5, p. 022209, 2011.

[50] K. Sollier, C. A. Mandon, K. A. Heyries, L. J. Blum, and C. A. Marquette, "“Print-n-Shrink” technology for the rapid production of microfluidic chips and protein microarrays," *Lab on a Chip,* vol. 9, pp. 3489-3494, 2009.

[51] D. Nguyen, D. Taylor, K. Qian, N. Norouzi, J. Rasmussen, S. Botzet, M. Lehmann, K. Halverson, and M. Khine, "Better shrinkage than shrinky-dinks," *Lab on a Chip,* vol. 10, pp. 1623-1626, 2010.

[52] J. Genzer and J. Groenewold, "Soft matter with hard skin: From skin wrinkles to templating and material characterization," *Soft Matter,* vol. 2, pp. 310-323, 2006.

[53] B. Li, Y.-P. Cao, X.-Q. Feng, and H. Gao, "Mechanics of morphological instabilities and surface wrinkling in soft materials: a review," *Soft Matter,* vol. 8, pp. 5728-5745, 2012.

[54] S. Yang, K. Khare, and P. C. Lin, "Harnessing surface wrinkle patterns in soft matter," *Advanced Functional Materials,* vol. 20, pp. 2550-2564, 2010.

[55] C. Cao, H. F. Chan, J. Zang, K. W. Leong, and X. Zhao, "Harnessing localized ridges for high-aspect-ratio hierarchical patterns with dynamic tunability and multifunctionality," *Advanced materials,* vol. 26, pp. 1763-1770, 2014.

[56] J. Zang, X. Zhao, Y. Cao, and J. W. Hutchinson, "Localized ridge wrinkling of stiff films on compliant substrates," *Journal of the Mechanics and Physics of Solids,* vol. 60, pp. 1265-1279, 2012.

[57] M. D. Huntington, C. J. Engel, A. J. Hryn, and T. W. Odom, "Polymer nanowrinkles with continuously tunable wavelengths," *ACS applied materials & interfaces,* vol. 5, pp. 6438-6442, 2013.

[58] T. Ohzono and M. Shimomura, "Geometry-dependent stripe rearrangement processes induced by strain on preordered microwrinkle patterns," *Langmuir,* vol. 21, pp. 7230-7237, 2005.

[59] K. Efimenko, M. Rackaitis, E. Manias, A. Vaziri, L. Mahadevan, and J. Genzer, "Nested self-similar wrinkling patterns in skins," *Nature materials,* vol. 4, pp. 293-297, 2005.

[60] C. C. Fu, A. Grimes, M. Long, C. G. Ferri, B. D. Rich, S. Ghosh, S. Ghosh, L. P. Lee, A. Gopinathan, and M. Khine, "Tunable nanowrinkles on shape memory polymer sheets," *Advanced materials,* vol. 21, pp. 4472-4476, 2009.

[61] E. S. Gil and S. M. Hudson, "Stimuli-reponsive polymers and their bioconjugates," *Progress in Polymer Science,* vol. 29, pp. 1173-1222, 2004.

[62] A. Lendlein, H. Jiang, O. Jünger, and R. Langer, "Light-induced shape-memory polymers," *Nature,* vol. 434, pp. 879-882, 2005.

[63] G. Li and W. Xu, "Thermomechanical behavior of thermoset shape memory polymer programmed by cold-compression: testing and constitutive modeling," *Journal of the Mechanics and Physics of Solids,* vol. 59, pp. 1231-1250, 2011.

[64] M. Behl and A. Lendlein, "Shape-memory polymers," *Materials Today,* vol. 10, pp. 20-28, 2007.

[65] A. Lendlein and S. Kelch, "Shape-memory polymers," *Angewandte Chemie International Edition,* vol. 41, pp. 2034-2057, 2002.

[66] D. Ratna and J. Karger-Kocsis, "Recent advances in shape memory polymers and composites: a review," *Journal of Materials Science,* vol. 43, pp. 254-269, 2008.

[67] B. K. Kim, S. Y. Lee, and M. Xu, "Polyurethanes having shape memory effects," *Polymer,* vol. 37, pp. 5781-5793, 1996.

[68] J. Morshedian, H. A. Khonakdar, and S. Rasouli, "Modeling of shape memory induction and recovery in heat-shrinkable polymers," *Macromolecular theory and simulations,* vol. 14, pp. 428-434, 2005.

[69] G. Barot and I. Rao, "Constitutive modeling of the mechanics associated with crystallizable shape memory polymers," *Zeitschrift für angewandte Mathematik und Physik ZAMP,* vol. 57, pp. 652-681, 2006.

[70] H. Tobushi, T. Hashimoto, S. Hayashi, and E. Yamada, "Thermomechanical constitutive modeling in shape memory polymer of polyurethane series," *Journal of intelligent material systems and structures,* vol. 8, pp. 711-718, 1997.

[71] K. Yu, H. Li, A. J. McClung, G. P. Tandon, J. W. Baur, and H. J. Qi, "Cyclic behaviors of amorphous shape memory polymers," *Soft Matter,* vol. 12, pp. 3234-3245, 2016.

[72] Y. Liu, K. Gall, M. L. Dunn, A. R. Greenberg, and J. Diani, "Thermomechanics of shape memory polymers: uniaxial experiments and constitutive modeling," *International Journal of Plasticity,* vol. 22, pp. 279-313, 2006.

[73] J. Diani, Y. Liu, and K. Gall, "Finite strain 3D thermoviscoelastic constitutive model for shape memory polymers," *Polymer Engineering & Science,* vol. 46, pp. 486-492, 2006.

[74] H. A. Khonakdar, S. H. Jafari, S. Rasouli, J. Morshedian, and H. Abedini, "Investigation and modeling of temperature dependence recovery behavior of shape-memory crosslinked polyethylene," *Macromolecular theory and simulations,* vol. 16, pp. 43-52, 2007.

[75] C. Buckley, C. Prisacariu, and A. Caraculacu, "Novel triol-crosslinked polyurethanes and their thermorheological characterization as shape-memory materials," *Polymer,* vol. 48, pp. 1388-1396, 2007.

[76] I. M. Ward and D. W. Hadley, *An introduction to the mechanical properties of solid polymers*, 1993.

[77] H. J. Qi, T. D. Nguyen, F. Castro, C. M. Yakacki, and R. Shandas, "Finite deformation thermo-mechanical behavior of thermally induced shape memory polymers," *Journal of the Mechanics and Physics of Solids,* vol. 56, pp. 1730-1751, 2008.

[78] Y.-C. Chen and D. C. Lagoudas, "A constitutive theory for shape memory polymers. Part I: large deformations," *Journal of the Mechanics and Physics of Solids*, vol. 56, pp. 1752-1765, 2008.

[79] Q. Yang and G. Li, "Temperature and rate dependent thermomechanical modeling of shape memory polymers with physics based phase evolution law," *International Journal of Plasticity,* vol. 80, pp. 168-186, 2016.

2 Chapter 2

Multi-step Proportional Miniaturization to Sub-Micron Dimensions Using Pre-stressed Polymer Films

Complete Citation:

S. Sayed and P. R. Selvaganapathy, "Multi-step proportional miniaturization to sub-micron dimensions using pre-stressed polymer films," *Nanoscale Advances,* vol. 2, pp. 5461-5467, 2020.

Copyright:

Contribution:

S. Sayed: Designed and performed all experiments, interpretation and analysis of data, wrote the manuscript draft.

P. R. Selvaganapathy: Supervised S. Sayed and provided guidance, revised and edited the manuscript, was responsible for the manuscript submission.

2.1 Abstract

The ability to define patterns and fabricate structures at the nanoscale in a scalable manner is crucial not only in integrated circuit fabrication but also in fabrication of nanofluidic devices as well as in nano and micromechanical systems. Top down fabrication at the nanoscale often involves fabrication of a master using a direct write method and then its replication using a variety of methods such as by hot embossing, nanoimprint lithography, or soft lithography. Nevertheless, fabrication of the master is a time consuming and expensive process. One interesting approach is to define patterns at larger dimensions on pre-stressed films using methods such as xurography or lithography which are scalable and heat them to de-stress and shrink which can reduce the size proportionally. Although attractive, suitable fabrication processes that can perform iterative shrinking of patterns over several cycles and into the nanoscale have not been demonstrated. Here, we demonstrate a fabrication process that is capable of accurately producing patterns and features over several cycles of miniaturization and shrinking to achieve resolution in the order of 100s of nanometers. In this approach, a pattern transfer method is developed by combining soft imprint lithography followed by reactive ion etching, both of which are scalable processes, to transfer the original patterns into a shrinkable polymer film. The patterned shrinkable film is heated to allow thermal shrinking. As a result, the pattern size was decreased by 60% of the original size in a single cycle. This reduced pattern was used as the master for the next cycle and three cycles of miniaturization was demonstrated. Sub-micron patterns of 750 nm were generated by the multi-step miniaturization method, showing approximately 20x reduction in size of the original patterns. Finally, these patterns are transferred into features on a silicon substrate to demonstrate its application in

semiconductor microfabrication or its use as a master template for microsystems applications.

2.2 Introduction

Fabrication of patterns and features in the nanoscale is important in many applications such as microelectronics, photonics, nanosystems and nanofluidics. Methods such as photolithography [1], nano imprint lithography [2] and soft lithography [3] exist for production of such patterns but require an expensively produced mask [4] or master mold which are often made using direct write approaches such as electron beam lithography or focused ion beam lithography [5] that consume a significant amount of time to produce complex and intricate features. An alternate process that can simplify production of mask patterns or master molds in a low cost, scalable manner can be effective in reducing the cost and complexity associated with nanofabrication.

One approach that has been investigated is to define patterns in the scale of hundreds of micrometers on pre-stressed, mechanically stretched polymeric films and to proportionally reduce their feature sizes by using a thermal trigger that relaxes the internal stresses and shrinks the film to dimensions that are a few tens of micrometers [6-8]. When these stretched polymer films are heated slightly above the glass transition temperature, the polymer reflows just enough to release the compressive stresses embedded in it which tends to recover to its original shape and up to 77% reduction in size is possible. When the shrinkable films are patterned, these patterns also tend to shrink in dimension when the entire film is exposed to the heat trigger and relaxes.

Many different methods including reactive ion etching (RIE) [9], hot embossing [10], and contact etching lithography [11] have been used to embed the pattern directly on

to the heat shrink film itself. Although these methods have been used to miniaturize patterns, they are unsuitable for repeated operation where the shrunk pattern itself is used as a master for the next cycle to enable their continued miniaturization into sub micrometer dimensions. For instance, the use of hot embossing and contact lithography produce shrunk patterns that have much lower aspect ratio than the original master which leads to loss of resolution in the next cycle. RIE patterns typically are generated using hard metal masks that are difficult to produce from the shrunk patterns generated from them for continued miniaturization.

Alternatively, soft lithography [12], and photolithography [13] have been used to pattern other materials on top of the heat shrink films which can enable miniaturization of such patterns. The limitation of this method is that the presence of another material can restrict the miniaturization of that region while the space between the patterns are miniaturized. Therefore, proportional miniaturization of the feature and the spacing between them is not possible.

In general, existing methods are suited for a single step miniaturization where the existing pattern is reduced by 30-70% of its original size. However, they are not ideally suited for a multi cycle miniaturization process where the shrunk pattern from the previous cycle can be used as a master for the next cycle for scalable miniaturization to sub micrometer and nanometer dimensions.

Here, we report a scalable miniaturization approach using heat shrinkable Polystyrene (PS) films that generates a proportionally miniaturized pattern which can in-turn be used as master for the next cycle of miniaturization. We demonstrate that this approach can be used multiple times to fabricate sub-micron patterns. Proportional

reduction in dimensional features of 20 times were demonstrated over three cycles of miniaturization. Starting from 15 µm features of the master, patterns as small as 750 nm were fabricated. We applied this new capability to fabricate patterns in a silicon wafer that can be used as a functional substrate for many applications such as diffraction grating based sensors [14, 15] or as a master template for soft lithography applications [16, 17].

2.3 Experimental

A multi-step miniaturization approach was developed that can be used repeatedly to produce patterns that are progressively smaller than the patterns in the previous step for scalable and continued miniaturization. A schematic illustration of the multi-step miniaturization process is shown in Figure 2-1. First, the original master pattern substrate was fabricated lithographically by patterning a photoresist (Microposit S1827) coated on a silicon wafer. Although lithography was used here, the master can be fabricated by other methods such as laser machining or xurography as well. Two different patterns were fabricated, namely: line-space pattern with line width of 15 µm and pillars pattern of 15 µm diameter. These dimensions are easy to produce using a variety of microscale patterning methods and hence were chosen. Then, an elastomer, poly(dimethylsiloxane) (PDMS, Sylgard 184, Dow Corning), was molded on the fabricated master by replica molding to be used as a master template. A photoresist (AZ-MIR 701) was spin-coated on the heat shrinkable Polystyrene film (Grafix) at 2000 rpm for 15 seconds, which ensured that the photoresist was uniformly distributed but still wet (Figure 2-1a). By soft imprint lithography, the PDMS mold was placed immediately on the coated photoresist to stamp it and transfer the pattern on to the photoresist layer (Figure 2-1b). The patterned photoresist was used as a mask in the subsequent RIE process (Figure 2-1c). The PDMS mold was

held in place for 10 min at room temperature to allow the photoresist to dry and then carefully removed. After patterning the photoresist, the sample was exposed to an O_2 plasma in a RIE chamber (Technics) (power 100 W, flow rate 16 sccm, pressure 210 mTorr) for 18-25 min. Both of the photoresist mask and the heat shrinkable film were etched which leads to transfer the pattern into the shrinkable film itself.

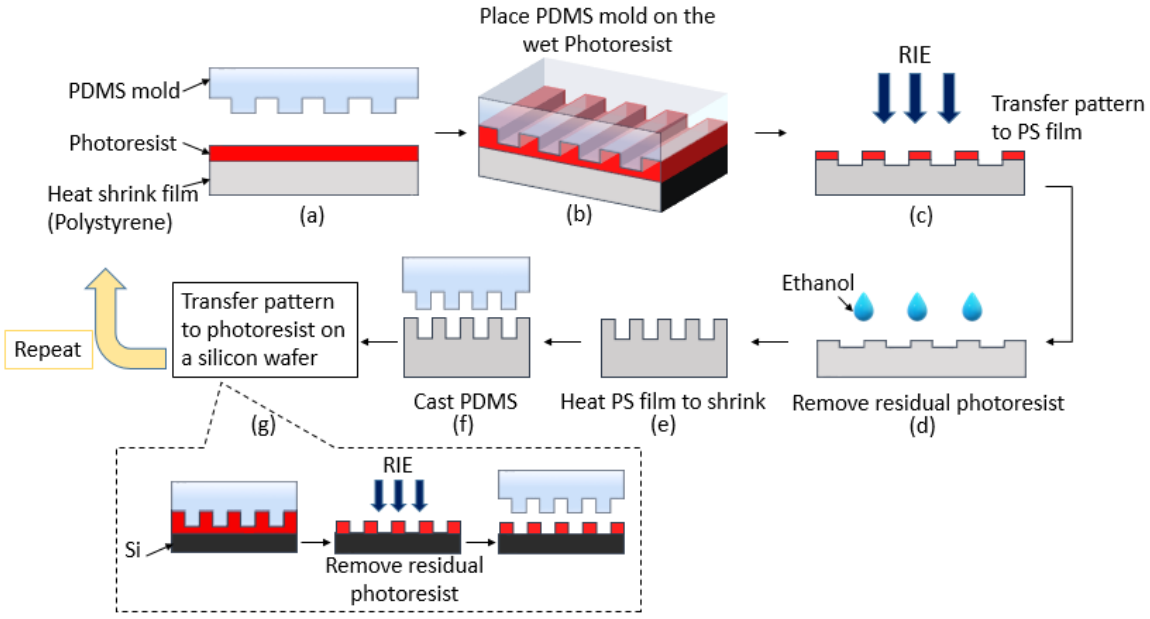

Figure 2-1 Schematic illustration of the multi-step miniaturization process using heat shrinkable films.

The remaining photoresist was removed by a quick rinse with ethanol followed by deionized water (Figure 2-1d). The PS film was heated in an oven at 135 ^{o}C for 15 min which allows it to thermally shrink by approximately 60% of the original size (Figure 2-1e). PDMS was cast onto the shrunk pattern to form a mold that was used as a new template for further miniaturization steps (Figure 2-1f). To improve the surface finish of the generated pattern which has a significant effect on the fidelity of the subsequent miniaturization steps, a silicon wafer coated with a photoresist was patterned by same soft imprint lithography process using the PDMS mold formed from the shrunk pattern (Figure

2-1g). Then the residual photoresist layer was etched by O_2 plasma RIE leaving behind clean and smooth Si surface in the regions where the photoresist pattern was not present. PDMS was then cast on this pattern to form the PDMS mold which was used for the next miniaturization step.

The combination of soft imprint lithography, reactive ion etching of heat shrinkable films as well as the use of the intermediate Si-photoresist hybrid mold, makes it possible to use the shrunk patterns of the previous step as a new master for the next step in a multi-step miniaturization that can be repeated multiple times to obtain nanoscale resolution. Thus, from a single master pattern, different smaller size patterns can be fabricated.

2.4 Results and Discussion

2.4.1 Multi-step Miniaturization Process

Pre-stressed polymer films have been used to demonstrate single step miniaturization of patterns. Previous attempts at multi step miniaturization have led to loss of resolution and fidelity after the 1st or the 2nd steps [7, 11]. Therefore, in order to demonstrate the scalability of the newly established process (Figure 2-1), a three step miniaturization sequence was used to show that large line patterns can be reduced to sub micrometer dimension. The initial master (Figure 2-2a) was fabricated lithographically as a line pattern with 15 µm line width and 30 µm spacing. These dimensions were chosen as they are easily achievable by low cost methods such as laser writing or 3D printing using stereolithography methods. This pattern was successively miniaturized three times with the final shrunk pattern of the previous step serving as the master mold for the next step to reduce the final dimension to 750 nm line width which is a 20x reduction in size of the original pattern. SEM images were taken at each step which are shown in Figure 2-2 (a-e).

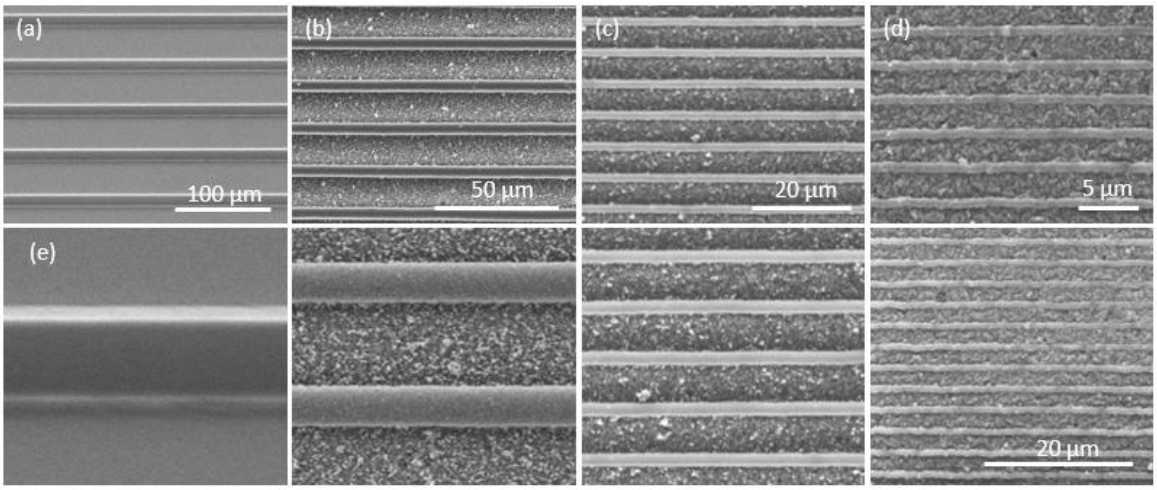

Figure 2-2 SEM images of the line-space pattern (a) master pattern (line-width w=15µm, spacing s=30µm), (b) first step miniaturization (w=5.4µm, s=11µm), (c) second step (w=2µm, s=4.5µm), (d) third step (w=0.75µm, s=1.9µm), (e) the master and three miniaturization steps at same magnification.

After the first miniaturization step (Figure 2-2b) the line width reduces to 5.4 µm (64% reduction) and the spacing to 11 µm. After the second step (Figure 2-2c), the line width reduces further to 2 µm (63% reduction) and the spacing to 4.5 µm. Finally, after the third step (Figure 2-2d), the line width reduces to 750 nm (62.5% reduction) and the spacing to 1.9 µm. It is interesting to note that the fidelity of the pattern is retained even when its size is reduced by ~ 20x to sub micrometer dimensions. Also, the original ratio of 0.5 (line width to spacing) was found to be maintained after the first step at 0.49 while it reduced to 0.44 and 0.4 in the subsequent steps.

These results align with the expected behavior of these pre-stressed films which shrink by 60-65% in both the lateral directions. The design of the fabrication process such that the shrunk pattern of one step can be used as the master of the next can be used to progressively achieve smaller and smaller patterns without any expensive equipment. The

fidelity of the pattern has been shown to be maintained throughout the successive miniaturization step.

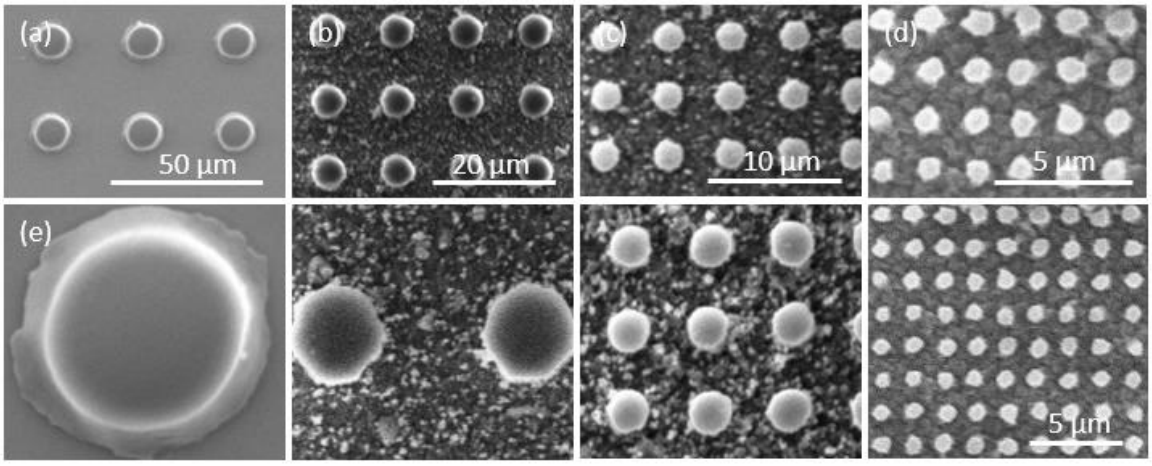

Figure 2-3 SEM images of the pillars pattern (a) master pattern (diameter d=14.5µm, spacing s=15.5µm), (b) first step miniaturization (d=5.5µm, s=5.8µm), (c) second step (d=2.2µm, s=2.3µm), (d) third step (d=0.86µm, s=0.9µm), (e) the master and three miniaturization steps at same magnification.

In order to show that the fabrication process can also be used to create features other than line patterns, a pillar array pattern was also microfabricated using the multi-step miniaturization process. The initial master (Figure 2-3a) was a pillar pattern with 14.5 µm diameter and 15.5 µm spacing which was fabricated lithographically. Using the same multi-step miniaturization process, this was reduced in size over three steps. SEM images were taken at each step which are shown in Figure 2-3 (a-e). After the first miniaturization step (Figure 2-3b) the diameter reduced to 5.5 µm (62% reduction) and the spacing to 5.8 µm. After the second step (Figure 2-3c), the diameter reduced further to 2.2 µm (60% reduction) and the spacing to 2.3 µm. Finally, after the third step (Figure 2-3d), the diameter reduced to 860 nm (61% reduction) and the spacing to 900 nm. The fidelity of the pattern is retained over the three miniaturization cycles. In addition, the original ratio of 0.935 (diameter to spacing) was found to be slightly increased after the first step to 0.95 while it

maintained constant at 0.955 in the subsequent steps. The results show that smaller size patterns can be generated from a single master and can be applied to different shape features.

2.4.2 Eliminating Surface Roughness Accumulation in Each Step

One of the challenges in a multi-step miniaturization process is that defects that originate in earlier steps accumulate in subsequent steps and leads quickly to loss of fidelity. This effect is particularly important in miniaturization of patterns using pre-stressed films and has led to previous attempts being restricted to only two steps or to large feature sizes [11, 13]. In the current fabrication process, the pre-stressed PS film is etched by RIE which leaves behind a rough surface in the exposed and etched regions. During the shrinking process the lateral dimensions of the film reduces by 60-65% while the vertical dimension of the features in it increase by a factor of ~ 6.25 due to volume conservation. This increase in height is desired to amplify the etched patterns embedded into these films; however, they also amplify the surface roughness in the etched regions.

Surface roughness can be detrimental as they create stress concentrations and can cause distorted shrinking of the films in subsequent steps. This effect becomes particularly important when the dimensions of the patterns are close to 1 μm or below. The use of a Si wafer intermediate in the process to form the mold for the next step can potentially mitigate the surface roughness in the etched regions due to RIE.

In order to demonstrate the effect of the intermediate step, experiments were performed wherein the PDMS replica mold of the shrunk pattern was used to pattern a photoresist coated on a Si wafer by soft imprint lithography (Figure 2-1g). Then, the residual photoresist layer (which produced by the undesired rough surface of the shrunk

pattern) was removed by a short O_2 RIE. A new PDMS mold was then cast on the patterned Si wafer and used to pattern the next miniaturization step. The PDMS mold directly made from the shrunk pattern was used as a control.

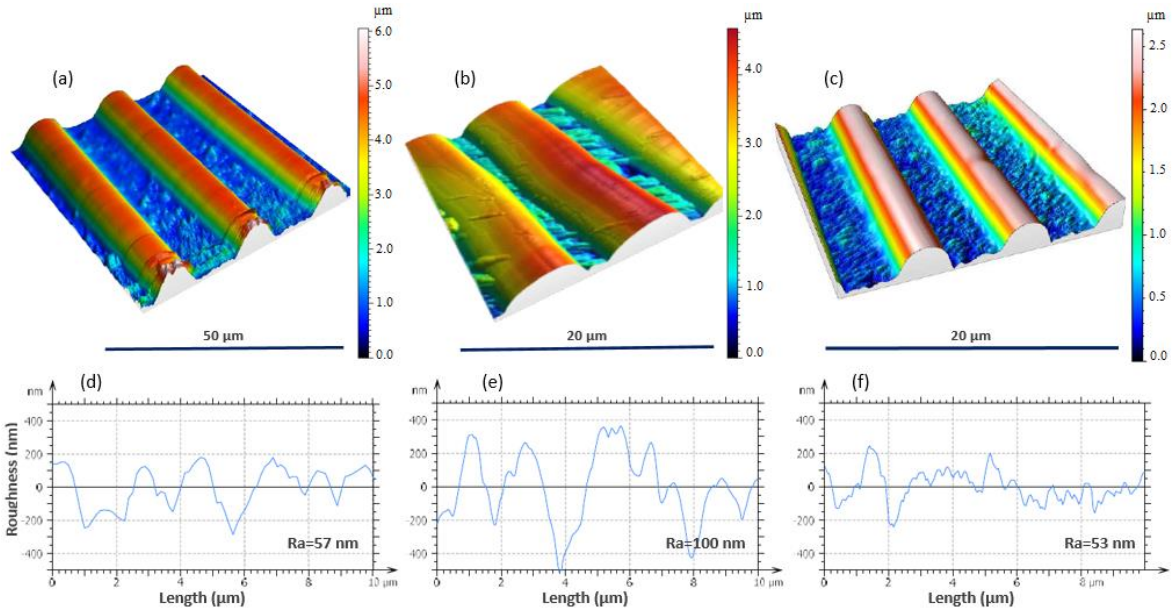

Figure 2-4 AFM images and the corresponding surface roughness measurements of (a, d) the first miniaturization step, (b, e) second miniaturization step directly, (c, f) second miniaturization step after modification by using Si wafer.

Atomic force microscopy was performed (Figure 2-4) on the patterns comparing the surface topography after the first miniaturization step (Figure 2-4a) and those formed after the second miniaturization step to determine the effect of the use of the Si intermediate mold (Figure 2-4c) vs. the control case (Figure 2-4b). It shows clearly that the surface roughness of the etched regions was significantly lower when the Si intermediate mold was used to then subsequently transfer the shrunk pattern to PDMS. The average surface roughness of the first miniaturization step after shrinkage was found to be ~ 57 nm, (Figure 2-4d). The surface roughness of the patterns generated after the second step of miniaturization was only ~ 53 nm (essentially unchanged, Figure 2-4f) when the Si

intermediate mold was used while it increased to ~ 100 nm (Figure 2-4e) in the control case where the PDMS mold was created directly from the shrunk pattern of the previous step.

These results show that the use of Si intermediate mold was able to mitigate the increase in surface roughness that occurs when the imprinting mold for the next step is directly cast from the shrunk mold of the previous step. This increase in surface roughness in the control case results in loss of resolution in each successive step and prevents the use of this method beyond one or two successive step. With the Si intermediate mold, successive miniaturization can be carried out indefinitely until the dimensions of the patterns approach the surface roughness of the heat shrinking polymer film.

2.4.3 Pattern transfer from heat shrunk polymer films onto functional substrates

The multi-step miniaturization process is used to reduce the dimensions of the patterns after which the reduced patterns have to be transferred on to a functional substrate. In order to demonstrate the pattern transfer and the features that are produced, Si was chosen as a functional substrate as it is widely used in electronic applications. The PDMS mold of the shrunk pattern after the first step of miniaturization (Figure 2-2b) was used to pattern a photoresist coated on a Si substrate by soft imprint lithography. Then the patterned substrate was exposed to a short O_2 RIE (20 sec) to remove any residual photoresist layer. The patterned photoresist was used as a mask to etch the Si substrate by RIE with mixed gases (C_4F_8 and SF_6) for 4-6 min.

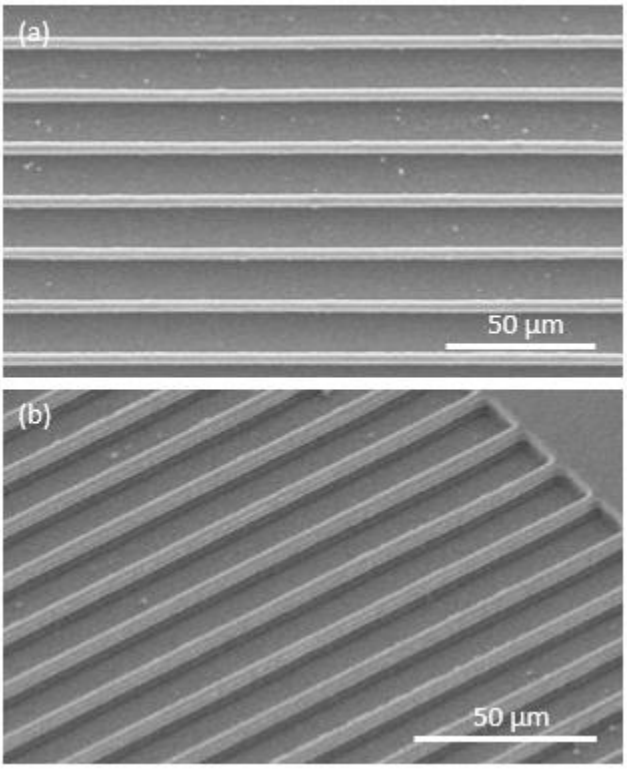

Figure 2-5 SEM images of the fabricated Si wafer after transferring the pattern of the shrunk film (a) top view, (b) incline view (tilt angle of 45^{o}).

The remaining photoresist mask was then removed by acetone or by O_2 plasma RIE. Figure 2-5 shows SEM images of the fabricated Si substrate after transferring the pattern. A top view of the patterned Si substrate is shown in Figure 2-5(a), and an incline view is shown in Figure 2-5(b). The line width is 5.2 µm, the spacing is 11.6 µm and the depth of the etched pattern is 4.8 µm. It clearly illustrates that the shrunk patterns generated from the miniaturization process can be transferred into a Si substrate in large-area and deep patterns.

2.4.4 Effect of aspect ratio of patterns on miniaturization

The height of the patterns formed after the RIE of the pre-stressed polymer films has a significant effect on the fidelity of the features formed after heat induced shrinking. This effect will then have a significant influence on the ability to miniaturize over a number of

steps. In order to identify the appropriate aspect ratio of the etched features that would be suitable, line-space patterns were fabricated at different aspect ratios (λ) which is defined as the ratio between the height of the pattern after shrinkage and the line width. The height of the features was controlled by the depth of etch during the RIE process. The SEM images of the patterns formed after shrinking are shown in both the top down (Figure 2-6a,c,e) and inclined (Figure 2-6b,d,f). When the aspect ratio was λ=1 (Figure 2-6a,b), the shrunk pattern had good fidelity with the original etched pattern and the lines were straight. At λ=1.5 (Figure 2-6c,d), the shrunk pattern began to lose some fidelity and was found to contain some kinks that were not present in the original etched pattern.

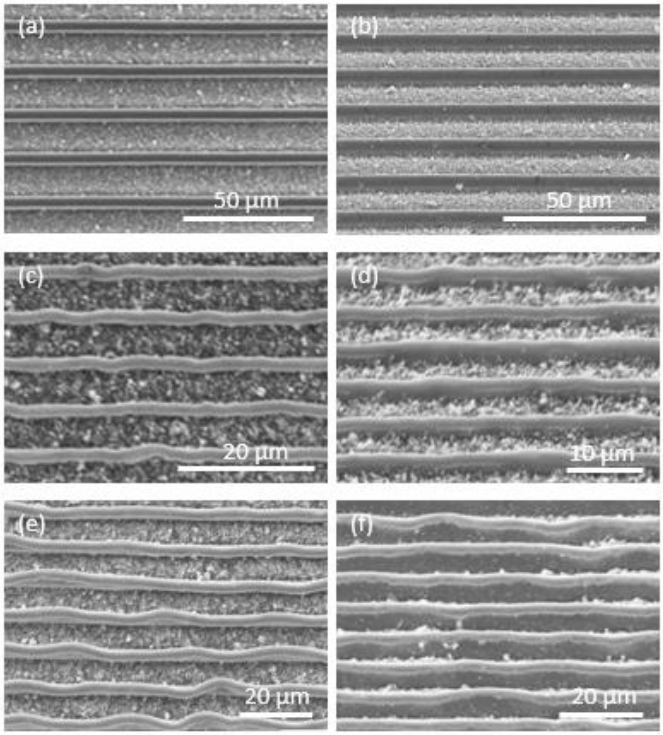

Figure 2-6 SEM images of the line-space pattern at different aspect ratios (λ). The aspect ratios are (a, b) λ=1, (c, d) λ=1.5, and (e, f) λ=2. (a, c, e) are top views and (b, d, f) are incline views.

These deformations were found to increase with the aspect ratio. For instance, when $\lambda=2$, large deformations were seen (Figure 2-6e,f). Thus $\lambda=1$ is suitable for proportional miniaturization of patterns in this format. This finding is important as the aspect ratio of the features etched into the pre-stressed polymer film has to be maintained at one in order to get the best feature fidelity. It implies that the etch depth of the features embedded into the polymer film such be reduced in each successive step of miniaturization. However, an etch depth that is comparable to the surface roughness of the pre-stressed film will also lead to the loss of fidelity. Therefore, the surface roughness of the pre-stressed film determines the minimum feature size that is achievable through this successive miniaturization process.

2.5 Conclusions

In summary, we have demonstrated a simple yet powerful multi-step miniaturization approach using pre-stressed polymer films that offers a sequential size reduction of micron and sub-micron patterns. A pattern transfer method was developed by a combination of soft imprint lithography and RIE that offers a way to use the shrunk patterns as new masters without the need of fabricating hard or metal templates. Thus, from a single master, new masters are created with different smaller feature sizes. A sequential miniaturization of different patterns have been demonstrated showing a 20x reduction in size of the original patterns, and achieving features as small as 750nm. Moreover, to show that the fabricated patterns are not limited to polymeric materials and can be converted into a functional substrate, they are transferred to a Si substrate. These capabilities are promising in micro and nano fabrication, and offer significant advantages over conventional photolithography in terms of resolution and over advanced lithography methods such as nanoimprint

lithography in terms of cost. In addition, the multi-step miniaturization approach introduces a new micron/sub-micron fabrication method that can be performed in any lab without the need of expensive instruments.

Acknowledgements

The authors acknowledge funding support from the Natural Sciences and Engineering Research Council of Canada (NSERC) and the Ontario Research Fund (ORF). PRS also acknowledges the Canada Research Chairs Program.

References

[1] D. P. Sanders, "Advances in patterning materials for 193 nm immersion lithography," *Chemical reviews*, vol. 110, pp. 321-360, 2010.

[2] M. C. Traub, W. Longsine, and V. N. Truskett, "Advances in nanoimprint lithography," *Annual review of chemical and biomolecular engineering*, vol. 7, pp. 583-604, 2016.

[3] D. Qin, Y. Xia, and G. M. Whitesides, "Soft lithography for micro-and nanoscale patterning," *Nature protocols*, vol. 5, pp. 491-502, 2010.

[4] N. Liaros and J. T. Fourkas, "Ten years of two-color photolithography," *Optical Materials Express*, vol. 9, pp. 3006-3020, 2019.

[5] E. M. Sebastian, S. K. Jain, R. Purohit, S. Dhakad, and R. Rana, "Nanolithography and its current advancements," *Materials Today: Proceedings*, 2020.

[6] P. J. Goodrich, F. Sharifi, and N. Hashemi, "Rapid prototyping of microchannels with surface patterns for fabrication of polymer fibers," *RSC Advances*, vol. 5, pp. 71203-71209, 2015.

[7] A. Yokoo, K. Wada, and L. C. Kimerling, "Pattern size reduction of nanoprint-fabricated structures on heat-shrinkable film," *Japanese Journal of Applied Physics*, vol. 46, p. 6395, 2007.

[8] S. Lin, E. K. Lee, N. Nguyen, and M. Khine, "Thermally-induced miniaturization for micro-and nanofabrication: progress and updates," *Lab on a Chip*, vol. 14, pp. 3475-3488, 2014.

[9] X.-M. Zhao, Y. Xia, O. J. Schueller, D. Qin, and G. M. Whitesides, "Fabrication of microstructures using shrinkable polystyrene films," *Sensors and Actuators A: Physical*, vol. 65, pp. 209-217, 1998.

[10] X. Zhu and T. Cui, "Polymer shrinkage of hot embossed microstructures for higher aspect ratio and smaller size," *Sensors and Actuators A: Physical*, vol. 195, pp. 21-26, 2013.

[11] H. Yabu and M. Shimomura, "Miniaturization of surface patterns by combination of contact etching lithography and multi-step shrinking of stretched polymer films," *Polymer journal*, vol. 40, p. 534, 2008.

[12] M. H. Lee, M. D. Huntington, W. Zhou, J.-C. Yang, and T. W. Odom, "Programmable soft lithography: solvent-assisted nanoscale embossing," *Nano letters*, vol. 11, pp. 311-315, 2010.

[13] D. Dyer, S. Shreim, S. Jayadev, V. Lew, E. Botvinick, and M. Khine, "Sequential shrink photolithography for plastic microlens arrays," *Applied Physics Letters*, vol. 99, p. 034102, 2011.

[14] C. Lv, Z. Jia, Y. Liu, J. Mo, P. Li, and X. Lv, "Angle-resolved diffraction grating biosensor based on porous silicon," *Journal of Applied Physics*, vol. 119, p. 094502, 2016.

[15] I. Yamada and Y. Ikeda, "Sol-gel zirconia diffraction grating using a soft imprinting process," *Applied optics*, vol. 56, pp. 5054-5059, 2017.

[16] D. Qin, Y. Xia, and G. M. Whitesides, "Soft lithography for micro-and nanoscale patterning," *Nature protocols*, vol. 5, p. 491, 2010.

[17] U. M. Sonmez, S. Coyle, R. E. Taylor, and P. R. LeDuc, "Polycarbonate Heat Molding for Soft Lithography," *Small*, 2020.

3 Chapter 3

Constrained shrinking of nanoimprinted pre-stressed polymer films to achieve programmable, high-resolution, miniaturized nanopatterns

Complete Citation:

S. Sayed and P. R. Selvaganapathy, "Constrained shrinking of nanoimprinted pre-stressed polymer films to achieve programmable, high-resolution, miniaturized nanopatterns," *Nanoscale Advances*, under review, 2021.

Contribution:

S. Sayed: Designed and performed all experiments, interpretation and analysis of data, wrote the manuscript draft.

P. R. Selvaganapathy: Supervised S. Sayed and provided guidance, revised and edited the manuscript, was responsible for the manuscript submission.

3.1 Abstract

Nanoimprint lithography (NIL) is an emerging technology to form patterns and features in the nanoscale. Production of large area molds for NIL is challenging particularly in the sub-50nm range. Pre-stressed polymer films with embedded microscale pattern can be miniaturized by shrinking induced due to thermal stress release. However, when pre-stressed films are thermally nanoimprinted with sub-micron features and shrunken, they lose all the topographical features due to material reflow. Here we report a new approach that prevents reflow and allows retention of shrunken patterns even at the scale of <50 nm. We have discovered that when the shrinking process is mechanically constrained in one direction, the thermal treatment only relieves the stress in the orthogonal direction leading to a uniaxial shrinkage in that direction while preserving the topographical features. A second step, with the constraint in the orthogonal direction leads to biaxial shrinkage and preservation of all of the topographical features. This new technique can produce well defined, high resolution and high fidelity nanostructures at dimensions below 50 nm. The process is programmable and the thermal treatment can be tuned to shrink features to various dimension below the original imprint which we use to produce tunable and gradient plasmonic structures.

Keywords: Nano fabrication, Nanoimprint lithography, prestressed films, constrained shrinking, plasmonics.

3.2 Introduction

Nanofabrication and the precise reproduction of features at the scale below 100 nm is crucial for a number of industrially relevant applications including semiconductor and IC fabrication, nanoelectromechanical systems (NEMS) as well as textured surfaces for biomedical applications. Nanolithography, which is associated with the nanofabrication, is a process of imprinting or fabrication of nanoscale patterns or features on a substrate [1]. One of the nanolithography techniques that has emerged over the last few decades is nanoimprint lithography (NIL) [2-4]. NIL has the ability to produce nano patterns of high density and high resolution at low cost and high throughput. However, it is a replication or duplication process that transfers the features on a master mold into a polymeric material fixed on another substrate [5]. The master molds are generally fabricated using focused ion beam lithography or electron beam lithography which are time-consuming and expensive processes [6-8]. Thus, the most expensive step in a complete NIL fabrication process is the fabrication of the master mold [9-11]. Since NIL is a 1:1 replication process, the resolution of the fabricated patterns depends on the resolution of the master mold. This will increase the complexity of master fabrication for nanoscale patterns (sub-100nm). Moreover, if different patterns or different dimensions are required, new master molds have to be fabricated for each new pattern or size. Thus, developing a process that can create patterns with different dimensions from the same master mold can be helpful in reducing the time and cost required for new master molds.

One interesting approach to produce miniaturized patterns from larger original patterns is using shape memory polymers (SMP). SMPs are formed of randomly oriented polymer chains that can be stretched and fixed in the new stretched form [12, 13]. They are

responsive to external stimuli that can be triggered by, for example, heating above the glass transition temperature T_g as in the heat shrinkable polymer films [14-16]. When an external stimulus is applied, shape recovery of the SMP takes place by relaxing the internal stresses where the polymer reflows and tends to recover to its original shape. By patterning the shrinkable films, these patterns also can be miniaturized when the entire film is triggered by the external stimulus and shrinks.

Thermal nanoimprint lithography (thermal-NIL) (which also known as hot embossing) has been used to pattern the pre-stressed films in order to miniaturize the features size after shrinking. A master mold which has relief structures is pressed against the polymer film to transfer the patterns by applying pressure and heating. However, the direct shrinking of embossed pre-stressed films fails to preserve the topographical features after shrinking [17, 18]. The reflow of material when the stress is relieved, causes reduction in pattern height and reduces the fidelity of the patterns. The reflow of material caused by the shape memory effect results in complete elimination of the imprinted patterns especially at the scale of a few hundred nanometers and below.

An alternative approach where reactive ion etching (RIE) is used to embed the topographical features instead of hot embossing can preserve patterns as material is physically removed [19]. Using RIE, the patterned area is physically removed, thus the polymer does not return to the original shape after shrinking and finally the height of pattern increases. The features dimensions achievable after miniaturization are limited to few microns [19, 20] and in recent work to sub-micron [21]. However, this method is not suitable for sub 500 nm resolution features due to the rough surface generated from RIE process.

Here, we report a new miniaturization approach that prevents reflow and allows retention of shrunken patterns on the pre-stressed polymer films even at the scale of <50 nm. By applying mechanical constraints in one direction during shrinking process, only the stress in the orthogonal direction is relieved and a uniaxial shrinkage is obtained in that direction while preserving the topographical features. Then, a biaxial shrinkage is obtained by a second thermal treatment with the constraint in the orthogonal direction. The developed approach can miniaturize the features size from that of the original master pattern while preserving all of the topographical features. Thus, the height of the shrunken patterns is preserved and well-defined patterns are generated. Nanoscale patterns with features size well below 50 nm were fabricated with high fidelity.

Moreover, we investigated the effect of hot embossing parameters on the quality of the generated patterns and the effect on the ability of the embossed film to shrink in order to determine the appropriate hot embossing parameters. We also demonstrate that this miniaturization approach can be programmed to fabricate different smaller size patterns from a single master mold. Varying the constraints spatially can also produce gradient shrinkages that may be of importance in certain applications. Finally, we applied this new capability to fabricate tunable and gradient plasmonic structures with different sizes and hence different optical properties that can reflect certain colors corresponding to each different size.

3.3 Experimental details and methods

3.3.1 Miniaturization process description

Thermal-NIL or hot embossing is a well-established fabrication process that can imprint complex structures over large areas at low-cost and high speed [22, 23]. However,

fabrication of master molds which are needed for the hot embossing process is challenging and time consuming, especially for large area patterning. Heat shrinkable films can be used to reduce the features size of an original master pattern. Thus, they can generate new features at higher resolution in a scalable manner without the need of fabricating new master molds. Therefore, a combination of hot embossing with the shrinking techniques could prove valuable in developing a low-cost, rapid and scalable nanofabrication approach. Nevertheless, such efforts in the past were not successful due to the shape memory effect of the pre-stressed films that result in material reflow and loss of pattern definition. In particular, the height of the patterns were significantly reduced to a few nanometers, especially for feature sizes in the sub micron scale.

We have discovered that if the same imprinted pre-stressed film were to be thermally shrunk with uniaxial constraint then it shrinks in the orthogonal direction with minimal loss of topographical features. With this finding, we developed a new fabrication process (Figure 3-1) to proportionally miniaturize nanometer scale imprinted features.

First, a master mold was used to imprint pre-stressed polystyrene (PS) films using a hot embossing process, Figure 3-1a,b. The film was embossed under specific conditions of force and temperature which were optimized so that the imprinting process does not affect the ability of the film to shrink (see supplementary information). After the hot embossing step, the film was cooled down while the embossing force was retained. At the separation temperature (50-60 ^{o}C), the patterned film was carefully separated from the master mold to avoid tearing or damage of the patterns that could happen during separation due to the difference in thermal expansion coefficients of the film and the mold, Figure 3-1b.

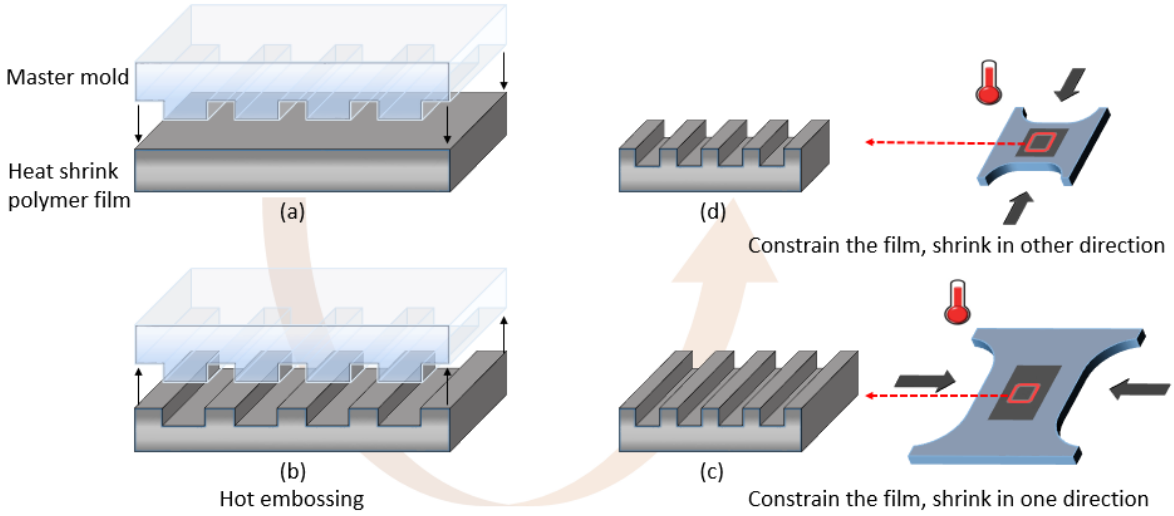

Figure 3-1 Schematic illustration of the miniaturization process of hot embossed patterns on heat shrinkable polymer films by applying directional constrains during thermal shrinking.

In order to miniaturize the embossed patterns, the film was heated above its T_g to allow thermal shrinking while applying unidirectional constraints on the film, Figure 3-1c. Due to this configuration, the film shrinks in a direction (shrink-direction) perpendicular to the constrained direction and a uniaxial shrinking was achieved. Then the film was cooled down to the room temperature. For a complete shrinking (biaxial shrinking), the film was constrained in the other direction and heated to allow shrinking in the shrink-direction, Figure 3-1d. This process will result in proportional miniaturization of the patterns in all directions while still preserving the topographical features.

3.3.2 Hot embossing

Polystyrene heat shrinkable films (Graphix Shrink Film, Maple Heights, Ohio) were used as a polymer substrate where the nano patterns were embossed onto it. Hot embossing equipment (EVG520 HE) was used. Master stamps were obtained from EVG and used to imprint the PS films. The PS film was cut into 4 inch size and placed on a 4 inch glass

wafer that was used as a carrier. The master stamp was then placed on top of PS film inside the hot embossing chamber. After closing the chamber, both top and bottom plates were warmed up at 80 ^{o}C, and the chamber was evacuated to the working vacuum pressure. The piston was then moved down to bring the master stamp and substrate into contact at a contact force of 500 N (which is the minimum allowable force). The temperature of both plates was continuously increased to the desired embossing temperature, at which the force also increased to the embossing force value. The embossing time was 5 min where the force and temperature were held constant. After that, the temperature started to decrease until reached 80 ^{o}C, at which the piston moved up and the force was removed (the demolding temperature was around 60 ^{o}C when the force was completely removed). The chamber was then vented and the sample was removed from the chamber. Immediately, the master stamp was separated from the imprinted film by inserting a thin razor blade between them at the edge and carefully separating them. During hot embossing optimization (see supplementary information), only the embossing temperature and force were changed while all other parameters were kept constant. The optimized values of temperature and force were 125 ^{o}C and 4500 N, respectively. These values were used for all experiments represented in this work.

3.3.3 Constrained miniaturization

After the nano patterns were imprinted onto the PS film, the film was cut into a square with the patterned area in the middle. Then, the film was placed on a silicon wafer and clamped by paper binder clips at two opposite ends while the patterned area was at the middle. The sample was heated at an oven at 130 ^{o}C for the desired shrinking time. Then, the sample was removed outside the oven and left for a few minutes to cool down at room temperature.

As a result, the film was miniaturized in one direction only (shrink direction) and a uniaxial shrinking was obtained. For a biaxial shrinking, the film was then clamped at the other two ends while keeping the patterned area at the middle. Then, it was placed in the oven at same temperature and removed from the oven after shrinking. The shrinking time was varied to obtain different shrink ratios.

3.3.4 Imaging and characterization

SEM images of the fabricated patterns onto PS films before and after shrinking were taken using JEOL JSM-7000F scanning electron microscope. All PS samples were coated with a thin gold layer (5-8 nm) for preparation prior to SEM imaging. The 3D topography and height profile of nano patterns were obtained by atomic force microscope TOSCA 400 using tapping mode. Optical microscope images of the plasmonic structures were taken using OLYMPUS SZ61 and attached camera Infinity1. The optical microscope was used to demonstrate the reflected different colors based on tuning the dimensions of the shrunk patterns. White LED light was pointed on the samples at a fixed incident angle, and the samples were placed at a fixed position with respect to the light source and the objective lens of the microscope. This configuration was used for comparing the different reflected colors based only on the variation of the pattern dimensions.

3.4 Results and Discussion

3.4.1 Miniaturization of hot embossed nano patterns by applying constraints

In order to demonstrate the miniaturization of hot embossed patterns using this new approach, a nanoscale line-space pattern (300 nm line width and 300 nm spacing) was used. The results were compared to the conventional direct shrinking process (without constraints).

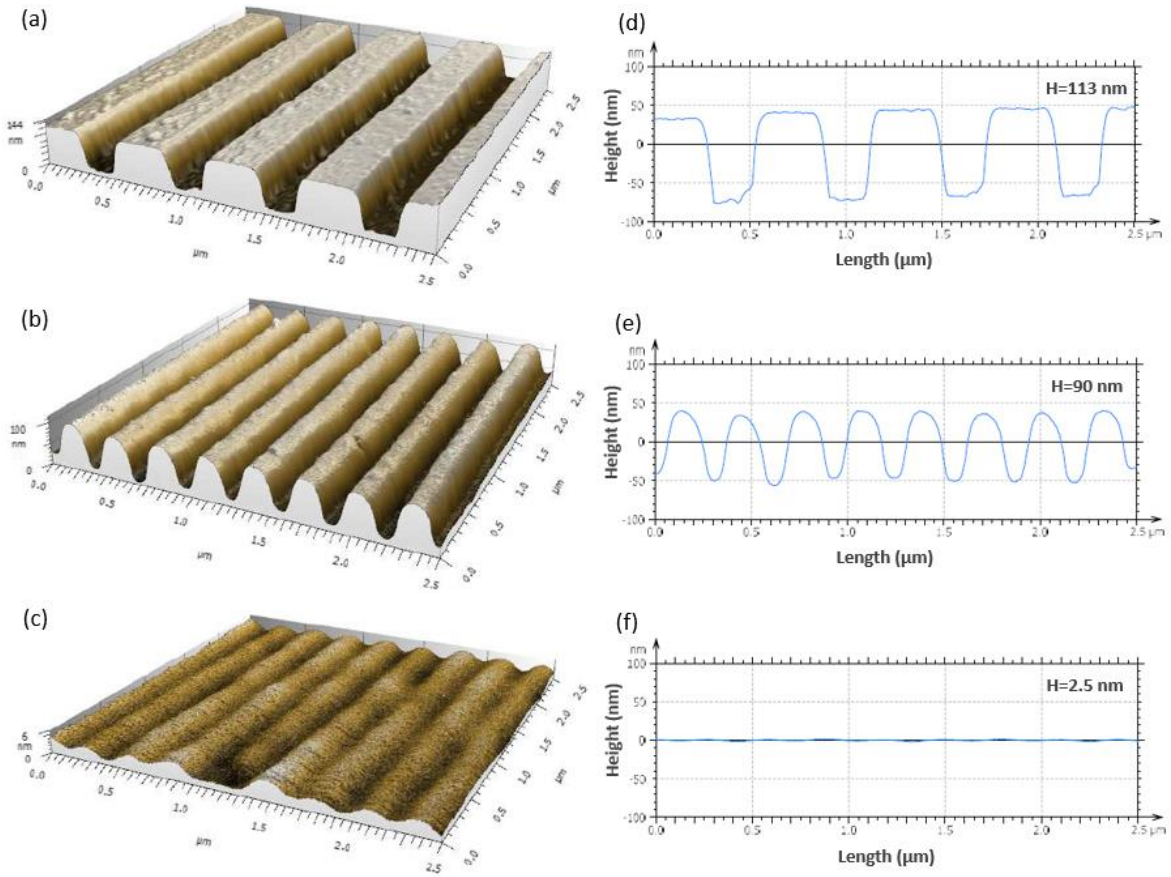

Figure 3-2 AFM images and the corresponding height profile of (a, d) the imprinted pattern by hot embossing , and the generated patterns after shrinking (b, e) by applying constrains, (c, f) without constrains. The height (H) of the imprinted pattern was initially 113 nm, and it slightly decreased to 90 nm after the constrained shrinking. However, it almost vanished in the case of direct shrinking where the height dramatically decreased to less than 2.5 nm.

Atomic force microscope (AFM) measurements of the imprinted pattern on PS film (Figure 3-2a) and those formed after miniaturization by applying constraints during shrinking (Figure 3-2b) and without constraints (Figure 3-2c) show that the topographical features were preserved during constrained shrinking process while they were completely removed during the conventional unconstrained shrinking. The height of the imprinted pattern which was found to be 113 nm, (Figure 3-2d) reduced to 90 nm upon miniaturization with constraints applied (Figure 3-2e), while it dramatically decreased to

less than 3 nm (Figure 3-2f) in the case of unconstrained direct shrinking. It should be noted that even though the height of the pattern slightly decreased by ~ 20% (from 113 nm to 90 nm) after the constrained shrinking, the aspect ratio (ratio of the pattern height to the line width) actually increased ~ 60% since the pattern size was reduced by ~ 50% in the lateral direction. These results explicitly show that uniaxial constraints during shrinking of hot embossed patterns can not only preserve the imprinted topographical features but also increase the aspect ratio of those features. Patterns can be miniaturized by ~ 50% from the original without any expensive processing.

When the pre-stressed polymer film with imprinted patterns on it is exposed to high temperatures ($>T_g$), the stress in the film is relieved in all directions causing a reflow of materials and therefore complete loss of the nanoscale imprinted patterns. However, by constraining the film uniaxially, an external tension is introduced which balances the internal compressive forces that manifest in that direction as the film tries to relieve its internal pre-stress. This balance not only prevents shrinkage in that direction but also maintains the topographical features embedded in the film. Since there is no constraint in the orthogonal direction, the film shrinks in that direction. The external tension in one direction is sufficient enough to prevent the complete stress relaxation in the imprinted regions of the film and therefore preserves the topographical features. In contrast, the unconstrained film is free to relax in all directions when exposed to temperatures higher than its T_g which results in the simultaneous reflow of material in all directions and loss of topographical features that were embedded. With the constrained shrinking, successful miniaturization of hot embossed patterns can be carried out with high fidelity and well-defined patterns smaller than the master pattern can be generated.

3.4.2 Scalability of the miniaturization approach and fabrication of nanoscale patterns down to 50 nm

The new nanofabrication method of miniaturization by constrained shrinking of the pre-stressed polymer films can enable accurate miniaturization of nanoscale patterns produced by a wide variety of methods including, lithography, nanoimprinting, hot embossing even further into the sub 100 nm scale as it overcomes the limitations of unconstrained shrinking due to stress relaxation. The scalability of this miniaturization process and its range was demonstrated by using three different dimensions of master patterns to imprint and shrink. Masters with line patterns containing line widths of 750 nm, 300 nm, and 150 nm with identical spacing were hot embossed on PS heat shrinkable films (Figure 3-3a, d, g respectively). These patterns were miniaturized by approximately 50% after the two-step constrained shrinking process (Figure 3-3b, e, h respectively). SEM images taken at inclined view for the shrunk patterns are shown in Figure 3-3c, f, i, respectively demonstrate that the patterns are relatively tall and retain the topographical features in all cases. For the 750 nm pattern, after miniaturization the line width reduces to 470 nm while the spacing reduces to 280 nm (50% total reduction). For the 300 nm pattern, the line width reduces to 170 nm and the spacing to 120 nm (52% total reduction). For the 150 nm pattern, the line width reduces to 92 nm and the spacing to 56 nm (51% total reduction).

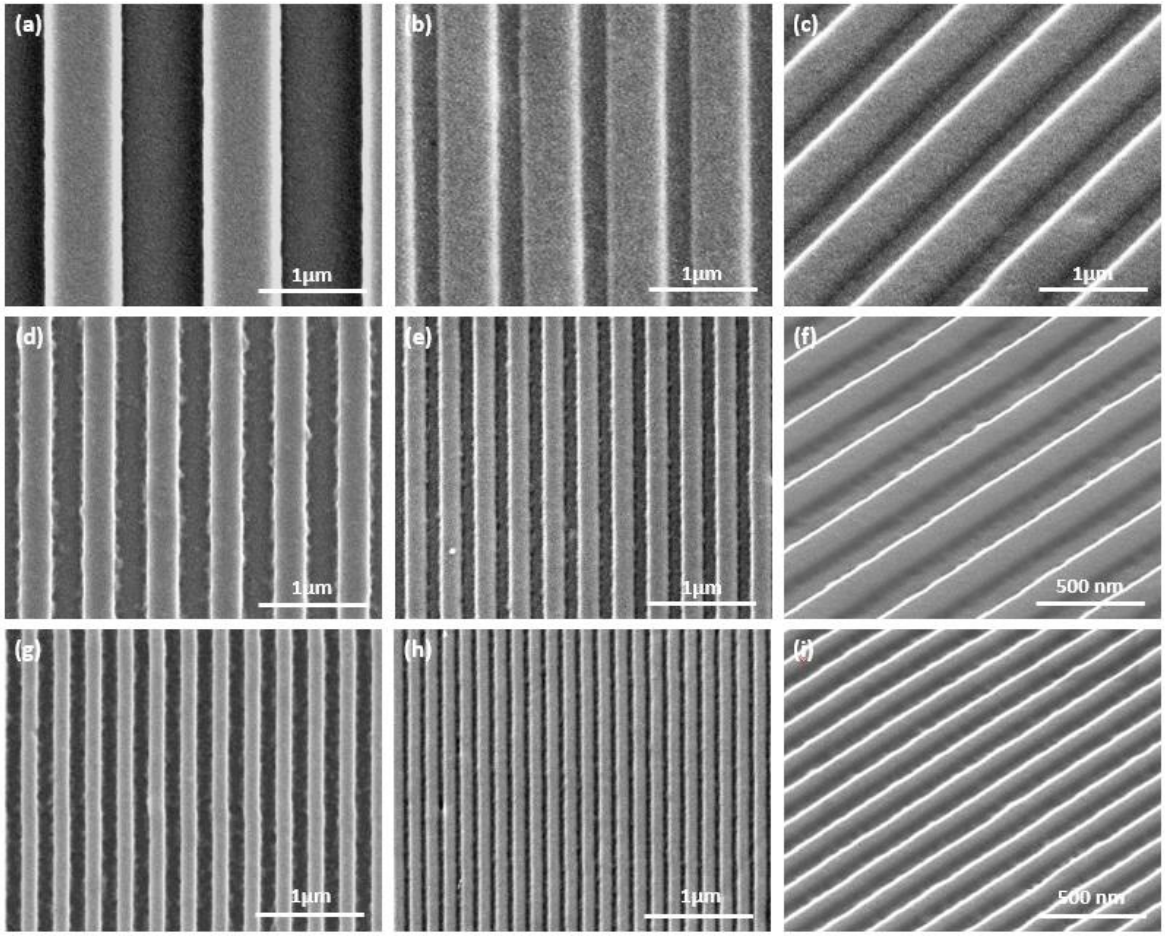

Figure 3-3 Miniaturization of line-space patterns with initial dimensions of 750 nm, 300 nm, and 150 nm. SEM images of (a, d, g) the hot embossed patterns, (b, e, h) the shrunk patterns, and (c, f, i) inclined views of the shrunk patterns. (a) 750 nm pattern with initial line-width w=750nm, spacing s=750nm, (b) after shrinking w=470nm, s=280nm. (d) 300 nm pattern w=s=300nm, (e) after shrinking w=170nm, s=120nm. (g) 150 nm pattern w=s=150nm, (h) after shrinking w=92nm, s=56nm.

It is interesting to note that higher resolution patterns than the original patterns were achieved with high fidelity even for the smallest pattern of sub-100 nm dimensions. It should be also noted that the spacing reduced more (37-40% of the original) than the line width (56-63% of the original) due to the stresses associated with the hot embossing process at the surface layer of the polymer film. The internal compressive stresses

embedded in the shrinkable film at the surface layer are partially released due to the hot embossing conditions and the polymer redistribution during patterning. When the patterned film is heated to thermally shrink, the internal compressive stresses in the core of the film push and compress the polymer material along the shrink-direction. Due to the absence of material in the spaces between the lines, the spacing is compressed and shrinks more than the line width. The partial release of the stress during hot embossing also explains why the hot embossed film shrinks by 50% overall instead of 60% with is typical for pristine pre-stressed PS films [21, 24, 25]. Despite the different shrinking ratios of the spacing and line width, highly uniform patterns with reduced dimensions were fabricated with high fidelity and reproducibility.

In order to show that the miniaturization process can be also used to fabricate features of different shapes other than line-space patterns, hole arrays with different dimensions were also nanofabricated by the constrained shrinking based miniaturization process. The initial master patterns were imprinted by hot embossing on PS shrinkable films. The imprinted patterns were hole arrays of square shape with hole size of 300 nm, and 150 nm (Figure 3-4a, d respectively). The spacing between the holes was the same as the hole size, i.e. 300 nm, and 150 nm respectively. Following same procedures of the constrained shrinking, the patterns were miniaturized by ~ 50% (Figure 3-4b, e respectively). SEM images taken at inclined view for the shrunk patterns are shown in Figure 3-4c, f, respectively demonstrate that the depth of these holes and topographical features are maintained. For the 300 nm hole array, after miniaturization, the hole size reduces to 135 nm while the spacing reduces to 165 nm (50% total reduction). For the 150 nm hole array, the hole size reduces to 68 nm and the spacing to 84 (49.5% total reduction).

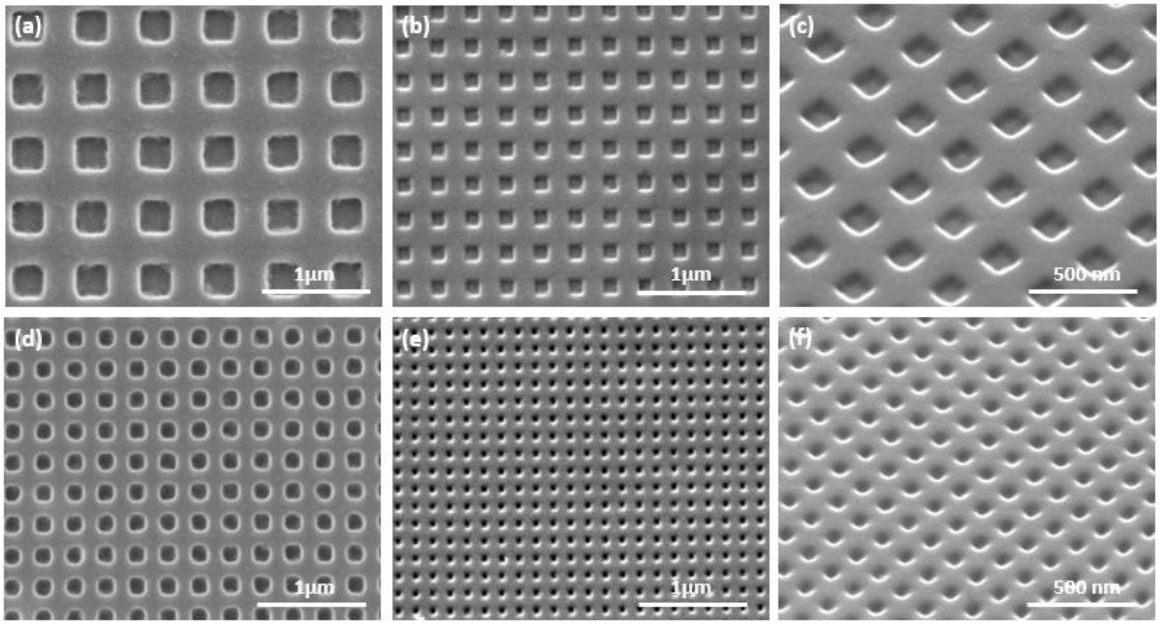

Figure 3-4 Miniaturization of hole array patterns with initial dimensions of 300 nm, and 150 nm. SEM images of (a, d) the hot embossed patterns, (b, e) the shrunk patterns, and (c, f) inclined views of the shrunk patterns. (a) 300 nm pattern with initial hole width w=300nm, spacing s=300nm, (b) after shrinking w=135nm, s=165nm. (d) 150 nm pattern w=s=150nm, (e) after shrinking w=68nm, s=84nm.

As described in the line-space pattern, the hole size reduced (45% of the original size) more than the spacing (55% of the original) between the holes due to the stress relaxation at the surface layer of the polymer film during the hot embossing process. However, the difference between the hole size and spacing in the hole array is smaller than the difference between the line width and spacing in the line-space pattern. This can be due to the additional connections that the hole array has in the direction of the constraint as compared with the line array. Thus, in the hole array, the compressive stresses push the interconnected material in the pattern and compress it more than the separated pattern. The results show that higher resolution patterns than the initial patterns can be generated and can be applied to different shape features.

3.4.3 Programmable size and shape patterns from a single master

The miniaturization process using constrained shrinking of heat shrinkable films offers a programmable approach to generate new smaller nanoscale structures with different pattern size and shape. Thus, scaling of nano patterns becomes possible without the need to fabricate new masters. The constraints also allow us to change the shape of the initial features by defining the shrinking direction, for example a rectangular shape can be generated from a square shape and an oval shape from a circular shape and vice versa. In order to demonstrate these capabilities, hot embossed patterns were shrunk in one direction only (uniaxial shrinking) to change the feature shape of the initial pattern. The embossed patterns were also miniaturized at different shrink ratios by controlling the heating time to create different feature sizes from same initial pattern. SEM images of the initial and shrunk patterns at different shrink ratios are shown in Figure 3-5. Two initial patterns were embossed on the PS films, line-space pattern (Figure 3-5a) and hole array (Figure 3-5e). The feature size of the initial imprinted patterns was 300 nm with same spacing. The imprinted film was constrained and heated uniformly at 130 oC for 4.5 min. As a result, the film was shrunk in one direction by 17% shrink ratio and consequently the embossed patterns (Figure 3-5b, f). When the film was heated for longer time (6 min), the patterns were shrunk by 32% (Figure 3-5c, g). Finally, the patterned film was heated for 9 min which allowed it to shrink by nearly 50% (Figure 3-5d, h). The final dimensions of the shrunk line-space pattern were 175 nm for the line width and 125 nm spacing between the lines. The hole array was shrunk to 140 nm for the hole width and 160 nm spacing between the holes. Note that the final shrink ratio of ~ 50% was the maximum achieve able shrink ratio of embossed PS films due to the used hot embossing parameters which affect the shrink-ability as discussed earlier.

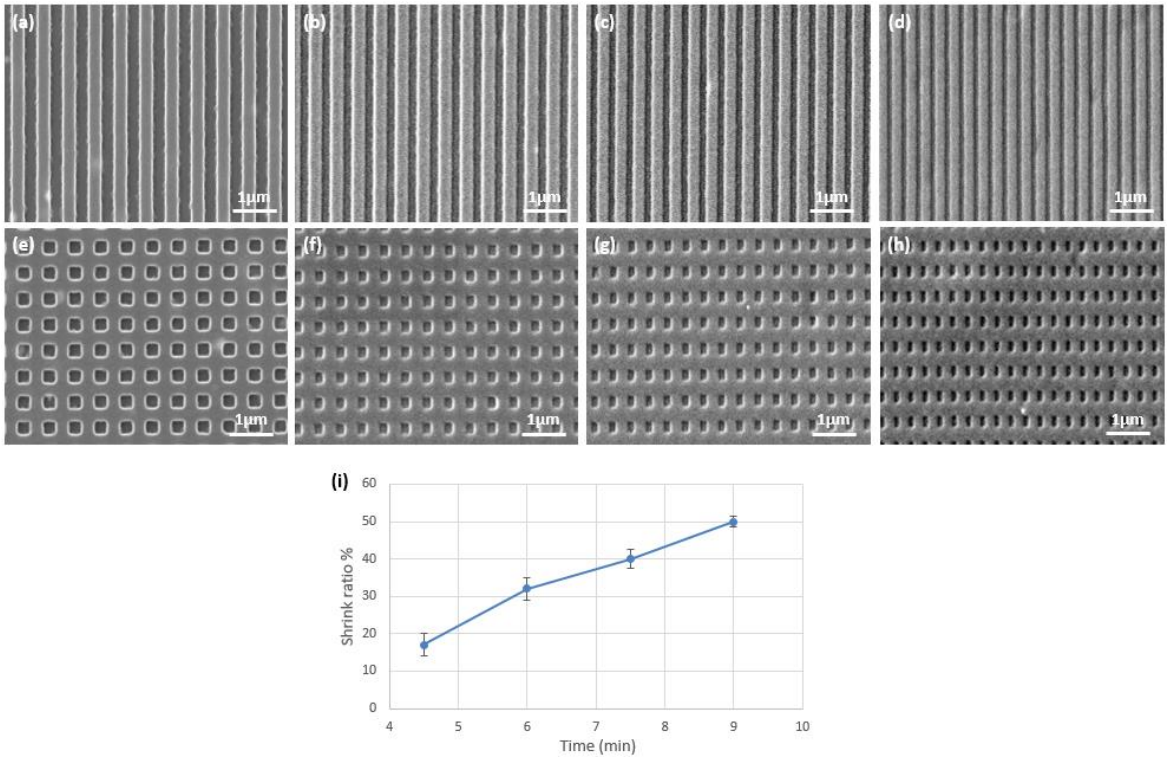

Figure 3-5 Programmable miniaturization process to control the size of the shrunk patterns. (a, e) Initial imprinted patterns. The shrunk patterns after uniaxial shrinking by (b, f) 17%, (c, g) 32%, and (d, h) 50%. (i) The shrink ratio by controlling the heating time at temperature of 130 ^{o}C.

The results show that the miniaturization process of patterned heat shrinkable films can be programmed to generate patterns of different sizes from the same master pattern. The resulted shrink ratio by carefully adjusting the shrinking time is shown in Figure 3-5i. By controlling the shrinking time, the desired pattern dimensions can be produced. In addition, not only the feature size but also the feature shape can be controlled and changed by the constrained shrinking. The feature shape of the hole array was initially a square hole (Figure 3-5e). After shrinking in one direction, the shape changed to a rectangular hole (Figure 3-5f-h). Typically, if patterns with different sizes or shapes are required, new masters must be fabricated for each pattern. However, we were able to overcome this limitation by the constrained miniaturization process of hot embossed PS shrinkable films.

This programmable approach can be a cost and time effective nanofabrication method that can create higher resolution patterns than the initial patterns.

3.4.4 Tunable plasmonic structures

The constrained shrinking of patterned prestressed films have shown the ability to produce new patterns with programmable sizes. We have applied this simple yet powerful nanofabrication approach to rapidly prototype plasmonic structures with tunable properties in a scalable manner. This can overcome a challenge in the field of plasmonics where there is a need to gradient feature size or spacing on the same substrate [26-28]. In order to demonstrate the ability to fabricate tunable plasmonic structures, a line-space pattern (grating structure) was imprinted on the PS shrinkable films by hot embossing. Then, the films were constrained and heated to perform uniaxial shrinking. Different shrink ratios were obtained by adjusting the heating (shrinking) time. The new miniaturized patterns were then coated by a thin gold layer (10 nm Au), by sputtering deposition, to activate the plasmonic effect and hence the optical properties. When a direct light is illuminated at an angle on the nanopatterned structure, the reflected light is determined by the plasmonic response of the surface [29, 30]. Depending on the shape and dimensions of the patterned surface structure, the reflected wavelengths can be controlled. If the reflected wavelength is in the visible spectrum region (400-700 nm), bright colors in the visible spectrum can be observed.

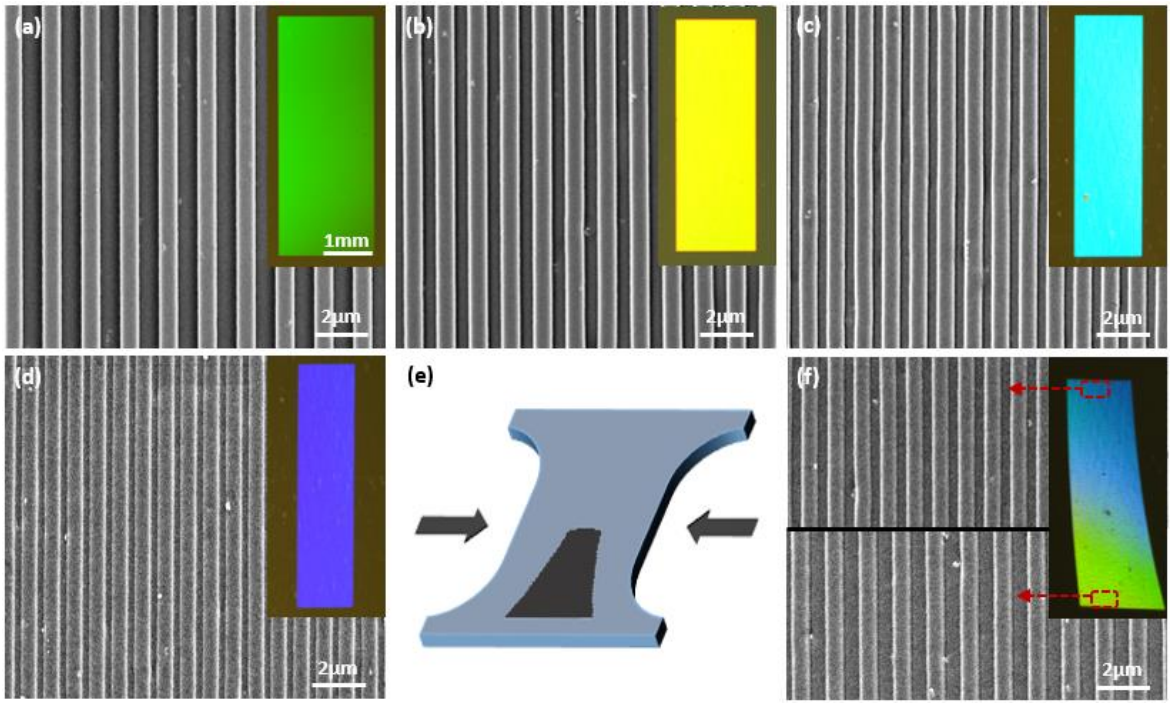

Figure 3-6 Fabrication of tunable plasmonic structures that reflect different bright colors based on changing the pattern dimensions. SEM and optical microscope (insets) images for (a) the initial imprinted pattern, and after shrinking by (b) 17%, (c) 30%, and (d) 48%. (e) Scheme of gradient pattern formation by changing the constraint conditions, (f) Gradient pattern.

SEM images taken for the initial and shrunk patterns and the corresponding optical microscope images are shown in Figure 3-6. The initial dimensions of the line-space pattern were ~ 750 nm line width and ~ 750 nm spacing (Figure 3-6a). Such dimensions were used to allow reflection of wavelengths in the visible region. Thus, visible bright colors can be detected by the optical microscope (and also by human eye). A bright green color was reflected by the initial embossed pattern, as shown in Figure 3-6a. When the pattern was miniaturized by ~ 17% (4.5 min) using the programmable shrinking method, a different color (yellow) was reflected from the pattern (Figure 3-6b). After ~ 30% miniaturization (6 min), the reflected color changed to cyan (Figure 3-6c). After further miniaturization by ~ 48% (9 min), the reflected color from the pattern was blue (Figure

3-6d). It can be clearly shown that the reflected colors are very uniform and homogeneous over the large patterned area. This indicates that the generated patterns by the constrained miniaturization process have high fidelity and uniformity over relatively large area. The results show that the developed process can be applied to rapidly generate plasmonic structures with tunable dimensions and hence optical properties just by changing the duration of time over which the material was shrunk.

It is also interesting to note that spatially tuned dimensions can be produced from the same pattern by modifying the constraint conditions spatially. A gradient pattern was obtained by placing the pattern closer to one of the constrained ends and relatively far from the other constrained end (Figure 3-6e), instead of placing the patterned area at the middle between the constrained ends as described before (Figure 3-1c, d). As a result, the pattern size slightly reduced at the end that is close to the constrain (bottom of Figure 3-6f) while it reduced more at the far end (top of Figure 3-6f). Therefore, the shrunken dimensions of the pattern can be changed continuously along the patterned area. This continuous change resulted in a multicolor gradient pattern with colors ranging from green to blue, as seen in the inset of Figure 3-6f. More broadly, these results indicate that by modulating the tension in the constraints spatially one can create any complex pattern of shrinkages which could be suitable in a variety of programmed miniaturization of nanoscale features.

3.4.5 Tunable fabrication of feature sizes below 50 nm

Feature sizes below 50 nm are of importance in IC processing where pattern definition at this scale are required to produce extremely small transistors. Features in this dimension are produced with high cost and complexity by using either ArF immersion lithography or EUV lithography. One way to lower the cost and complexity is to produce patterns at larger

dimension (50-100 nm) and shrink them to lower dimensions. In order to determine the extension of our process to dimensions lower than 50 nm, we conducted a study using 100 nm hole array (Figure 3-7a) which was subjected to constrained miniaturization with different heating time to achieve different final dimensions. The imprinted pattern was successfully miniaturized by 37% (7 min), where the hole size reduced to 55 nm and spacing between them reduced to 72 nm (Figure 3-7b). After further miniaturization (8.5 min), a total reduction of 46% was achieved. The hole size reduced to 43 nm while spacing reduced to 65 nm (Figure 3-7c).

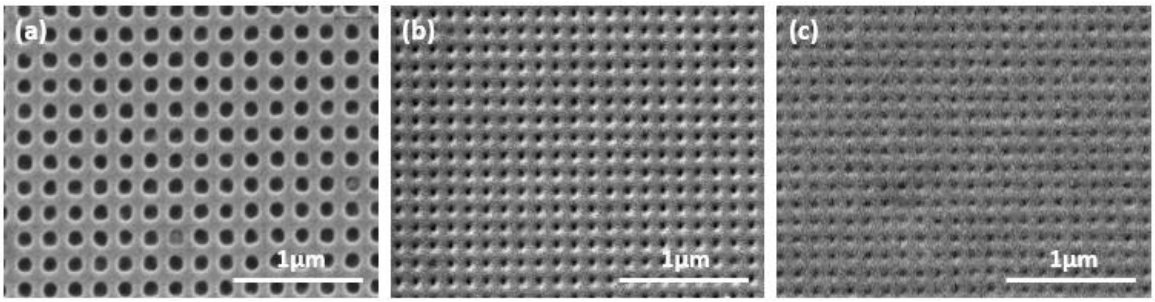

Figure 3-7 Miniaturization to sub-50 nm dimensions. SEM images of (a) the imprinted pattern of initial 100 nm hole size, and after miniaturization by (b) 37%, hole size 55 nm, and (c) 46%, hole size 43 nm.

These results show that the constrained miniaturization process can achieve feature sizes below 50 nm easily. One of the challenges in visualizing the features produced at this scale especially in a polymer is the need to metalize it. Deposition of even a thin gold layer (10-15 nm) in thickness results in loss of resolution of the embedded features as can be seen in (Figure 3-7c). Nevertheless, these results show a promising fabrication and miniaturization process that can accurately produce high resolution features at sub-50 nm dimensions. We believe that the theoretical limit of this approach is the diameter of the uncoiled polymer

used in the film which can be anywhere between 1-10 nm depending on the molecular weight of the polymer used.

3.5 Conclusion

In summary, we have developed a miniaturization approach of the hot embossed patterns using heat shrinkable films by applying directional constrains to control the polymer flow during shrinking process. This powerful approach was able to overcome the limitation that the hot embossed features almost disappear after direct shrinking. Using the constrained miniaturization, the height of the shrunk patterns increased from 2.2% to 80%. Moreover, new smaller patterns with higher resolution were fabricated from a single master. Nanoscale patterns with features size as small as 56 nm were fabricated with high fidelity over large area. This nanofabrication ability offers rapid fabrication of new masters that has significant advantages over master fabrication by direct-write methods in terms of cost and scalability. The influence of hot embossing process parameters on the quality of the replicated patterns and the shrink-ability of the heat shrinkable films was demonstrated in order to optimize the miniaturization process. We have shown that the developed process can be programmed to change the features size and shape. These capabilities were applied to fabricate tunable plasmonic structures by continuously changing the pattern dimensions and hence controlling optical properties. This process shows a simple, rapid, cost effective and scalable nanofabrication approach that can be used for a wide range of applications including plasmonic structures with tunable wavelengths, high capacity storage devices or fabrication of higher resolution masters for soft lithography and nanoimprint lithography.

References

[1] E. M. Sebastian, S. K. Jain, R. Purohit, S. Dhakad, and R. Rana, "Nanolithography and its current advancements," *Materials Today: Proceedings*, vol. 26, pp. 2351-2356, 2020.

[2] S. Y. Chou and P. R. Krauss, "Imprint lithography with sub-10 nm feature size and high throughput," *Microelectronic Engineering*, vol. 35, pp. 237-240, 1997.

[3] A. Cattoni, E. Cambril, D. Decanini, G. Faini, and A. Haghiri-Gosnet, "Soft UV-NIL at 20 nm scale using flexible bi-layer stamp casted on HSQ master mold," *Microelectronic Engineering*, vol. 87, pp. 1015-1018, 2010.

[4] H. Schift, "Nanoimprint lithography: An old story in modern times? A review," *Journal of Vacuum Science & Technology B: Microelectronics and Nanometer Structures Processing, Measurement, and Phenomena*, vol. 26, pp. 458-480, 2008.

[5] M. C. Traub, W. Longsine, and V. N. Truskett, "Advances in nanoimprint lithography," *Annual review of chemical and biomolecular engineering*, vol. 7, pp. 583-604, 2016.

[6] J. Chen, J. Shi, A. Cattoni, D. Decanini, Z. Liu, Y. Chen, and A.-M. Haghiri-Gosnet, "A versatile pattern inversion process based on thermal and soft UV nanoimprint lithography techniques," *Microelectronic Engineering*, vol. 87, pp. 899-903, 2010.

[7] R. Menon, A. Patel, D. Gil, and H. I. Smith, "Maskless lithography," *Materials Today*, vol. 8, pp. 26-33, 2005.

[8] A. Pimpin and W. Srituravanich, "Review on micro-and nanolithography techniques and their applications," *Engineering Journal*, vol. 16, pp. 37-56, 2012.

[9] B. Kwon and J. H. Kim, "Importance of molds for nanoimprint lithography: hard, soft, and hybrid molds," *Journal of Nanoscience*, vol. 2016, 2016.

[10] G. Jeong, J. Park, K. Lee, J. Jang, C. Lee, H. Kang, C. Yang, and S. Suh, "Fabrication of low-cost mold and nanoimprint lithography using polystyrene nanosphere," *Microelectronic Engineering*, vol. 87, pp. 51-55, 2010.

[11] F. D. Arisoy, I. Czolkos, A. Johansson, T. Nielsen, and J. J. Watkins, "Low-cost, durable master molds for thermal-NIL, UV-NIL, and injection molding," *Nanotechnology*, vol. 31, p. 015302, 2019.

[12] A. Lendlein, *Shape-memory polymers* vol. 226: Springer, 2010.

[13] J. Hu, Y. Zhu, H. Huang, and J. Lu, "Recent advances in shape–memory polymers: Structure, mechanism, functionality, modeling and applications," *Progress in Polymer Science*, vol. 37, pp. 1720-1763, 2012.

[14] S. Lin, E. K. Lee, N. Nguyen, and M. Khine, "Thermally-induced miniaturization for micro-and nanofabrication: progress and updates," *Lab on a Chip*, vol. 14, pp. 3475-3488, 2014.

[15] P. T. Mather, X. Luo, and I. A. Rousseau, "Shape memory polymer research," *Annual Review of Materials Research,* vol. 39, pp. 445-471, 2009.

[16] W. Small IV, P. Singhal, T. S. Wilson, and D. J. Maitland, "Biomedical applications of thermally activated shape memory polymers," *Journal of materials chemistry,* vol. 20, pp. 3356-3366, 2010.

[17] A. Yokoo, K. Wada, and L. C. Kimerling, "Pattern size reduction of nanoprint-fabricated structures on heat-shrinkable film," *Japanese Journal of Applied Physics,* vol. 46, p. 6395, 2007.

[18] X. Zhu and T. Cui, "Polymer shrinkage of hot embossed microstructures for higher aspect ratio and smaller size," *Sensors and Actuators A: Physical,* vol. 195, pp. 21-26, 2013.

[19] X. M. Zhao, Y. Xia, D. Qin, and G. M. Whitesides, "Fabrication of polymeric microstructures with high aspect ratios using shrinkable polystyrene films," *Advanced materials,* vol. 9, pp. 251-254, 1997.

[20] X.-M. Zhao, Y. Xia, O. J. Schueller, D. Qin, and G. M. Whitesides, "Fabrication of microstructures using shrinkable polystyrene films," *Sensors and Actuators A: Physical,* vol. 65, pp. 209-217, 1998.

[21] S. Sayed and P. R. Selvaganapathy, "Multi-step proportional miniaturization to sub-micron dimensions using pre-stressed polymer films," *Nanoscale Advances,* vol. 2, pp. 5461-5467, 2020.

[22] S.-M. Park, X. Liang, B. D. Harteneck, T. E. Pick, N. Hiroshiba, Y. Wu, B. A. Helms, and D. L. Olynick, "Sub-10 nm nanofabrication via nanoimprint directed self-assembly of block copolymers," *ACS nano,* vol. 5, pp. 8523-8531, 2011.

[23] J. Sun, J. Zhuang, Y. Liu, H. Xu, J. Horne, E. K. Wujcik, H. Liu, J. E. Ryu, D. Wu, and Z. Guo, "Development and application of hot embossing in polymer processing: a review," *ES Materials & Manufacturing,* vol. 6, pp. 3-17, 2019.

[24] D. Nguyen, D. Taylor, K. Qian, N. Norouzi, J. Rasmussen, S. Botzet, M. Lehmann, K. Halverson, and M. Khine, "Better shrinkage than shrinky-dinks," *Lab on a Chip,* vol. 10, pp. 1623-1626, 2010.

[25] C. M. Gabardo, Y. Zhu, L. Soleymani, and J. M. Moran-Mirabal, "Bench-top fabrication of hierarchically structured high-surface-area electrodes," *Advanced Functional Materials,* vol. 23, pp. 3030-3039, 2013.

[26] D. Graham-Rowe, "Tunable structural colour," *Nature Photonics,* vol. 3, pp. 551-553, 2009.

[27] Y. Shen, V. Rinnerbauer, I. Wang, V. Stelmakh, J. D. Joannopoulos, and M. Soljacic, "Structural colors from Fano resonances," *Acs Photonics,* vol. 2, pp. 27-32, 2015.

[28] A. Kristensen, J. K. Yang, S. I. Bozhevolnyi, S. Link, P. Nordlander, N. J. Halas, and N. A. Mortensen, "Plasmonic colour generation," *Nature Reviews Materials,* vol. 2, pp. 1-14, 2016.

[29] F. Lütolf, M. Stalder, and O. J. Martin, "Metallized Gratings Enable Color Effects and Floating Screen Films by First-Order Diffraction," *Advanced Optical Materials*, vol. 3, pp. 1793-1799, 2015.

[30] A. B. Christiansen, E. Højlund-Nielsen, J. Clausen, G. P. Caringal, N. A. Mortensen, and A. Kristensen, "Imprinted and injection-molded nano-structured optical surfaces," in *Nanostructured Thin Films VI*, 2013, p. 881803.

4 Chapter 4

High resolution fabrication of nano patterns by multi-step iterative miniaturization of hot embossed pre-stressed polymer films and constrained shrinking

Complete Citation:

S. Sayed and P. R. Selvaganapathy, "High resolution fabrication of nano patterns by multi-step iterative miniaturization of hot embossed pre-stressed polymer films and constrained shrinking", in progress, 2021.

Contribution:

S. Sayed: Designed and performed all experiments, interpretation and analysis of data, wrote the manuscript draft.

P. R. Selvaganapathy: Supervised S. Sayed and provided guidance, revised and edited the manuscript.

4.1 Abstract

Fabrication of nano structures and patterns is the basis of diverse technologies and applications in our life ranging from microelectronics and semiconductors to nanofludics, biomedical and biosensors. However, creation of nano patterns by means of conventional nanofabrication techniques such as electron beam lithography is expensive and time consuming. Here we develop a multi-step miniaturization approach using pre-stressed polymer films to generate nano patterns from microscale patterns without the need of complex nanolithography methods. Pre-stressed polymer films have been used as a miniaturization technique to fabricate features with smaller size than the initial imprinted features. However, the height of the imprinted features is significantly reduced after thermal shrinking of the pre-stressed films due to shape memory effect of the polymer, and as a result the topographical features tend to disappear after shrinking. We have developed a miniaturization approach that controls the material flow and maintain the shrunken patterns by applying mechanical constraints during shrinking process. The combination of hot embossing and the constrained shrinking opens the way to reduce the size of the initial imprinted features even at nanoscale. The developed multi-step miniaturization approach allows using the shrunk pattern as a master for a next miniaturization cycle. Well defined patterns as small as 100 nm are fabricated showing 10-fold reduction in size of the original master. The developed approach also allows the transfer of the shrunk polymeric patterns into a silicon substrate which can be used as a functional substrate for many applications or directly as a master for nanoimprint lithography.

4.2 Introduction

Nanolithography plays a pivotal role in integrated circuit (IC) and semiconductor industry as well as for fabrication of microelectronics and biosensors. The current breakthrough and success of IC manufacturing relies on the ability to continuously miniaturize features and patterns areas on the substrate surface that can increase the density of transistors while reducing the overall size and dimensions of the chip [1, 2]. This trend requires fabrication of high resolution master patterns which are generally fabricated using serial writing nanolithography methods [3-6]. These methods often involve high-cost processes and equipment, they are also time consuming specially for large area patterning at nanoscale dimensions [7-9]. Thus, developing a simple miniaturization approach that can significantly reduce the features size from a microscale to a nanoscale can be potentially crucial for fabrication of nano patterns at lower cost without the need of conventional nanolithography techniques.

Pre-stressed polymer films have been used as a miniaturization approach in the microscale to reduce the size of the original patterns by patterning the polymer films, then thermally releasing the pre-stresses by heating above the glass transition temperature [10, 11]. As a result, it allows shrinking of the film and hence reducing the size of the imprinted patterns on that shrinkable film [12]. The common patterning methods that have been used to pattern shrinkable films include printing [13-15], reactive ion etching (RIE) [16, 17], and hot embossing [18].

Hot embossing is a well known patterning process that is used to transfer patterns from a master mold into a polymeric substrate. It is one of the important nanolithography methods which is used to replicate nano features and patterns through thermal nanoimprint

process [19, 20]. Although hot embossing has been used to pattern pre-stressed films, it fails to retain nanoscale patterns after shrinking without losing the topographical features [21, 22]. Due to the shape memory effect, the polymer material relaxes during shrinking process that results in erasure of the patterns embedded on the polymer film. This results in significant reduction of the height of the imprinted patterns and the patterns tend to disappear. We have discovered a miniaturization approach that controls the polymer reflow and preserves the topographical features after shrinking by mechanically constraining the film during shrinking process [22]. The film is mechanically constrained in one direction which allows releasing the stresses only in the orthogonal direction while minimizing the change in height of the imprinted features. Then the film is constrained in the orthogonal direction to obtain biaxial shrinkage which finally leads to reduce the size of the features and preserve the topographical features. Although we have demonstrated that this constrained shrinking process is scalable down to nanoscale, the shrunk pattern that it produces is not suitable for multistep iterative miniaturization which can reduce the size even further.

Here, we report such a multi-step miniaturization approach that significantly reduces the patterns size from microscale to nanoscale over several cycles without the need to use conventional nanolithography techniques to fabricate nano patterns. A combination of hot embossing and constrained shrinking of the pre-stressed polymer films was developed in this process to transfer the master patterns into the polymer films and allow retention of shrunken patterns. After shrinking, the miniaturized pattern was used to fabricate a new master which is then used as a master for the next miniaturization cycle. After three miniaturization steps, the size of the patterns was reduced by total reduction of 10x and

high resolution patterns as small as 100 nm are fabricated. This multi-step miniaturization approach can potentially be applied to fabricate nanoimprint lithography masters for integrated circuit manufacturing and overcome the challenges associated with fabricating masters at that scale using e-beam lithography.

4.3 Experimental details and methods

4.3.1 Multi-step miniaturization process

Nanoimprint lithography is a well-established fabrication process which is used to replicate master patterns onto another substrate over large area at high throughput and low cost. However, fabrication of master molds required for the nanoimprint lithography process is challenging. Master molds are primarily fabricated by electron beam lithography or focused ion beam techniques which require expensive equipment and long processing time particularly for large area patterning. Thus, developing a fabrication process that can create nanoimprint lithography masters without using such complex processes could be valuable for rapid, low cost and scalable nanofabrication. One approach that can be pursued is to create low resolution patterns using scalable and high throughput fabrication methods such as photolithography and then proportionally miniaturize that microscale pattern into a nanoscale pattern.

Following this approach, we have developed a new multi-step miniaturization approach based on constrained shrinking of hot embossed pre-stressed polymer films to significantly reduce the size of the initial microscale patterns into the nanoscale while maintaining the topographical features. The developed approach allows the use of the shrunk pattern from a previous step as the master for the next miniaturization cycle which

can be repeated iteratively in order to achieve the required resolution. A schematic illustration of the multi-step miniaturization process is shown in Figure 4-1.

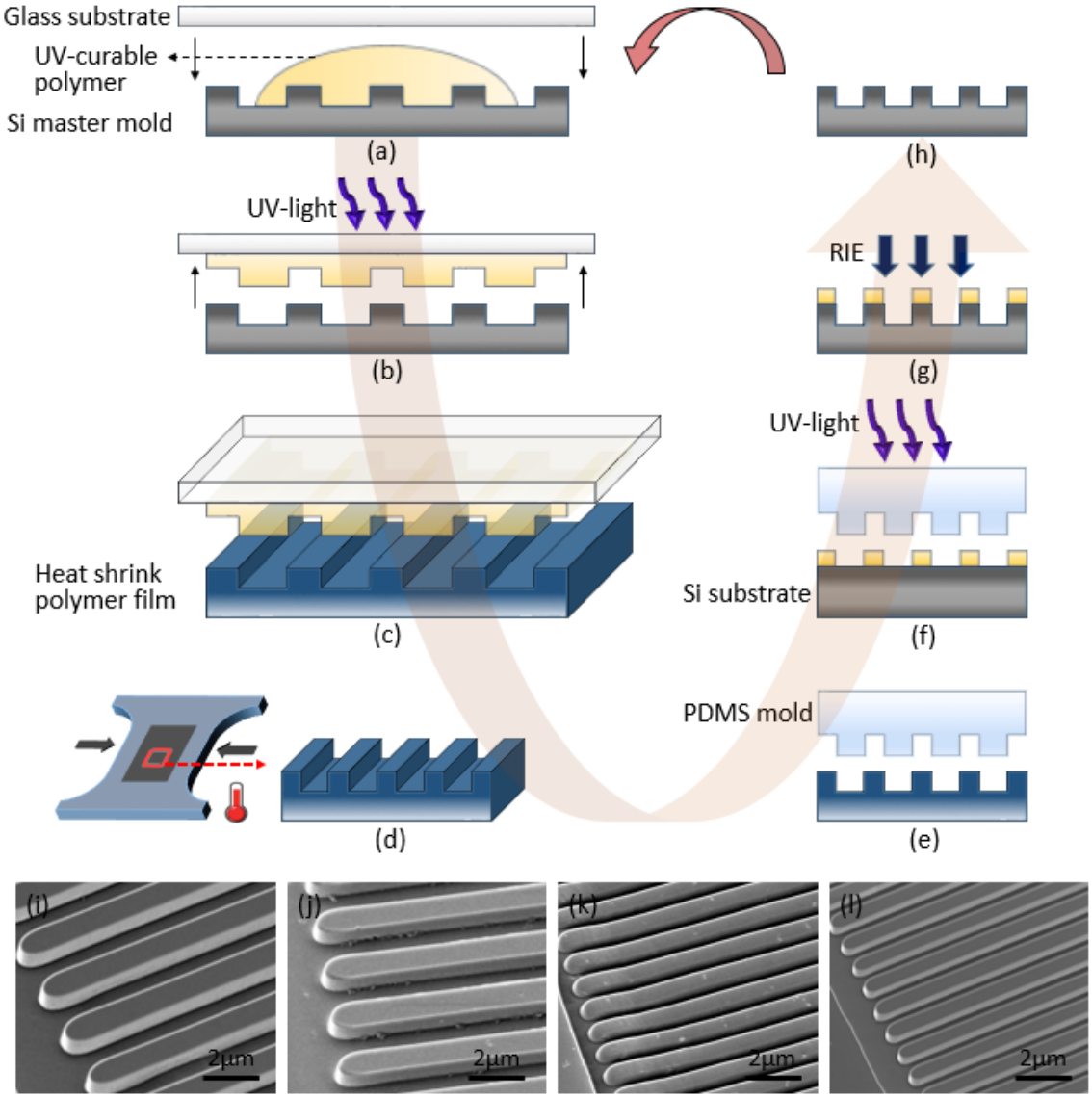

Figure 4-1 Scheme of the multi-step miniaturization approach using pre-stressed polymer films. (a, b) Fabrication of polymer working stamp. (c) Hot embossing the pre-stressed film. (d) Constrained shrinking. (e) Cast PDMS mold. (f) Soft imprint polymer pattern on Si substrate. (g) RIE Si substrate. (h) Clean patterned Si substrate which is used as a master for next miniaturization step. SEM images of the results of a complete miniaturization cycle for (i) Si master, (j) imprint on pre-stressed film, (k) shrunk pattern, (l) new Si master.

First, a Si master mold was fabricated using direct laser writing to create microscale (1 μm) patterns although they can be also fabricated by photolithography. Then, a polymer working stamp was replicated from the Si master mold to be used directly to imprint the pre-stressed polymer films. Although the Si master can be used directly for hot embossing, the polymer working stamp was found to be better for demolding of the imprinted film from the stamp (see supplementary information, section 1) [23, 24]. The working stamp was fabricated using UV-curable polymer that was attached to a glass substrate and cured under UV light source, Figure 4-1a,b. Then, a polystyrene (PS) heat shrinkable film was imprinted using the fabricated working stamp in a hot embossing process under optimized conditions of molding force, temperature and time, Figure 4-1c. These conditions were optimized to ensure the quality of the imprinted patterns while not affecting the ability of the embossed film to shrink. After hot embossing, the film was carefully demolded from the stamp at a specific separation temperature to avoid damage or deformation of the imprinted patterns during separation.

In order to shrink the patterned film, the film was mechanically constrained in one direction and heated above its glass transition temperature which allowed shrinking only in the orthogonal direction, Figure 4-1d. Then, to obtain biaxial shrinkage, the film was constrained in the orthogonal direction and heated. As a result, the size of the patterned features reduced without losing the topographical features. Now, the shrunk patterns were used to generate a new master to be used for the next miniaturization cycle. After thermal shrinking, the surface of the shrunk film was not completely flat compared to a Si substrate. Besides, the edges and sidewalls of the shrunk features become more curved due to softening of the polymer during heating. Finally, the aspect ratio of the structures increased

which can result in instability of the line features especially at the nanoscale. Thus, it was found that fabricating an intermediate Si master was better than using the shrunk PS film directly in terms of obtaining a completely flat substrate surface and decoupling the aspect ratio of the structure from the shrink dynamics enabling precise structures with vertical sidewalls even in the nanoscale.

In order to generate the new master, polydimethylsiloxane (PDMS) was cast on the shrunk PS film (Figure 4-1e) and used to transfer the patterns onto a Si substrate by soft UV imprint lithography (Figure 4-1f). Then, the transferred resist pattern was then used as a mask to etch the Si substrate by RIE, Figure 4-1g. The RIE was optimized using mixed gas process to successfully transfer patterns into the Si substrate (see supplementary information, section 2). Finally, the etched Si substrate was cleaned to remove the remaining resist mask and was used as a master for a next miniaturization cycle, Figure 4-1h.

Scanning electron microscope (SEM) images of the initial master, imprinted PS film, shrunk film, and the new Si master are shown in Figure 4-1i,j,k,l respectively as an example of the feature evolution through the complete miniaturization cycle. As shown in the figure, the pattern was significantly miniaturized after shrinking while the topographical features were preserved. In contrast, direct shrinking resulted in losing topographical features where the pattern height was dramatically decreased (see supplementary information). It can be noted that the edges of the shrunk pattern became curved (Figure 4-1k) compared to the imprinted pattern before shrink (Figure 4-1j). However, a pattern with well-defined edges was obtained after RIE of a Si substrate (Figure 4-1l) which allows faithful reproduction of the pattern in the next miniaturization step. Due to the introduction of the intermediate

Si transfer stamp using the soft UV imprint lithography followed by RIE, the master produced after each step can have independent control over miniaturization in the X-Y and Z directions and enable successful and proportionate miniaturization over a large number of steps. The multi-step miniaturization approach allows reducing the size of the initial patterns several times to nanoscale dimensions and generate new masters of smaller size patterns.

4.3.2 Polymer working stamp fabrication

The working stamp was fabricated using UV-curable polymer (MD700, Solvay) attached to a glass substrate. The glass substrate was first coated with adhesion promoter (EVGprimK) to improve polymer adhesion to the glass surface. The working stamp was replicated from a Si master which was fabricated by direct laser writer (Heidelberg, µPG 101) to pattern a photoresist layer (S1808) coated on a Si substrate, then Si is etched by RIE process and the remaining photoresist mask was removed. The Si master was coated with anti-stick layer before working stamp fabrication. The UV-curable polymer was mixed with photoinitiator (2% by weight) and placed in a vacuum chamber to outgas. Then, the polymer mixture was poured on the Si master and the glass substrate was placed on top of them. The polymer was exposed to UV light source for 5 min to cure. Finally, the working stamp was carefully separated from Si master and the excess polymer was rinsed with HFE solvent.

4.3.3 Hot embossing pre-stressed films

Polystyrene pre-stressed films (Graphix Shrink Film, Maple Heights, Ohio) were imprinted by hot embossing using (EVG520 HE) equipment. The fabricated polymer working stamp was used to imprint pre-stressed films. Hot embossing process parameters were as follow:

molding temperature 125 ^{o}C, molding force 4500 N and molding time 5 min. After hot embossing, the imprinted film and polymer stamp were cooled down while the molding force was still applied. Then the imprinted film was carefully demolded from the stamp at demolding temperature around 60 ^{o}C.

4.3.4 Constrained shrinking

After imprinting patterns onto the pre-stressed film, the film was mechanically constrained at two opposite ends along one direction using paper binder clips. The patterned area was placed at the middle between the two constrained ends. The assembly was placed in an oven and heated at 130 ^{o}C for 9-10 min. This resulted in shrinking the film in one direction only orthogonal to the constrained direction. In order to obtain biaxial shrinkage, the film was then constrained in the orthogonal direction with the patterned area at the middle and heated again at same temperature and time.

4.3.5 Reactive ion etching RIE

The shrunk patterns were transferred to Si substrate by RIE to fabricate a master for the next miniaturization step. RIE equipment (Oxford PlasmaPro 100) was used. Mixed gases RIE process was used to etch Si patterns with gases C_4F_8 and SF_6 of flow rates 100 sccm and 50 sccm respectively. The RIE time was 1-2 min depending on the required etch depth. The SF_6 flow rate was reduced to 40 sccm when etching the smaller patterns to improve selectivity.

4.3.6 SEM imaging

SEM images were taken using (JEOL JSM-7000F). The imprinted pre-stressed films were coated with a thin gold layer (8 nm) for preparation of the samples prior to SEM imaging. The Si patterns were imaged without coating.

4.4 Results and Discussion

4.4.1 Fabrication of nanoscale patterns

The new multi-step miniaturization approach can be used as a nanofabrication method that can reduce the size of larger patterns several times down to nanoscale. This approach demonstrates that constrained shrinking of hot embossed patterns on pre-stressed films can generate well defined patterns at higher resolution which then can be used as a master for further miniaturization steps even at 100 nm scale.

The scalability of this approach was demonstrated by miniaturization of a micrometer master pattern into approximately 100 nm pattern over three miniaturization steps. The initial master pattern is a line-space pattern with a line width of 1 µm and 1 µm spacing (Figure 4-2a), which was fabricated by using a laser lithographic process. After hot embossing, the imprinted pattern on the PS shrinkable film has same dimensions of the master (Figure 4-2b). The patterned film was then miniaturized by applying constrained shrinking which resulted in 50% reduction in size approximately (Figure 4-2c). The shrunk pattern was used to fabricate a new Si master which was used for the next miniaturization cycle.

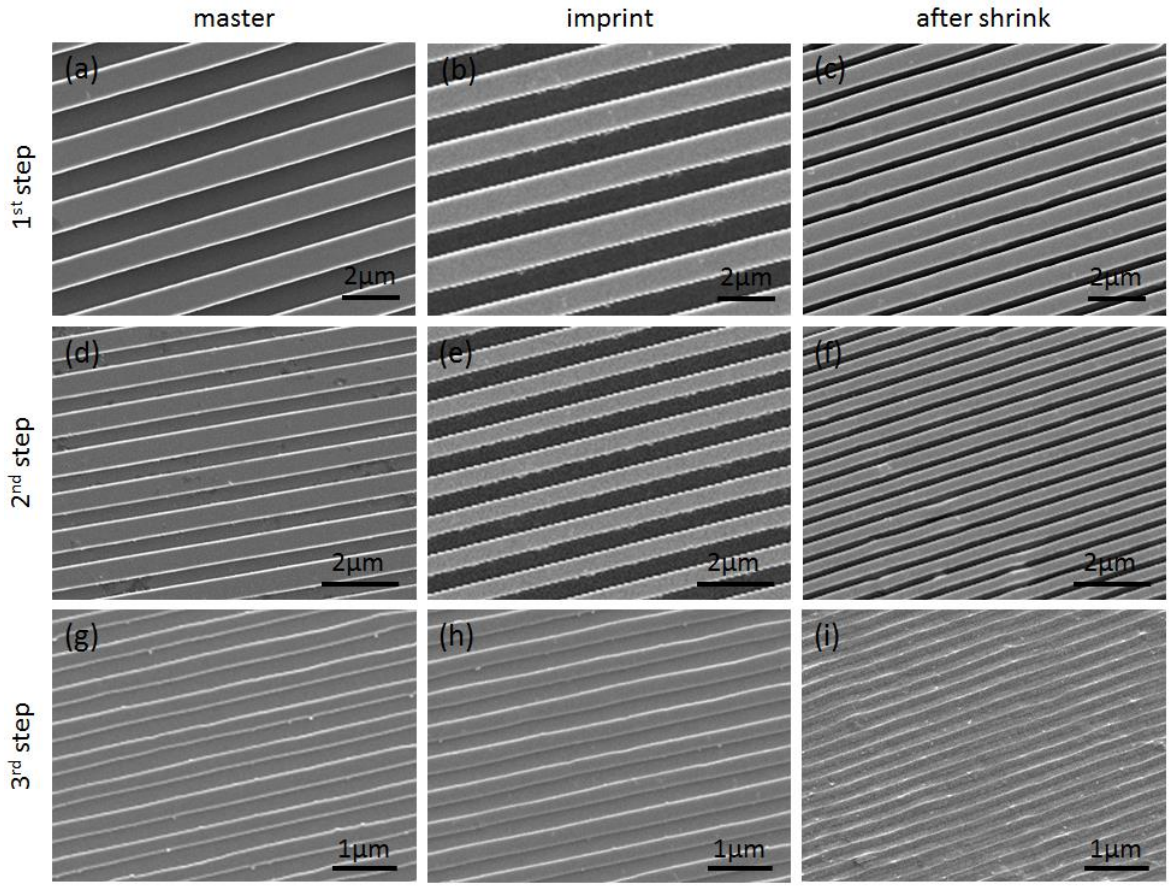

Figure 4-2 Multi-step miniaturization of line-space pattern for three successive cycles. SEM images of (a, d, g) Si master, (b, e, h) imprinted pre-stressed film, and (c, f, i) shrunk pattern for each miniaturization step. The initial master pattern has line width w=1µm, spacing s=1µm. After shrinking of first step w=675nm, s=320nm, after second step w=280nm, s=190nm, after third step w=130nm, s=100nm.

Following the procedures described in Figure 4-1, the miniaturization process was repeated for three cycles. The initial master and the new fabricated masters that were used for the three miniaturization cycles are shown in Figure 4-2a, d, g. The imprinted patterns on pre-stressed films are shown in Figure 4-2b, e, h. The shrunk patterns after each miniaturization step are shown in Figure 4-2c, f, i. After the first miniaturization step, the pattern size was shrunk by 50%, the line width reduced to 675 nm and the spacing to 320 nm. After the second step, the line width reduced to 280 nm and the spacing to 190 nm,

showing 77% total reduction from the initial pattern. After the third miniaturization step, the line width reduced to 130 nm while the spacing reduced to 100 nm, which resulted in 89% total reduction compared to the initial pattern. The results of the multi-step miniaturization approach show that from a single master pattern, three higher resolution patterns were fabricated with high fidelity achieving features size as small as 100 nm for the smallest pattern. It should be noted that the spacing between the lines reduced more than the line width itself probably because of the effect of the imprinting process. When the imprinted film is thermally heated, the compressive stresses embedded in the pre-stressed film are released leading to shrink the polymer material into smaller size. However, the imprinting process that creates the features also plastically deforms the material and introduces additional stresses at the surface in addition to the pre-stress in the bulk. During the imprint process material is moved from the spacing region and into the line width region. This creates a large stress at the surface in the spacing as compared with that in the linewidth region. Therefore, release of this stress by thermal shrinking can potentially shrink the spacing more than the linewidth. Since the stress induced is dependent on the imprinting process and the amount of material displaced, one would expect that the asymmetry in the shrinkage will reduce as smaller and smaller patterns are imprinted. This is seen in the results obtained where the asymmetry in the shrinkage is larger when the 1 μm patterns are imprinted as compared with smaller patterns. Here, the applied hot embossing conditions lead to 50-55% shrink ratio, instead of 60% shrink ratio for typical PS shrinkable films [25, 26].

4.4.2 Aspect ratio of the fabricated nanopillar array

The multi-step miniaturization process can be used for nanofabrication of different feature shapes. In order to demonstrate the variety of features that can be miniaturized, pillars array was fabricated. The initial master of the pillars array has circular pillars of 1 μm diameter with similar spacing between pillars (Figure 4-3a). The initial pattern was imprinted and miniaturized for three sequential miniaturization cycles. The initial master and the following fabricated masters are shown in Figure 4-3a, d, g. The imprinted patterns on PS films after hot embossing are shown in Figure 4-3b, e, h. The miniaturized patterns after constrained shrinking are shown in Figure 4-3c, f, i.

After the first miniaturization step, the pillars diameter reduced from 1 μm to 630 nm while the spacing reduced to 350 nm showing an overall reduction of 51%. After the second step, the pillars diameter reduced further to 275 nm and spacing to 190 nm achieving 77% total reduction in size from the initial master. After the third miniaturization step, the pillars diameter reduced more to 105 nm and the spacing to 100 nm, which resulted in a significant total reduction of 90% compared to the initial pattern. The proportional size reduction of the pillar array over three miniaturization steps is shown in Figure 4-3j. Similar to the line-space pattern, the spacing between pillars shrinks more than the pillars diameter due to the stress induced during the imprinting process. However, the difference between pillars diameter and spacing decreases when the shrunk pattern was transferred into a Si substrate to fabricate a master for the next step. After patterning the UV-curable polymer mask on the Si substrate (Figure 4-1f), the residual polymer layer was removed by a quick RIE using Oxygen to expose the Si surface. During this RIE process, the polymer pattern features were also slightly etched in the lateral directions which leads to reduction the pillar's diameter and increase in spacing between them. Then, the pattern was transferred

to the Si substrate by selective RIE of Si. The results show that the pattern integrity was maintained and high resolution patterns were fabricated with 10x reduction in size of the original pattern.

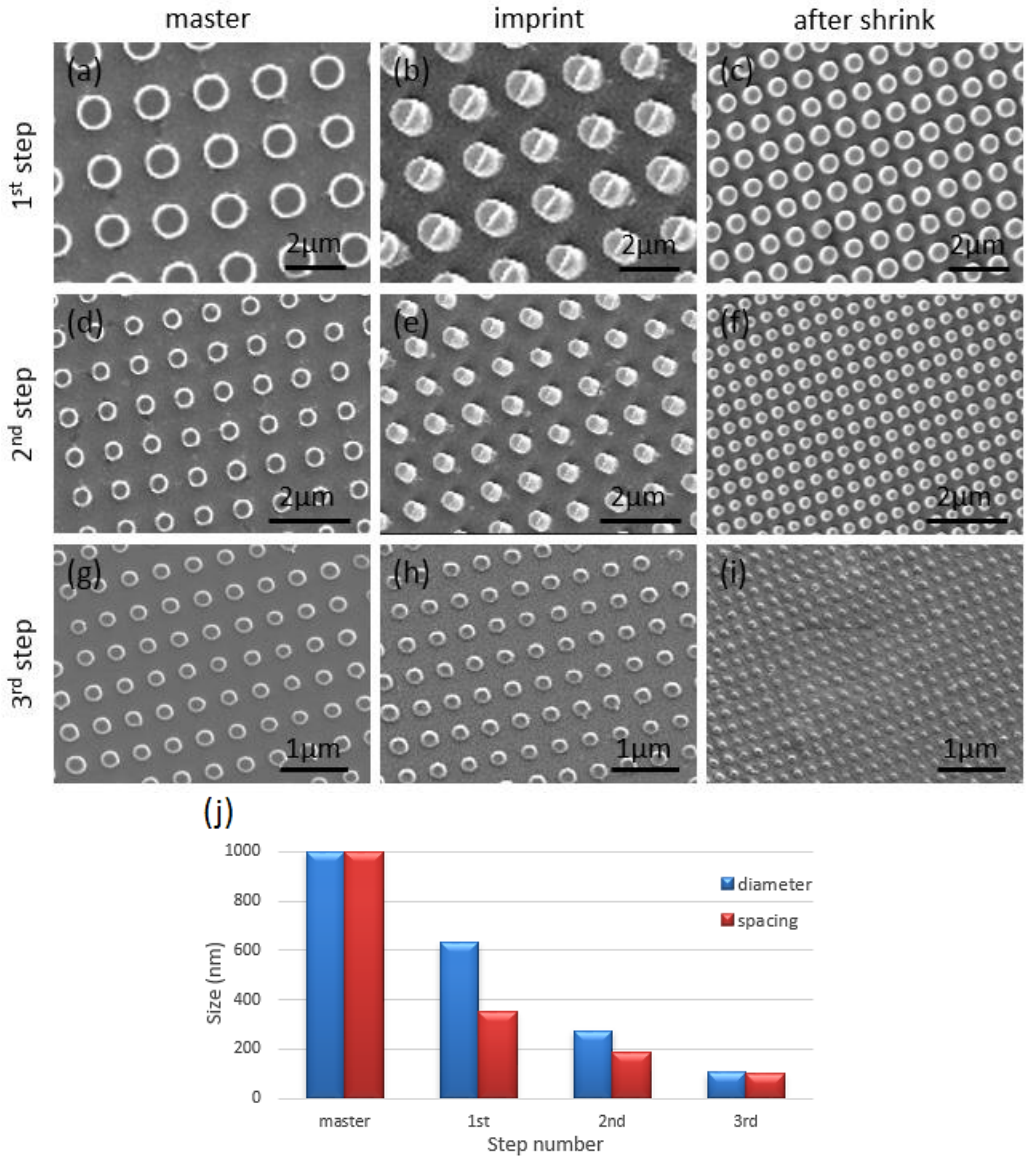

Figure 4-3 Multi-step miniaturization of pillars array for three successive cycles. SEM images of (a, d, g) Si master, (b, e, h) imprinted pre-stressed film, and (c, f, i) shrunk pattern for each miniaturization step. (j) Graph of size reduction over miniaturization steps. The initial master pattern has pillar diameter d=1μm, spacing s=1μm. After shrinking of first step d=630nm, s=350nm, after second step d=275nm,

The multi-step miniaturization approach is based on shrinking patterns on pre-stressed polymer films that were imprinted by hot embossing. However, direct shrinking of hot embossed patterns results in decrease in the height of the patterns dramatically and the patterns tend to disappear after shrinking (see supplementary information, section 3). As a result, the aspect ratio is also dramatically reduced. In contrast, the developed constrained shrinking process allows to reduce the patterns size without losing the topographical features. In particular, the height of the patterns is retained or slightly decreased when applying directional constraints during shrinking while the in plane feature size dramatically reduces. Thus, the aspect ratio is expected to increase which is considered an advantage in nanofabrication. However, increase in aspect ratio during successive steps can result in tall and weak structures that can prevent precise pattern imprinting.

The intermediate step to transfer the patterns obtained from constrained shrinkage onto a Si master allows for independent control of the height of the pattern and therefore the aspect ratio over several miniaturization cycles. Figure 4-4 shows the aspect ratio of the pillars array over three miniaturization cycles. For each cycle, SEM images were taken at an inclined view for the master patterns (Figure 4-4a, b, c) and the shrunk patterns (Figure 4-4d, e, f) in order to demonstrate the height of fabricated pillars. The aspect ratios of the master and shrunk patterns are shown in Figure 4-4g. It can be seen that the aspect ratio of features on the shrunken films increased after constrained shrinking compared to the initial master for each miniaturization step. In addition, the aspect ratio was maintained for the first and second miniaturization cycles as the height of the patterns in the master was controlled by RIE of the Si intermediate master. However, the aspect ratio of the master and shrunk patterns of third step was lower. It may be due to an unoptimized RIE

process when fabricating the third step master at such small dimensions. The polymer mask was etched quickly, and hence deeper etch of the Si could not be achieved. However, in the future a more resistant mask can be used and RIE process can be optimized to maintain the required aspect ratio [27-29].

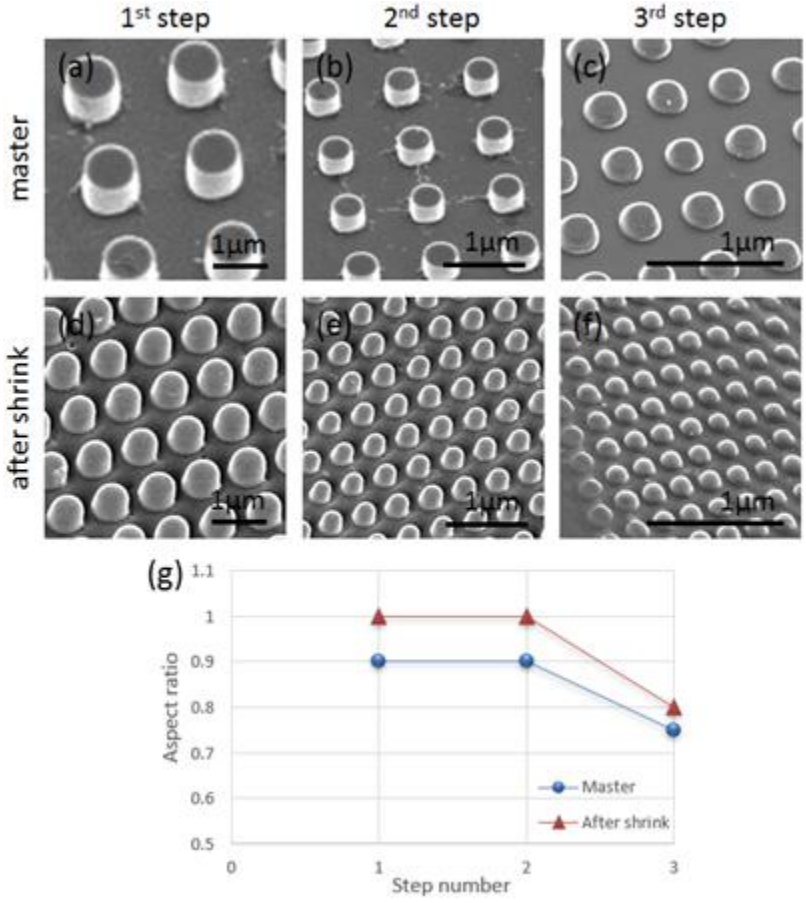

Figure 4-4 Aspect ratio of the fabricatted patterns. SEM images of (a, b, c) Si master, and (d, e, f) shrunk patterns for three miniaturization steps. (g) Aspect ratio of the master and shrunk patterns for each miniaturization step.

4.4.3 Fabrication of complex patterns

In order to demonstrate that the multi-step miniaturization approach is versatile, a more complicated pattern with alphabets, ("MCMASTER") was also fabricated and miniaturized for three sequential miniaturization cycles (Figure 4-5). The total reduction in size that was

achieved after each miniaturization cycle was 51%, 78%, and 88% respectively. The line that forms each letter of MCMASTER has an initial width of 2 µm. After each miniaturization step the line width was reduced to 970 nm, 450 nm, and 240 nm respectively. It can be seen that all different letters were miniaturized in the same proportion even for the letters that include inclined lines such as "A". This indicates that the technique is versatile and can proportionally miniaturize not only line and dot patterns but any complex pattern of choice. It can be noticed that the shrunk pattern of the third miniaturization step was slightly distorted (Figure 4-5i). This may be due to misalignment in the constrained direction during shrinking process. Often when the constraints on either side are not aligned with each other such distortions can occur. Use of a more optimized jig for constraining would address this issue. Nevertheless, the results show that the multi-step miniaturization approach can be used for almost any kind of patterns and different feature shapes to significantly reduce the size of the original features from a micrometer scale into nanoscale. This can overcome the challenges of directly fabricating nano patterns using conventional photolithography methods.

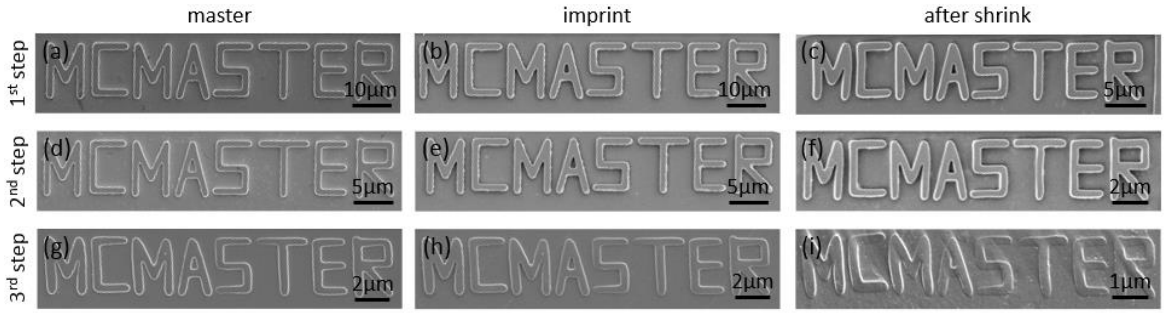

Figure 4-5 Multi-step miniaturization of "MCMASTER" name for three successive cycles. SEM images of (a, d, g) Si master, (b, e, h) imprinted pre-stressed film, and (c, f, i) shrunk pattern for each miniaturization step.

4.5 Conclusion

In summary, we have demonstrated a multi-step miniaturization approach using pre-stressed polymer films that can reduce the size of the original patterns dramatically from micrometer scale to nanoscale. Imprinted patterns on pre-stressed films by hot embossing were miniaturized using constrained shrinking process which allowed to reduce the size of the initial patterns without losing topographical features. The miniaturization process can be repeated several times for further size reduction by using shrunk patterns to generate new masters for next miniaturization steps. We have fabricated well defined, high resolution, nanoscale patterns with sizes as small as 100 nm starting from a master with patterns 1 μm in size. From a single master, three smaller patterns were fabricated achieving 10x reduction in size over three miniaturization steps. This powerful approach can be used to fabricate masters with nanoscale features and overcome the challenges of nanofabrication using serial writing techniques. Moreover, we have shown that the aspect ratio of the miniaturized patterns can be maintained over several miniaturization cycles which improves the pattern fidelity. The multi-step miniaturization approach described here is a scalable and versatile nanofabrication process that can be used for a wide range of applications including integrated circuit manufacturing and nanoimprint lithography.

References

[1] S. Sreenivasan, "Nanoimprint lithography steppers for volume fabrication of leading-edge semiconductor integrated circuits," *Microsystems & nanoengineering*, vol. 3, pp. 1-19, 2017.

[2] E. M. Sebastian, S. K. Jain, R. Purohit, S. Dhakad, and R. Rana, "Nanolithography and its current advancements," *Materials Today: Proceedings*, vol. 26, pp. 2351-2356, 2020.

[3] P. van Assenbergh, E. Meinders, J. Geraedts, and D. Dodou, "Nanostructure and microstructure fabrication: from desired properties to suitable processes," *Small*, vol. 14, p. 1703401, 2018.

[4] M. Roeder, T. Guenther, and A. Zimmermann, "Review on fabrication technologies for optical mold inserts," *Micromachines*, vol. 10, p. 233, 2019.

[5] R. Menon, A. Patel, D. Gil, and H. I. Smith, "Maskless lithography," *Materials Today*, vol. 8, pp. 26-33, 2005.

[6] J. Chen, J. Shi, A. Cattoni, D. Decanini, Z. Liu, Y. Chen, and A.-M. Haghiri-Gosnet, "A versatile pattern inversion process based on thermal and soft UV nanoimprint lithography techniques," *Microelectronic Engineering*, vol. 87, pp. 899-903, 2010.

[7] H. Lan and H. Liu, "UV-nanoimprint lithography: structure, materials and fabrication of flexible molds," *Journal of nanoscience and nanotechnology*, vol. 13, pp. 3145-3172, 2013.

[8] S. E. Kapl, H. Loeschner, W. Piller, M. Witt, W. Pilz, F. Letzkus, M. Jurisch, M. Irmscher, and E. Platzgummer, "Characterization of CMOS programmable multi-beam blanking arrays as used for programmable multi-beam projection lithography and resistless nanopatterning," *Journal of Micromechanics and Microengineering*, vol. 21, p. 045038, 2011.

[9] H. Matsumoto, H. Inoue, H. Yamashita, H. Morita, S. Hirose, M. Ogasawara, H. Yamada, and K. Hattori, "Multi-beam mask writer MBM-1000 and its application field," in *Photomask Japan 2016: XXIII Symposium on Photomask and Next-Generation Lithography Mask Technology*, 2016, p. 998405.

[10] J. Hu, Y. Zhu, H. Huang, and J. Lu, "Recent advances in shape–memory polymers: Structure, mechanism, functionality, modeling and applications," *Progress in Polymer Science*, vol. 37, pp. 1720-1763, 2012.

[11] P. T. Mather, X. Luo, and I. A. Rousseau, "Shape memory polymer research," *Annual Review of Materials Research*, vol. 39, pp. 445-471, 2009.

[12] S. Lin, E. K. Lee, N. Nguyen, and M. Khine, "Thermally-induced miniaturization for micro-and nanofabrication: progress and updates," *Lab on a Chip*, vol. 14, pp. 3475-3488, 2014.

[13] D. Nguyen, D. Taylor, K. Qian, N. Norouzi, J. Rasmussen, S. Botzet, M. Lehmann, K. Halverson, and M. Khine, "Better shrinkage than shrinky-dinks," *Lab on a Chip*, vol. 10, pp. 1623-1626, 2010.

[14] P. J. Goodrich, F. Sharifi, and N. Hashemi, "Rapid prototyping of microchannels with surface patterns for fabrication of polymer fibers," *RSC Advances*, vol. 5, pp. 71203-71209, 2015.

[15] A. Grimes, D. N. Breslauer, M. Long, J. Pegan, L. P. Lee, and M. Khine, "Shrinky-Dink microfluidics: rapid generation of deep and rounded patterns," *Lab on a Chip*, vol. 8, pp. 170-172, 2008.

[16] X.-M. Zhao, Y. Xia, O. J. Schueller, D. Qin, and G. M. Whitesides, "Fabrication of microstructures using shrinkable polystyrene films," *Sensors and Actuators A: Physical*, vol. 65, pp. 209-217, 1998.

[17] S. Sayed and P. R. Selvaganapathy, "Multi-step proportional miniaturization to sub-micron dimensions using pre-stressed polymer films," *Nanoscale Advances*, vol. 2, pp. 5461-5467, 2020.

[18] X. Zhu and T. Cui, "Polymer shrinkage of hot embossed microstructures for higher aspect ratio and smaller size," *Sensors and Actuators A: Physical*, vol. 195, pp. 21-26, 2013.

[19] J. Sun, J. Zhuang, Y. Liu, H. Xu, J. Horne, E. K. Wujcik, H. Liu, J. E. Ryu, D. Wu, and Z. Guo, "Development and application of hot embossing in polymer processing: a review," *ES Materials & Manufacturing*, vol. 6, pp. 3-17, 2019.

[20] S.-M. Park, X. Liang, B. D. Harteneck, T. E. Pick, N. Hiroshiba, Y. Wu, B. A. Helms, and D. L. Olynick, "Sub-10 nm nanofabrication via nanoimprint directed self-assembly of block copolymers," *ACS nano*, vol. 5, pp. 8523-8531, 2011.

[21] A. Yokoo, K. Wada, and L. C. Kimerling, "Pattern size reduction of nanoprint-fabricated structures on heat-shrinkable film," *Japanese Journal of Applied Physics*, vol. 46, p. 6395, 2007.

[22] S. Sayed and P. R. Selvaganapathy, "Constrained shrinking of nanoimprinted pre-stressed polymer films to achieve programmable, high-resolution, miniaturized nanopatterns," *Nanoscale Advances*, vol. under review, 2021.

[23] T. Glinsner, T. Veres, G. Kreindl, E. Roy, K. Morton, T. Wieser, C. Thanner, D. Treiblmayr, R. Miller, and P. Lindner, "Fully automated hot embossing processes utilizing high resolution working stamps," *Journal of Vacuum Science & Technology B, Nanotechnology and Microelectronics: Materials, Processing, Measurement, and Phenomena*, vol. 28, pp. 36-41, 2010.

[24] L. Peng, Y. Deng, P. Yi, and X. Lai, "Micro hot embossing of thermoplastic polymers: a review," *Journal of Micromechanics and Microengineering*, vol. 24, p. 013001, 2013.

[25] D. Dyer, S. Shreim, S. Jayadev, V. Lew, E. Botvinick, and M. Khine, "Sequential shrink photolithography for plastic microlens arrays," *Applied Physics Letters*, vol. 99, p. 034102, 2011.

[26] C. M. Gabardo, Y. Zhu, L. Soleymani, and J. M. Moran-Mirabal, "Bench-top fabrication of hierarchically structured high-surface-area electrodes," *Advanced Functional Materials*, vol. 23, pp. 3030-3039, 2013.

[27] E. Baquedano, R. V. Martinez, J. M. Llorens, and P. A. Postigo, "Fabrication of silicon nanobelts and nanopillars by soft lithography for hydrophobic and hydrophilic photonic surfaces," *Nanomaterials*, vol. 7, p. 109, 2017.

[28] P. Doll, A. Al-Ahmad, A. Bacher, A. Muslija, R. Thelen, L. Hahn, R. Ahrens, B. Spindler, and A. Guber, "Fabrication of silicon nanopillar arrays by electron beam lithography and reactive ion etching for advanced bacterial adhesion studies," *Materials Research Express*, vol. 6, p. 065402, 2019.

[29] F. Laermer, S. Franssila, L. Sainiemi, and K. Kolari, "Deep reactive ion etching," in *Handbook of silicon based MEMS materials and technologies*, ed: Elsevier, 2020, pp. 417-446.

5 Chapter 5

Conclusion and future work

5.1 Conclusion

This thesis presents development and improvement of miniaturization approaches using shape memory polymer films for micro/nano fabrication. Shape memory films were introduced into microfabrication as alternative techniques to the conventional lithography methods which are generally expensive and require advanced equipment. Thus, creating patterns using shape memory films offers inexpensive, rapid, and scalable fabrication method and can be also integrated into sensors and lab-on-chip systems. However, all the miniaturization approaches that have been developed so far have focused mainly on the microscale fabrication. The resolution limits, total reduction ratio that can be achieved and master mold requirements are the main challenges facing these approaches. This thesis contributes to overcome the above mentioned challenges and to extends the use of shape memory films in nanofabrication field for proportional miniaturization.

The resolution of features that could be obtained using miniaturization of heat shrink films was limited to few microns in most of the reported methods. Alternatively, when nano patterns made using soft lithography were miniaturized, they did not shrink proportionally. The maximum size reduction ratio that could be achieved was also a limitation in some methods where the amount of reduction compared to the original

features was quite low (less than 30%). If the miniaturization cycle was sequentially repeated to increase the total size reduction, it resulted in a significant loss of resolution in the second cycle and failed to achieve further miniaturization.

In order to address these challenges, a new multi-step miniaturization approach was developed in this thesis for pre-stressed polymer films. This approach offers a sequential size reduction to achieve sub-micron resolution. A pattern transfer method was developed by combination of soft imprint lithography and RIE that enables using the shrunk patterns from one step as new master for the subsequent miniaturization step without the need of fabricating hard or metal templates. The developed process significantly reduces or eliminates defects from one cycle propagating into the next one and hence enables scalable miniaturization. Thus, from a single master, new patterns were created with various smaller feature sizes. Sequential size reduction of different patterns was demonstrated showing a 20x reduction in size of the original patterns (more than 99.7% reduction in area) and achieving features as small as 750 nm. Moreover, to show that the fabricated patterns are not limited to polymeric materials and can be converted into a functional substrate, the patterns were transferred to a silicon substrate. It should be noted that the increase of surface roughness due to RIE of polymer films limited fabrication of higher resolution patterns (smaller feature sizes). However, the process design that allowed iterative miniaturization introduces a new micron/sub-micron fabrication method that can be performed in any lab without the need of expensive instruments.

In order to improve the resolution and achieve nanoscale patterns, a new miniaturization approach was discovered by applying mechanical constraints during shrinking of imprinted pre-stressed films. Hot embossing can be used to imprint nano

patterns into pre-stressed polymer films. However, direct shrinking of embossed patterns results in loss of the topographical features due to stress relaxation and flow of material causing a shape memory effect. In the approach developed in this thesis, it was found that when the shrinking process is mechanically constrained in one direction, the thermal treatment only relieves the stress in the orthogonal direction leading to a uniaxial shrinkage in that direction while preserving the topographical features. A second step, with the constraint in the orthogonal direction leads to biaxial shrinkage and preservation of all of the topographical features. This miniaturization approach was able to reduce the feature size of the initial imprinted pattern while maintaining the height of pattern. It allows controlling the polymer reflow of not only the in-plane direction but also the out-off plane direction. Thus, the height of the shrunk patterns was preserved and well-defined patterns were generated. The constrained shrinking overcomes the limitations of using hot embossing with the shrinkable films. Using the constrained miniaturization, the height of the shrunk patterns increased from 2.2% to 80%. Shrunken nanoscale patterns of sub-50 nm were generated without losing the topographical features. The hot embossing process parameters were optimized by investigating the effect of these parameters on the quality of the imprinted patterns and the effect on the ability of the embossed film to shrink. The programmability of this approach was demonstrated by fabricating different scale patterns with different feature sizes from the same initial master pattern. Finally, these new capabilities were applied to fabricate tunable and gradient plasmonic structures and hence different optical properties. This process shows a simple, rapid, cost effective and scalable nanofabrication ability that can be used for a wide range of applications.

Next, a multi-step miniaturization approach based on the constrained shrinking process was developed to significantly reduce the patterns size from micro to nanoscale without using a master fabricated by nanolithography methods. Thus, it overcomes the limitations of fabricating nanoscale master molds which often involves using expensive and time consuming processes. This approach allows using the miniaturized pattern to fabricate a new master which was then used as a master for the next miniaturization cycle. This powerful approach reduced the patterns size by 10x over three cycles, and generated high resolution patterns as small as 100 nm. Simple shape patterns as well as complex patterns were fabricated with high fidelity. In addition, the aspect ratio of the features can be maintained even after shrinking multiple times which improves the pattern reproducibility. This scalable nanofabrication approach can be used to fabricate masters for nanoimprint lithography.

The work presented in this thesis has a great potential in nanofabrication of various patterns and structures. The developed fabrication approaches can proportionally miniaturize patterns from tens of micrometers which are easy to fabricate at that scale to sub 100 nm dimensions. This would solve a major challenge in producing nanoscale patterns for microelectronics as well as other applications including sensors, functional surfaces and lab-on-chip devices.

5.2 Recommendations for future work

The developed miniaturization approaches using pre-stressed polymer films have a great potential as unconventional nanofabrication methods. However, these methods can be further improved to achieve even better resolution, scaling and use. Below are a few recommendations and direction for investigations that can result in further improvements.

(i) RIE process for polymer films: In chapter two, the patterns were transferred to the shape memory polystyrene films by RIE using O_2. Depending on the process parameters, the resulting surface roughness could be variable. Due to shrinking process, the lateral dimensions of the patterned features are reduced while the height increases as the total thickness of the film increases. Thus, the peaks and valleys of the rough surface also increase which lead to a significant increase in the surface roughness. As a result, the resolution is limited as any small features on the surface may disappear in the rough surface. Different refinements of the process parameters were performed including the gas flow rate, chamber pressure and the power in order to improve the etched surface. However, the resulted surface roughness is still affecting the resolution. Thus, further improvement can be achieved by optimizing of the RIE process. One recommended adjustment that was found in the literature is reducing the working pressure at a very low value (0.1 Pa). Another approach is to introduce other gases such as argon or nitrogen at a certain percentage along with the reactive gas during etching to either control the reactive gas flow rate while maintaining same pressure or induce ion bombardment effect. It is suggested that increasing ion bombardment energy can decrease the surface roughness particularly for polystyrene.

It was also noticed that these commercial polystyrene films have high density of impurities embedded in the polymer which represent an obstacle for etching smaller size features. Thus, it is recommended to use industrial grade polymer films of higher quality. In addition, preparation of high efficiency shape memory polymers in the laboratory may be considered.

(ii) UV-NIL for patterning shrinkable films: Pre-stressed polymer films have been used to miniaturize features of other materials patterned on the surface of the films. In the nanoscale, if the patterned features have a strong adhesion to the polymer film, they can be miniaturized proportionally with thermal shrinking of the film. The strong adhesion will transfer the compressive stresses applied by the pre-stressed film to the patterned features. It is recommended to use UV-NIL to pattern a thin layer of UV-curable polymer coated on top of the pre-stressed film. Subsequently, the film is thermally heated to allow shrinking which is expected to miniaturize the polymer features as well. There are two important factors to be taken into consideration: the UV-curable polymer properties and the thickness of the residual layer of the polymer after patterning. In order to allow miniaturization of the polymeric features, they need to respond to the applied compressive stress. Thus, the polymer should be partially soften during shrinking. This means the glass transition temperature of the chosen UV-curable polymer should be close to the heating temperature. The other factor is the thickness of the remaining residual layer after imprinting, this layer should be as thin as possible. If the residual layer is too thick, it may exhibit high resistance to shrink and/or produce buckling effect (wrinkles).

(iii) Investigation of constrained shrinking behavior: Constrained shrinking of embossed patterns has shown promising results (chapter three). In order to achieve further improvement, there are two research directions can be investigated. First, the effect of the constraints position on the quality of the shrunken patterns can be investigated. The distance between the two constrained ends with the patterned area placed between them can affect the quality of the shrunk pattern. If the distance is too large, the loss in the resolution will be greater. On the other hand, if the distance is too small, the constraints

may prevent the pattern from shrinking. Second, the hot embossing process parameters are important not only for the replication quality of the imprinted pattern, but also for the quality of the consequently shrunk pattern after thermal treatment. In general, the molding temperature and molding force are more important and effective than the molding time in hot embossing polymer substrates. An optimization has been performed in order to study the effect of hot embossing parameters on the imprint quality and the shrink-ability (shape recovery) of the patterned film. However, regarding to shape memory polymers, the molding time is also a crucial parameter. The molding time can affect the partial stress release of the shape memory polymer during hot embossing and hence shape recovery and the resulted shrunk pattern. Thus, further investigation of the hot embossing parameters would be critical.

6 Appendix 1

Supplementary Information for Chapter 3

Constrained shrinking of nanoimprinted pre-stressed polymer films to achieve programmable, high-resolution, miniaturized nanopatterns

6.1 Hot embossing optimization and its effect on the height of the embossed pattern and on the shrink-ability of the embossed film

Hot embossing is a replication process that replicates the features in the master mold into the polymer film. Thus, changing the process parameters could affect the quality of the replicated features [1, 2]. As our main goal is to combine the hot embossing based pattern transfer with the heat shrink technology to fabricate smaller features while maintaining their height after shrinking, it is important to ensure the quality and identicality of the hot embossed patterns.

Briefly, the hot embossing cycle consists of the following steps: heating of the polymer film and the mold to the molding temperature, while the film and the mold are brought into contact. When the molding temperature is reached, the mold and the polymer film are pressed against each other by increasing the force until it reaches the required molding force and then it is kept constant during the defined holding time. After that the cooling step starts where the temperature decreases to the demolding temperature while the force is still maintained. Finally, the force is removed and the embossed polymer film is demolded from the master mold.

A typical representation of the time-dependent behaviour of the applied process parameters (force and temperature) is shown in Supplementary Figure 6-1b. First, the temperature is increased to preheat the mold and the heat shrinkable PS film to 80 ^{o}C. Then, the mold and the polymer film are brought into contact while the force increases to the contact force value (500 N) and was kept constant. The temperature continues to increase until it reaches the molding temperature (T), which is above the glass transition temperature T_g of the polymer, and then kept constant. When the molding temperature is reached, the

embossing force increases to reach the required molding force (P), which is held constant during the embossing time (5 min). During this step, the polymer material flows into the cavities of the mold and the features of the mold are replicated into the PS film. When the embossing time is over, the cooling step starts while the molding force is still applied. The temperature decreases to 80 ^{o}C, at which the force is decreased until it is completely removed. Then, the mold and the patterned film are separated and demolded. The values of the molding force (P) and the molding temperature (T) represented in Supplementary Figure 6-1b are 4500 N and 125 ^{o}C, respectively. These values represent the chosen parameters after the process optimization, which is discussed in the following paragraphs.

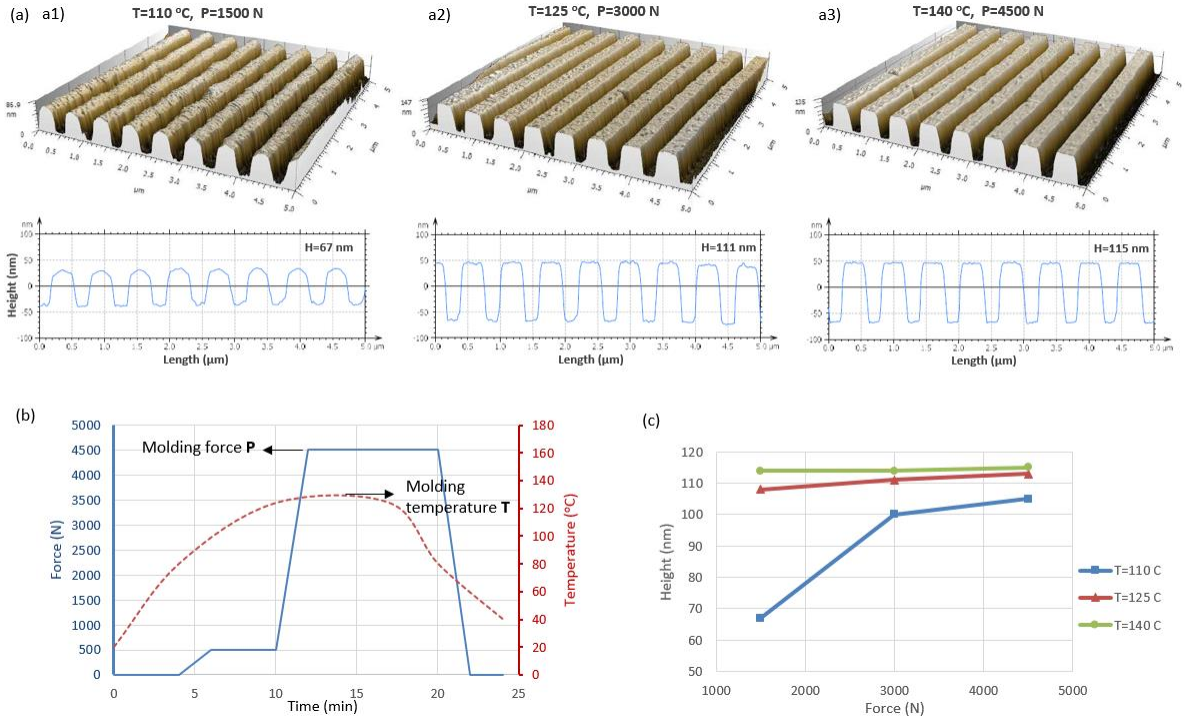

Supplementary Figure 6-1 The effect of the hot embossing parameters (temperature and force) on the quality of the replicated patterns. (a) AFM measurements of the embossed patterns that replicated from a master pattern with initial height of 115 nm. (b) Typical hot embossing cycle showing the behavior of the process parameters force and temperature. (c) The measured height of embossed patterns at different values of molding temperature and force.

The main process parameters for the hot embossing that affect the filling of the polymer into the mold cavities and the quality of the replicated features are the molding force (P), the molding temperature (T) and the embossing time [3-5]. For the nano scale patterns, we found that the embossing time has no significant effect on the embossed patterns and a few minutes (5-6 min) are sufficient for the embossing process. Thus, the molding force and the molding temperature were studied while all other parameters were remained unchanged. Hot embossing experiments were performed on the PS heat shrinkable films at three different values of molding temperature (T) of 110 ^{o}C, 125 ^{o}C, and 140 ^{o}C. Note that the glass transition temperature T_g of PS is around 110 ^{o}C. At each T, the molding force (P) was varied at three different values of 1500 N, 3000 N, and 4500 N. AFM measurements were performed on the embossed patterns to determine the quality and the height of the patterns. Supplementary Figure 6-1a shows three examples of the embossed patterns at the lowest, middle, and highest values of T and P. The initial master pattern was a line-space pattern with a line width of 300 nm and height of 115 nm. The height of the embossed patterns was measured as it can represent the filling of the mold cavities. At the lowest values of T and P (T=110 ^{o}C, P=1500 N), the height of the embossed pattern was found to be 67 nm (Supplementary Figure 6-1 a1). While at the middle values of T and P (T=125 ^{o}C, P=3000 N), the height was increased to be 111 nm (Supplementary Figure 6-1 a2). When the highest values of T and P were applied (T=140 ^{o}C, P=4500 N), the height was increased further to 115 nm (Supplementary Figure 6-1 a3) which is the same height of the master pattern. These results show that the height of the embossed pattern increased with the increase of T and P. In addition to the height increase, the shape and the surface finish of the pattern were also improved.

The measured heights of the patterns after hot embossing at all different values of T and P are shown in Supplementary Figure 6-1c. This can show the effect of increasing T and P on the height. When the pattern was embossed at a temperature equal to T_g ($T=T_g=110\ ^oC$), the force had a significant effect on the height of the embossed pattern. However, when the temperature was increased over T_g the effect of the molding force was minimized as the height slightly increased. At relatively higher temperature than T_g, the embossing force had almost no effect on the height and the height of the embossed pattern reached its maximum value even at lower force values. This illustrates the effect of increasing the temperature as the polymer is soften which makes it easier for the polymer material to flow and fill the cavities in the mold. Thus, the molding temperature has an important role in achieving better replication results.

It is clearly shown that the height and the shape of the replicated patterns are improved when the molding temperature and the force are increased. Therefore, applying higher temperature and force is expected to optimize the hot embossing results and hence the miniaturization process, however this is not the ideal case. Hot embossing conditions affect the ability of the heat shrinkable films to shrink. During hot embossing, the embedded stresses in the prestressed polymer film are partially released while the film is fixed in position and its size does not change. Thus, when the film is heated to allow thermal shrinking, the film does not shrink completely. In order to demonstrate the effect of hot embossing conditions on the shrink-ability of the prestressed PS films, embossed films at different values of T and P were heated to shrink. The embossed films were heated at 130 ^oC for 7 min. Then, the shrunk size was measured and compared to the initial size before shrinking, the results are shown in Supplementary Figure 6-2. It is clearly shown

that the shrink ratio significantly decreased when T was increased. However, the embossing force did not significantly affect the shrink ratio. It is interesting to note that when the film was embossed at higher temperature (T=160 ^{o}C), the film completely lost its ability to shrink (shrink ratio 0%) even when it was heated for 1.5 hours at 180 ^{o}C.

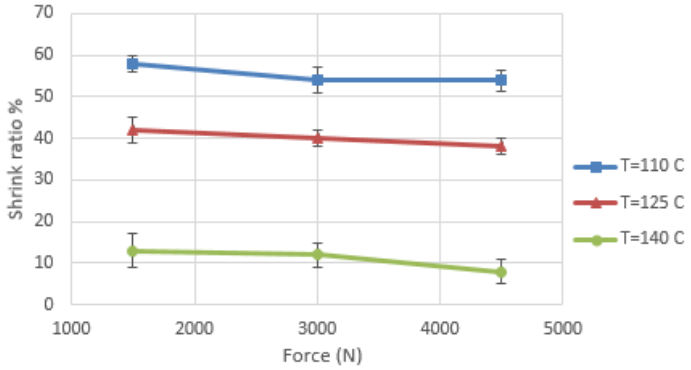

Supplementary Figure 6-2 Effect of hot embossing parameters (temperature and force) on the shrink-ability of the embossed PS films.

Therefore, to choose the appropriate hot embossing conditions for the developed miniaturization process, the conditions should attain high quality embossed patterns without significantly losing the ability to shrink. The molding temperature should be higher than T_g to achieve better replicated patterns (Supplementary Figure 6-1c), but not too high to affect the shrink-ability of the embossed film (Supplementary Figure 6-2). The molding force can be increased to improve the replicated patterns (Supplementary Figure 6-1c), however this increase doesn't significantly affect the shrink-ability (Supplementary Figure 6-2). Due to these requirements, T and P of values 125 ^{o}C and 4500 N were used as optimized hot embossing process parameters for the miniaturization process. For these values, high quality replicated patterns can be generated with high shrink-ability of shrink ratio up to 52% (when heated for longer time to shrink completely).

References

[1] H. D. Rowland, A. C. Sun, P. R. Schunk, and W. P. King, "Impact of polymer film thickness and cavity size on polymer flow during embossing: toward process design rules for nanoimprint lithography," *Journal of Micromechanics and Microengineering*, vol. 15, p. 2414, 2005.

[2] J. Wang, P. Yi, Y. Deng, L. Peng, X. Lai, and J. Ni, "Recovery behavior of thermoplastic polymers in micro hot embossing process," *Journal of Materials Processing Technology*, vol. 243, pp. 205-216, 2017.

[3] R.-D. Chien, "Hot embossing of microfluidic platform," *International communications in heat and mass transfer*, vol. 33, pp. 645-653, 2006.

[4] J. Li, C. Liu, and J. Peng, "Effect of hot embossing process parameters on polymer flow and microchannel accuracy produced without vacuum," *Journal of Materials Processing Technology*, vol. 207, pp. 163-171, 2008.

[5] S. Lan, H.-J. Lee, E. Kim, J. Ni, S.-H. Lee, X. Lai, J.-H. Song, N. K. Lee, and M. G. Lee, "A parameter study on the micro hot-embossing process of glassy polymer for pattern replication," *Microelectronic Engineering*, vol. 86, pp. 2369-2374, 2009.

7 Appendix 2

Supplementary Information for Chapter 4

High resolution fabrication of nano patterns by multi-step iterative miniaturization of hot embossed pre-stressed polymer films and constrained shrinking

7.1 Using polymer working stamp for hot embossing

In the developed multi-step miniaturization approach a polymer working stamp which was replicated from the original Si master was used for hot embossing. However the Si master can be used directly for hot embossing, the polymer working stamp has several advantages over Si master. These advantages include: the polymer stamp is better in terms of demolding and repeatability, the imprinted pattern has same polarity as the original master, and increase lifetime of the master.

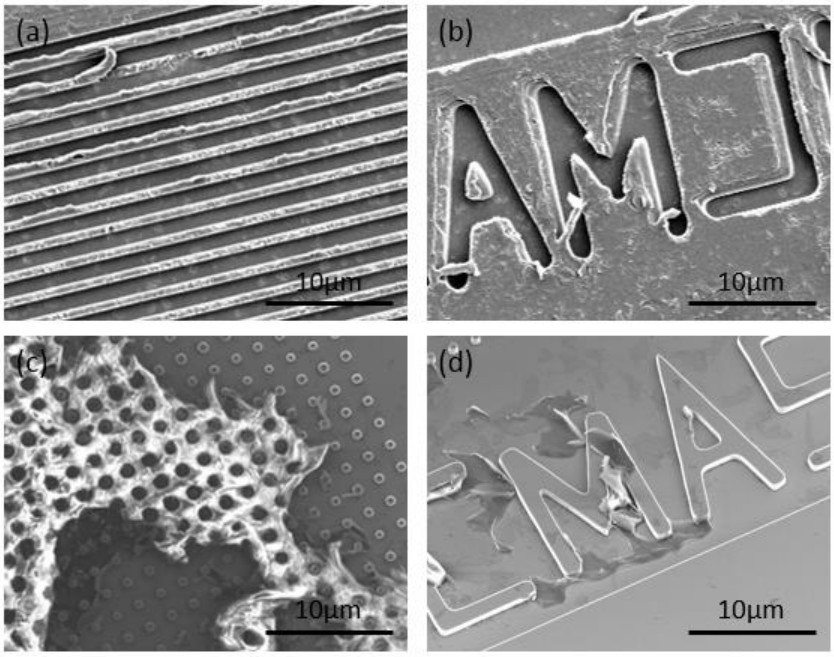

Supplementary Figure 7-1 Demolding issues of using Si master for hot embossing pre-stressed films. (a, b) Pre-stressed film after imprint using Si master, however Si master was coated with anti-stick layer. (c, d) Si master after hot embossing twice, large areas of polymer film stick to the Si master.

The polymer working stamp was easier for demolding after hot embossing and did not have sticking issues as the Si master. Supplementary Figure 7-1 illustrates demolding issues associated with using Si master directly for hot embossing. However an anti sticking layer was coated on the Si master before hot embossing, the imprinted patterns on the PS

shrinkable film were damaged during demolding (Supplementary Figure 7-1a, b) due to sticking to the Si master. In addition, if the Si master is used to imprint another sample, it should be cleaned and coated again with anti sticking layer each time before hot embossing. When Si master was used for hot embossing twice without coating anti sticking layer before the second hot embossing, larger areas of the imprinted film stick to the Si master (Supplementary Figure 7-1c, d). However, the polymer stamp can be used for many times without further treatments.

7.2 Optimization of RIE

The multi-step miniaturization approach allows using the shrunk pattern of a miniaturization cycle to fabricate a Si master that can be used for the next cycle. In order to transfer the pattern to fabricate a Si master, the Si substrate is etched through a RIE process. Different Si RIE recipes were used including Bosch process, mixed gases process, and a combination of both processes (the results are shown in Supplementary Figure 7-2). Bosch process which is a cyclic process of deposition/etch steps is used to obtain high aspect ratio structures. A protection layer which is generally a fluorocarbon-based film is deposited on the surface to protect sidewalls of the pattern. Then, the Si is etched at the bottom surface during the etch step while sidewalls are protected by the deposited layer. However, in our results, the deposited layer was insufficient to protect sidewalls which resulted in etching sidewalls completely (Supplementary Figure 7-2a).

A combination of mixture gases etch followed by Bosch process was used (Supplementary Figure 7-2b, c, d). First, Si etch using gases mixture of C_4F_8/SF_6 was performed which resulted in a good etch profile with smooth surface. Then, Bosch process was used to increase etch depth but it started to etch sidewalls as well (Supplementary

Figure 7-2c). When Bosch process was performed for more cycles, the sidewalls were completely etched and the pattern was damaged (Supplementary Figure 7-2d). Thus, only mixture gases process was used to etch Si substrate for the desired depth with C_4F_8:SF_6 gases ratio of 2:1 which resulted in good etch profile with smooth surface and nearly vertical sidewalls (Supplementary Figure 7-2e, f). This mixture gases RIE process was used for each miniaturization cycle in the multi-step miniaturization process.

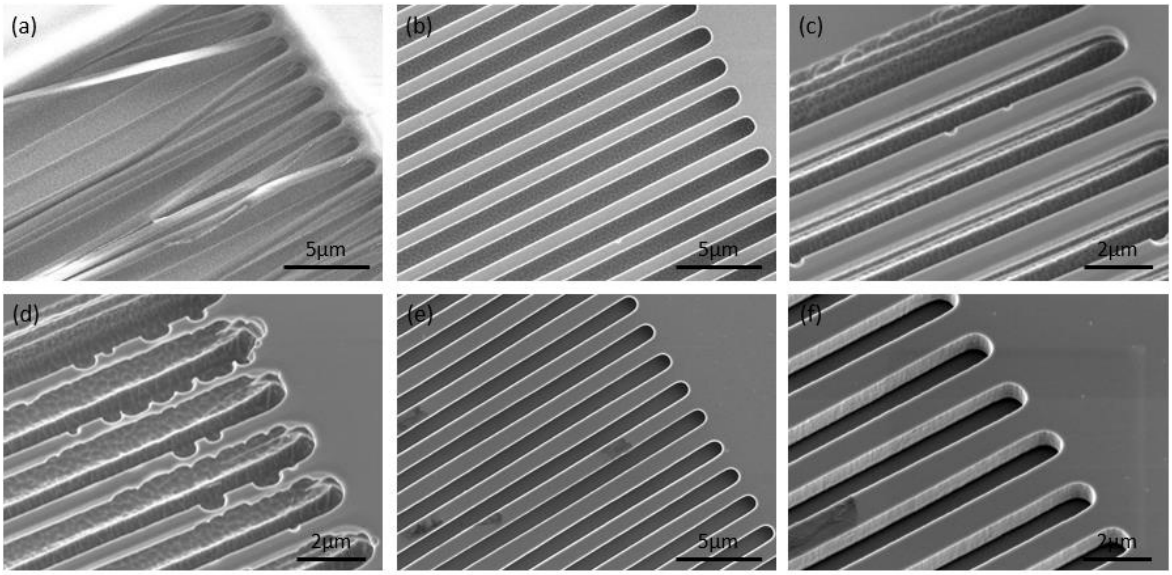

Supplementary Figure 7-2 Si RIE using different processes. (a) Bosch process. (b, c) Mixed gases followed by Bosch process. (d) Mixed gases followed by Bosch process for longer time. (e, f) Mixed gases etch process.

7.3 Direct shrinking of embossed pattern

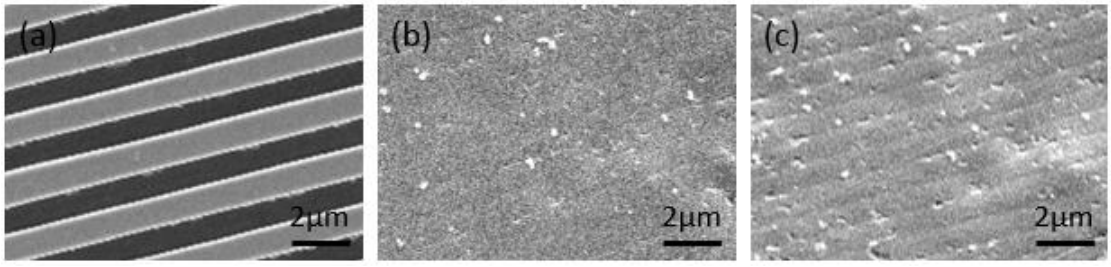

Supplementary Figure 7-3 Direct shrinking of embossed pre-stressed film. SEM of (a) imprint, (b) shrunk pattern, (c) inclined view of the shrunk pattern.

Direct shrinking of hot embossed pre-stressed films leads to loss of resolution as the height of the pattern dramatically decreased due to polymer reflow during shrinking (Supplementary Figure 7-3). The pre-stressed polymer film was imprinted by same hot embossing process, the imprinted pattern is shown in Supplementary Figure 7-3a. After direct shrinking, the pattern was almost disappeared (Supplementary Figure 7-3b). An inclined view for the shrunk pattern (Supplementary Figure 7-3c) shows that the pattern height is very small.